QATAR UNIVERSITY

COLLEGE OF HEALTH SCIENCES

DIFFERENTIAL EXPRESSION OF MICRORNAS BY ANTI-OBESITY TREATMENT SULFORAPHANE IN SKELETAL MUSCLE OF DIET-INDUCED OBESITY IN MICE

BY

DIMA RIYAD ALASMAR

A Thesis Submitted to

the College of Health Sciences

in Partial Fulfillment of the Requirements for the Degree of

Masters of Science in Biomedical Sciences

January 2023

COMMITTEE PAGE

The members of the Committee approve the Thesis of
Dima Alasmar defended on 05/01/2023.

_____
Nasser M. Rizk
Thesis/Dissertation Supervisor

_____
Dr. Mohammed Elrayess
Committee Member

_____
Dr. Layla Al-Mansoori
Committee Member

_____
Dr. Nader Eldweik
Committee Member

_____
Add Member

Approved:

_____
Hanan Abdul Rahim, Dean, College of Health Science

ABSTRACT

ALASMAR, DIMA, R., Masters of Science: January : 2023, Biomedical Sciences

Title: Differential Expression of miRNAs by Anti-Obesity Treatment Sulforaphane in Skeletal Muscle of Diet-Induced Obesity in Mice

Supervisor of Thesis: Nasser M. Rizk.

Background: Skeletal muscles account for 40-60% of total body weight and are responsible for 30% of resting metabolic rate. They are essential for metabolic homeostasis in the body as they provide the leading site for glucose uptake into tissues by insulin induction. Sulforaphane (SFN), a natural isothiocyanate compound extracted from cruciferous vegetables, acts mainly as an antioxidant; but multiple research studies have shown that it can also act as an anti-obesity drug. Recent studies have shown that microRNAs (miRNAs) play a critical role in regulating skeletal muscle dysfunction; however, their exact mechanism of regulation is not well known. **Aim:** To study the expression profile of miRNA in the skeletal muscles of diet- induced obesity (DIO) mice treated with SFN and determine their role by identifying pathways and gene ontology involved in the metabolic functions of skeletal muscles. **Methods:** The study included ten male mice of CD1 strain (five-SFN treated and five-vehicle as control); they were randomized at four weeks old and fed ahigh-fat diet to induce DIO condition. Total RNA was extracted from the skeletal muscles of DIO mice, and small RNA sequencing was utilized to identify the microRNA expression profiles. Pathway mapping and gene ontology (GO) tools were used to evaluate the biological processes and signaling pathways affected by the differentially expressed miRNAs. **Results:** Body weight, food intake, plasma glucose, and leptin levels were significantly decreased in SFN-treated mice compared to control groups. Furthermore, we identified eight

differentially expressed miRNAs in SFN-treated DIO mice, of which five were upregulated (mmu-miR-150-5p, mmu-miR-486a-3p, mmu-miR-126b-5p, mmu-miR-140-3p, mmu-miR-92a-3p) and three were downregulated (mmu-miR-101a-3p, mmu-miR-29c-3p, mmu-miR-3074-5p). Furthermore, we confirmed that SFN treatment dysregulates miRNAs that regulate genes involved in insulin signaling, MAPK, and PI3K/Akt signaling pathways, which are important regulators of skeletal muscle metabolism, including insulin resistance and obesity. **Conclusion:** Our study showed that SFN induced a change in the expression profiles of miRNAs in the skeletal muscle of DIO mice, which regulate gene targets of miRNAs involved in multiple biological processes to combat obesity.

DEDICATION

To my beloved family

ACKNOWLEDGMENTS

I would like to express my gratitude to everyone who helped to fulfill this work. The greatest thanks to my supervisor, Dr. Nasser Rizk, for all the help, support, and guidance throughout the study. I would also extend my gratitude to my committee members, Dr. Layla Al-Mansoori, Dr. Mohammed Elrayess, and Dr. Nader al-Dewik. A great thanks to Qatar National Research Fund (QNRF) – National Priorities Research Program (NPRP) for the grant (NPRP9-351-3-075) and Qatar University QUST-1-CHS-2022-353 for their support. Also, I would like to thank the team of Dr. Nasser's lab in the present study at the Biomedical research center Omnia Mohamed, Abdulrahman El-Gamal, Amina Fadel, and Dina Elsayegh. Thanks to my colleagues in the Genomics core lab at Weill Cornell Medical College, especially Yasmin Mahmoud and Ayeda Ahmed, for their continuous support and help. Lastly, all my gratitude to my family for their support and care for me throughout my studies.

TABLE OF CONTENTS

LIST OF TABLES

LIST OF FIGURES

LIST OF ABBREVIATIONS

AMP	Adenosine monophosphate
AMPK	AMP-activated protein kinase
ATP	Adenosine triphosphate
BMI	Body mass index
CA	Cinnamic aldehyde
CoA	Coenzyme A
DGCR8	DiGeorge syndrome critical region 8
DIO	Diet-induced obesity
FFAs	Free fatty acids
FTO	Fat mass-and obesity-associated gene
FOXO1	Forkhead Box O1
GLUT4	Glucose transporter
GWAS	Genome-wide association studies
IKKβ	Inhibitor of nuclear factor kappa-B kinase subunit beta
IL-6	Interleukin-6
IRS	Insulin receptor substrate
miRNAs	microRNAs
miRISC	miRNA-induced silencing complex
MSCs	Mesenchymal stem cells
MyoR	Myogenic repressor
NAD(P)H	Nicotinamide adenine dinucleotide phosphate

ncRNAs	Non-coding RNAs
NF-κB	Nuclear factor-κB
NQO1	NAD(P)H Quinone Dehydrogenase 1
Nrf2	Nuclear factor (erythroid-derived 2)-like 2
Pax7	Paired box transcription factor 7
PEPCK	Phosphoenol pyruvate carboxykinase
PKC	Protein kinase C
qPCR	quantitative polymerase chain reaction
RIN	RNA integrity number
ROS	Reactive oxygen species
SFN	Sulforaphane
sRNA	Small RNA
STZ	Streptozotocin
T2DM	Type-2 diabetes
TLR	Toll like receptor
TNF-α	Tumor necrosis factor-alpha, 11
TRBP	Transactivation-responsive RNA-bin ding protein
WHO	World Health Organization
γ-GCS	Gamma-glutamyl cysteine synthetase

CHAPTER 1: INTRODUCTION

Obesity is a multifactorial metabolic disorder characterized by hyperplasia and hypertrophy of adipocytes. It is considered a primary nutritional condition underlying the cause of other serious health problems, such as hypertension, cardiovascular diseases, and diabetes, along with other diseases (Martins et al., 2018; Mayoral et al., 2020). The rising prevalence of obesity has been a major concern as the increased weight gain increases the risk for other diseases and economic hardship worldwide (Engin, 2017). According to the World Health Organization (WHO), the German Federal Court, the European Parliament, and the German Obesity Association, obesity is considered a chronic disorder with a high morbidity and mortality rate with the need for lifelong treatment (Wirth et al., 2014). Moreover, obesity negatively affects the human skeletal muscles (SMs) as it causes loss of muscle mass and quality; it decreases locomotor performance and contractility of the skeletal muscles, resulting in hampered movements in obese individuals (Tallis et al., 2018). In addition, various studies have demonstrated that epigenetic regulation, such as modifying histones, microRNAs (miRNAs), and DNA methylation, can stably adjust gene expressions (Fan et al., 2012).

There is evidence that miRNAs' function regulates gene expression by recruiting silencing complexes to complimentary sequence regions in target mRNAs (Ortega et al., 2013). Small RNA molecules called miRNAs, ranging in size from 19 to 24 nucleotides (nt), often regulate gene expression by repressing translation or deadenylating and degrading target mRNAs (Bartel, 2004). Substantial evidence has shown that miRNAs have a vital role in various biological processes such as cell differentiation, proliferation, apoptosis, and hematopoiesis (Chen et al., 2004; Dostie et al., 2003; Wang et al., 2009; Xu et al., 2003). Expression profiles of miRNAs can be biomarkers of various diseases as they play a role in multiple physiological

and pathological processes, such as cell proliferation and death and differentiation of tissue cells (Landrier et al., 2019; Qian Yao et al., 2019; Q. Yao et al., 2019). An example of pathological conditions regulated by miRNAs is obesity, where several miRNAs contribute to the development and metabolism of adipose cells, such as miR-14, miR-278, and let-7, which are responsible for lipid metabolism (Frost & Olson, 2011; Krützfeldt & Stoffel, 2006). Furthermore, they act as epigenetic modulators as they affect the protein expression of the target mRNAs without changing the gene sequences. They act either as adipogenic suppressors or pro-adipogenic effects based on their target cell function in adipocytes (Landrier et al., 2019; Shi et al., 2016).

A recent study in Dr. Nasser's lab has suggested that SMs are the primary site of action for Sulforaphane (SFN) in diet-induced obesity (DIO) mice (Cakir et al., 2022). As a continuation of the previous study, we hypothesize that DIO mice treatment with SFN as an anti-obesity drug induces dysregulation of miRNAs profile expression, which changes gene expression and consequently affects the metabolic functions of skeletal muscles in obese mice. The objectives of this study are to characterize the profile of miRNA in the skeletal muscles of DIO mice treated with SFN and to identify the role of miRNAs after SFN treatment in SMs of DIO mice. These roles will be further recognized using bioinformatics tools to identify pathways and gene ontology involved in the metabolic functions of skeletal muscles.

CHAPTER 2: LITERATURE REVIEW

2.1 Obesity

Obesity is usually classified based on the body mass index (BMI, kg/m2), which is measured by dividing an individual's weight by height. It is considered the internationally accepted method for classifying obesity (Engin, 2017). According to the BMI measures, individuals are allocated into four categories; underweight, where BMI is less than 18.5 kg/m2; normal weight, with a BMI between 18.5–24.9 kg/m2; overweight 25-29.9 kg/m2, and a BMI of more than 30 kg/m2 is considered within the obesity range (Engin, 2017). Furthermore, obesity is classified into three classes; BMI of 30-34.9 is class 1, BMI of 35-39.9 is class 2, and BMI of more than 40 is considered class 3, which is the highly severe obesity class (Engin, 2017). According to WHO, the global obesity rate has tripled three times since 1975 worldwide; in 2016, 39% of adults above 18 years old were overweight, and 13% were considered obese, while an estimated 38.2 million children aged less than five years were either overweight or obese in 2019 (*Obesity and overweight*, 2021). Furthermore, being overweight and obese is highly associated with increased insulin resistance and diabetes type 2 (T2DM) (Haslam, 2010). According to a study conducted by Keaver et al., obesity and overweight would reach up to 89% in men and 85% in women by the year 2030, contributing to the increased levels of chronic diseases related to obesity, such as diabetes and cardiovascular diseases (Keaver et al., 2013).

Although a diet accompanied by exercise as well as anti-obesity drugs can be used to treat obesity, a BMI higher than 30 kg/m^2 is hard to lower with only diet, and other treatments may cause other diseases and/or adverse side effects in the long term. Therefore, the most successful obesity treatment is bariatric surgery, but it is highly associated with short- and

long-term complications; therefore, there is a high urge to find a medication to resolve this condition (Cakir et al., 2022). The homeostatic control of energy balance involves the balance between food intake and energy expenditure and is regulated mainly through the hypothalamus, which integrates various central circuitries to establish the homeostatic responses (Andermann & Lowell, 2017; Rossi & Stuber, 2018). Among these circuitries, leptin-melanocortin circuitry is the primary regulator of homeostatic balance (Cakir et al., 2022). Leptin is considered a sensor of fat mass in the body and is involved in a negative feedback loop to maintain the fat stores in the body at a specific set point (Oswal & Yeo, 2007). Thus, Leptin production increases with greater adipogenesis, and leptin concentrations in the blood mirror the levels of body fat reserves (Oswal & Yeo, 2007). Increased leptin production allows leptin to bind to its receptors in various tissues reducing food intake and increasing energy expenditure, leading to weight loss (Klok et al., 2007). Although this mechanism has been demonstrated in rodents, it does not seem to apply to humans similarly. However, most obese individuals have high leptin levels without weight loss, implying resistance to leptin actions in humans (Oswal & Yeo, 2007). Furthermore, DIO mice are resistant to both the endogenous leptin released by adipose tissues and the administration of exogenous leptin (Frederich et al., 1995; Myers et al., 2010). As a result, considering ways to alleviate leptin resistance or increase leptin receptors' sensitivity to leptin is important in treating obesity. (Cakir et al., 2022).

Usually, low-grade systematic inflammation and oxidative stress accompany obesity due to high levels of free fatty acids (FFAs) and glucose (Ellulu et al., 2017; Manna & Jain, 2015; Weisberg et al., 2003; Wellen & Hotamisligil, 2003). Increased FFAs elicited chemotactic pro-inflammatory signals via TLR 4, resulting in the release of tumor necrosis factor-alpha

(TNF-α) and interleukin-6 (IL-6). TNF-α acts on increasing lipolysis, nuclear factor κB (NF-κB)/IKKβ pathway activation, and phosphorylation of insulin receptor substrate 1 (IRS1) (Weisberg et al., 2003; Wellen & Hotamisligil, 2003). On the other hand, IL-6 inhibits the expression of GLUT4 and IRS1 in skeletal muscle leading to increased resistance to insulin (Kaul & Forman, 1996), (Kahn & Flier, 2000). Insulin resistance causes a decrease in glucose uptake by insulin-dependent tissues and cells. It also increases adipocyte utilization of FFA, increasing mitochondria β-oxidation and eventually elevating the levels of reactive oxygen species (ROS) and other inflammatory markers (Kaul & Forman, 1996). The nuclear factor (erythroid-derived 2)-like 2 (Nrf2) is a master regulator of alleviating oxidative stress induced by obesity or other redox conditions (Gupte et al., 2013), (Vomund et al., 2017). The accumulation of ROS leads to the activation of Nrf2, which is normally sequestered in the cytoplasm by Kelch-like ECH-associated protein 1 (KEAP1) (Vomund et al., 2017) (Lugrin et al., 2014). Interactions of ROS with the cysteine residues on (KEAP1) lead to the release of Nrf2 to the nucleus inducing the expression of antioxidative genes such as NAD(P)H quinone oxidoreductase 1, glutathione S-transferases, and glutamate-cysteine ligase, which eliminates the ROS molecules (Lugrin et al., 2014) (Vomund et al., 2017). Several studies have indicated that activation of Nrf2 leads to protection against obesity and diabetes. For example, a study by Zheng et al. identified whether Nrf2 activation by dietary compounds could alleviate renal damage in streptozotocin (STZ)-induced diabetic nephropathy (Zheng et al., 2011). In this study, diabetes was induced by injection of STZ in Nrf2 +/+ and Nrf2 -/- mice two weeks later, and sulforaphane (SFN) or cinnamic aldehyde (CA) was given to the mice (Zheng et al., 2011). After that, diabetes markers such as blood glucose, weight loss, polydipsia, polyuria, and insulin levels were assessed (Zheng et al., 2011). The results of this

study showed that SFN and CA both are capable of decreasing diabetes symptoms in Nrf2 +/+ mice and not in Nrf2 -/-, which indicates that activation of the Nrf2 specific pathway indicated by increased levels of the Nrf2, NQO1, and γ-GCS proteins by SFN and CA helps to alleviate the pathological alterations caused by diabetes (Zheng et al., 2011). Through Nrf2 activation, oxidative damage was eliminated through ROS neutralization, protecting the glomerulus against oxidative damage and the development of diabetic nephropathy (Zheng et al., 2011). Moreover, Nrf2 activation mediates glucose metabolism and glycogen formation in the liver of SFN, and CA-treated mice of Nrf2 +/+ strain, reducing blood glucose (Zheng et al., 2011).

2.2 Predisposing factors of obesity

Although obesity is mainly triggered by an imbalance between energy intake and energy loss through physical and metabolic activities, the disease's etiology is not yet fully identified (Wright & Aronne, 2012). Furthermore, it is related to highly complex factors that could be genetic, environmental, physiological, psychological, or even social and economic factors contributing to obesity (Wright & Aronne, 2012). However, the most common factors are genetics, behavior, and sociodemographic (Endalifer & Diress, 2020).

2.2.1 Sociodemographic factors

Sociodemographic factors, including age, gender, education, income, marital status, employment, ethnicity, and living location, can contribute to the obese status of an individual (Cheah et al., 2020; Endalifer & Diress, 2020). A study by Cheah et al. to understand the relationship between sociodemographic factors and confectionery consumption among obese and non-obese adults in Malaysia showed that education, employment, income, gender, and

ethnicity correlate with increased consumption of confectionery. However, no relation was found with age, marital status, or living location (Cheah et al., 2020).

A study by Kerkadi et al. examined the link between lifestyle factors and overall abdominal obesity in Qatar among 14-18-year-olds. The study found a significant incidence of abdominal and overall obesity, with males having a higher risk than females (Kerkadi et al., 2019). 44% of the population was inactive, with women more so than men (Kerkadi et al., 2019). In addition, 48% and 27.3% of teens routinely consume sugary drinks and fast food, respectively (Kerkadi et al., 2019). Half of the teens eat candy and chocolate four times a week. The higher prevalence among females (60.2% vs. 39.8%, p 0.001) (Kerkadi et al., 2019). Physical inactivity, poor diet, insufficient sleep, and excessive sedentary behavior have been reported to be great contributors to obesity among children (Castro et al., 2016; Poitras et al., 2016; Tanaka et al., 2014).

2.2.2 Behavioral factors

As identified by multiple studies, irregularities in physical exercise and lack of physical activity, decreased sleep duration, stress, smoking, and urban and industrial environment contribute to obesity (Endalifer & Diress, 2020). For example, sitting still for more than 2 hours, watching electronic devices, and when the brain is simply observing, it stops utilizing glucose, leading to fat accumulation (Endalifer & Diress, 2020). Moreover, hormonal changes can lead to obesity, such as stress, whereas cortisol increases appetite and excess abdominal fat production (Endalifer & Diress, 2020).

2.2.3 Genetic factors

Family history of obesity could also be a predisposing risk factor for obesity; numerous studies have referred to genetic factors as crucial in obesity, and 250 genes have been

associated with it by Genome-wide association studies (GWAS) (Endalifer & Diress, 2020). For example, the fat mass- and obesity-associated gene (FTO) has been strongly associated with the advancement of obesity and type 2 diabetes (Endalifer & Diress, 2020). Furthermore, a study by Li et al. showed 12 obesity-predisposed loci; they tested those loci to identify their relationships with BMI, waist circumference, weight, height, and obesity risk predictive value, and they found that they indeed increased weight as well as the risk of obesity by 10.8% (Apovian, 2016; Li et al., 2010). Furthermore, a study of identical twins who were separated identified that genetics is involved in differences in body fat between individuals, with about 60%, while the rest is attributed to the environment (Apovian, 2016; Price & Gottesman, 1991).

2.3 Adipose tissue structure and function

Adipose tissue plays a pivotal role in physiological processes due to its endocrine and secretory functions, and it is highly abundant in the human body (Niemelä et al., 2008). It is mainly found surrounding the inner organs and in the loose subcutaneous connective tissue (Niemelä et al., 2008). It mainly consists of mature adipocytes; nevertheless, other cell types include fibroblasts, epithelial cells, pericytes, smooth muscle cells, and adipogenic progenitor cells known as preadipocytes (Niemelä et al., 2008). Adipose tissue constitutes two main subtypes: white and brown fat (Niemelä et al., 2008). White fat is the main site of fat digestion and storage and is an important energy reservoir site (Niemelä et al., 2008). In case of increased energy situations, it is capable of triglyceride storage, while in energy scarcity cases, it frees fatty acids to compensate for the low energy (Gregoire et al., 1998).

On the other hand, brown fat is rare and mainly provides heat for the body (Niemelä et al., 2008). Additionally, adipose tissue is essential for estrogen biosynthesis as well as steroidal hormones storage (Deslypere et al., 1985; Kley et al., 1980; Nimrod & Ryan, 1975); not only

that, it secretes various peptides, cytokines, and complements that function to regulate adipocyte growth and metabolism (Gregoire et al., 1998; Kim & Moustaid-Moussa, 2000). Moreover, the secretion of endocrine signals establishes energy homeostasis in the body (Gregoire et al., 1998; Kim & Moustaid-Moussa, 2000). Despite the crucial functions of adipose tissue in normal pivotal processes, it contributes to the formation of multiple human diseases due to the accumulation of increased fat composition in the body, causing obesity which underlies multiple pathological disorders, including diabetes type-2 (Moller & Flier, 1991), hypertension, and cardiovascular diseases (Spiegelman et al., 1993), in addition, it has been considered as a high-risk factor to breast, renal, ovarian and colorectal cancer (Bjørge et al., 2004; Engeland et al., 2003; Jonsson et al., 2003; Tamakoshi et al., 2004). Adipose tissue is further regulated by the central nervous system, which is innervated by the sympathetic nervous system, which promotes fat mobilization by secreting adrenergic hormones like epinephrine and norepinephrine (Tang & Lane, 2012).

2.3.1 Adipocytes

Adipocytes, which account for most of the cell types in the adipose tissue, are derived from pluripotent mesenchymal stem cells (MSCs) that inhabit the bone marrow and adipose tissue vascular stroma (Tang & Lane, 2012). Upon stimulation, pluripotent MSCs are committed to the adipocyte lineage, which gives rise to the preadipocytes, which undergo a mitotic clonal expansion through several rounds of mitosis and eventually differentiate into mature adipocytes (Tang & Lane, 2012). A mature adipocyte comprises a big fat droplet within a thin cytoplasm frame surrounded by a plasma membrane (Tang & Lane, 2012). In case of energy deprivation in the body, cytoplasmic hormone-sensitive lipase (Egan et al., 1992) and adipocyte-triglyceride lipase (Ahmadian et al., 2011; Ahmadian et al., 2010), upon stimulation

by lipolytic hormones (Egan et al., 1992), move to the surface of the fat droplet in which they break down triglyceride into glycerol and fatty acids (Londos et al., 1999); thereafter, fatty acids are transported into the blood to provide energy to the peripheral tissue in need, especially for heart, liver and skeletal muscles (Tang & Lane, 2012). On the other hand, if there is an energy excess due to high caloric intake, triglyceride is synthesized by lipogenic enzymes found in the cytoplasm and endoplasmic reticulum (ER), which are then integrated into the fat droplet in the adipocyte (Tang & Lane, 2012).

Furthermore, mature adipocytes release the leptin hormone (Batra et al., 1995; Friedman, 2002, 2009; Leroy et al., 1996; Zhang et al., 1994), which regulates body weight, food intake, and other effects on the appetite by interacting with specific hypothalamus receptors (Flier, 1998; Kim & Moustaid-Moussa, 2000; Sternson et al., 2005). Although leptin is an anorectic hormone that decreases energy storage when adipose tissue is filled by reducing the food intake, individuals with obesity could be leptin resistant, decreasing its effectiveness (Tang & Lane, 2012). Additionally, adipocytes can secrete other factors that interact with vascular diseases and immunological responses and regulate individuals' appetite (Niemelä et al., 2008).

2.4 Skeletal muscle structure and function

Skeletal muscle is an organ of integrated tissues of skeletal muscle fibers, blood vessels, nerves, and connective tissue (Biga et al., 2020). Each skeletal muscle has three layers of connective tissue, which maintains its structure and categorizes the muscle fibers inside (Biga et al., 2020). The first layer of connective tissue is the epimysium, a dense irregular connective tissue separating the muscle from internal organs and functions in the muscle contraction independent from other tissue without losing its structural integrity (Biga et al., 2020). The

middle layer of connective tissue is the perimysium surrounding fascicles, bundles of muscle fibers (Biga et al., 2020). Finally, the endomysium's last layer of connective tissue is a thin layer of collagen and reticular fibers. It carries the force of the contraction from the muscle fibers to the tendons that allow the pulling of the bones to help in the movement of the skeleton (Biga et al., 2020). All in all, signals from the nervous system signal the contraction of muscle fibers, which are transferred to the tendons that move the skeleton of an individual, resulting in human movement.

2.4.1 Muscle fibers

The type of fiber determines the contractile function of the skeletal muscle in muscle, and the deleterious effect of obesity on the muscle is caused due to its effect on different fiber types (Tallis et al., 2018). Classification of the muscle fibers depends on their content of myosin heavy chain isoform composition (Tallis et al., 2018). They are further classified into slow and fast-twitch fibers, where the slow type I and IIa fibers in human are ready to go into aerobic metabolism as they are rich in mitochondria and myoglobin and has a high fatigue resistance ability but generate a low power (Tallis et al., 2018). On the other hand, the fast type IIb and IId/x fibers go into anaerobic metabolism, which, although it could produce fast strength power, has a low fatigue resistance as it is independent of oxygen (Tallis et al., 2018). Moreover, slow muscle fibers are associated with higher insulin sensitivity and glucose uptake through GLUT4 transporter than fast fibers (Tallis et al., 2018).

2.5 Skeletal muscle metabolism

The metabolism and function of skeletal muscles are regulated by various signaling pathways controlled by hormonal, inflammatory, nervous, and nutritional stimuli (Moro & Capel, 2019). Glucose, glycogen, and free fatty acids are the main fuels for muscle energy

metabolism (Felig & Wahren, 1975; Wahren, 1977). The main energy source for the slow fibers is the β-oxidation of free fatty acids. In contrast, fast fibers are rich in glycogen and glycolysis enzymes that result in glucose production (Agarwal et al., 2013). Moreover, muscle metabolism is regulated by hormones such as insulin which increases the muscle uptake of glucose and fatty acids (Agarwal et al., 2013). Simultaneously, insulin activates the formation of proteins, triglycerides, and glycogen (Agarwal et al., 2013).

2.6 Skeletal muscles and obesity

Obesity has a negative effect on skeletal muscle function in obese individuals, lowering their mobility by reducing their locomotor performance (Tallis et al., 2018). As a result, it causes a reduction in movement, activity levels, and energy expenditure causing more weight gain and, thus, poor life quality (Tallis et al., 2018). Calcium signaling and protein activity of contraction and relaxation in the muscle define its contractile function, and both are controlled by the fiber type (Tallis et al., 2018). Obesity causes a shift from slow fiber composition to fast fiber as a response to the increased sugar-fat diet altering the force and power production and disrupting the calcium signaling pathway (de Wilde et al., 2008; Helge et al., 1999; Seebacher et al., 2017; Stuart et al., 2013; Tallis et al., 2018; Tanner et al., 2002). In addition, obesity causes an imbalance of energy; AMPK is a central regulator of the energy balance. It is activated in low-energy states due to a lower ratio of ATP: AMP in cases of either muscle contraction or low-calorie intake and facilitates ATP production (Kristensen et al., 2015; Narkar et al., 2008; Steinberg, 2018). In obesity, AMPK activity is repressed (Steinberg et al., 2006), and low ATP will be produced, leading to fat deposition and a shift from slow-fiber to fast-fiber muscle expression (Tallis et al., 2018).

Moreover, obesity causes insulin resistance in skeletal muscles, the primary site for glucose uptake after a high-sugar meal, through an insulin-dependent mechanism. After a meal high in glucose, an increase of glucose in the blood causes stimulation of insulin secretion from the pancreas, which in turn lowers FFA levels in the plasma as it represses the lipolysis process and facilitates the uptake of glucose by skeletal muscles through GLUT 4 glucose transporter leading to a high rate of glucose oxidation and energy production (Abdul-Ghani & DeFronzo, 2010; DeFronzo, 1988; Groop et al., 1989). Skeletal muscles can use FFAs or glucose as energy sources (Abdul-Ghani & DeFronzo, 2010). In the case of low plasma insulin, glucose uptake by skeletal muscles is low, and FFA is high; therefore, they are the primary source of energy production (Abdul-Ghani & DeFronzo, 2010). Obese individuals have a high rate of insulin resistance in skeletal muscles that boosts with increasing BMI (Bogardus et al., 1984); this could be caused due to the accumulation of fat in the muscle cells and increased FFA in the plasma impairing the insulin signaling pathways (Abdul-Ghani & DeFronzo, 2010).

The basis of insulin resistance in obese individuals could be attributed to reduced glucose transport or defective glucose handling intracellularly in obese individuals (Mengeste et al., 2021). Changes in skeletal muscle metabolism due to severe obesity include decreased insulin-stimulated glucose uptake, oxidative metabolism, and high lactate production (Elton et al., 1994; Friedman et al., 1994). The decreased insulin action is caused by insulin receptor signaling deficiency, leading to lower stimulated glucose uptake (Dohm et al., 1988; Goodyear et al., 1995). In obese individuals' skeletal muscles, serine phosphorylation of insulin receptors such as IRS1 and other kinases are activated, such as protein kinase C (PKC), which decreases signal transduction by insulin and lowers

glucose transport stimulation, glycogen synthesis, non-oxidized glycolysis and glucose oxidation (Houmard et al., 2011, 2012).

Moreover, changes in lipid metabolism have been observed between lean and obese individuals (Mengeste et al., 2021). Obese individual's skeletal muscles show high intramuscular/intramyocellular triacylglycerol (Goodpaster et al., 2001; Goodpaster et al., 2000; Simoneau et al., 1999) along with reduced oxidative lipid capacity (Anderson et al., 2009; Hulver et al., 2003; Kelley et al., 1999; Kim et al., 2000; Mogensen et al., 2007) and fatty acid oxidation (Houmard et al., 2012). Low lipid oxidation could be due to impaired lipid metabolism, like an increased expression of stearoyl coenzyme A (CoA) denaturase-1 and decreased mitochondrial content (Houmard et al., 2011, 2012). Hence the metabolic capacity of skeletal muscles in obese individuals is directed towards fatty acid storage and esterification and not oxidation (Bandyopadhyay et al., 2006; Fritzen et al., 2020; Simoneau et al., 1999).

2.7 Animal models of obesity

Over the years, animal models have remained vital to understanding the pathophysiology of diseases and finding effective therapeutics for various diseases without harming humans (Suleiman et al., 2020). The advantage of animal models is that they can be easily controlled, fed under a standard diet, and kept under certain conditions free of pathogens (Suleiman et al., 2020). There are different types of animal obesity models, either genetic such as monogenic (like ob/ob mouse and db/db mouse), polygenic (like Tsumura and Suzuki obesity and diabetes mouse and New Zealand obese mouse), and transgenic models (like CRF–Transgenic mouse and Glucose transporter subtype 4 transgenic mouse) or non-genetic which is induced by high-fat diet (like Diet-induced

obese (DIO) rats), surgical or chemical (like Lesion of the ventromedial hypothalamus (VMH lesion) and Lesion of the hypothalamic paraventricular nucleus (PVN lesion)), exotic (such as bats and seals) and large animal models (such as dogs and pigs) (Suleiman et al., 2020) (Lutz & Woods, 2012).

2.7.1 Diet-induced obesity mice (DIO)

A DIO mouse model is made obese by a special high-fat diet (Suleiman et al., 2020). They are a useful model in studying the progression of metabolic diseases and have lower sensitivity to leptin activity and low insulin levels (Suleiman et al., 2020). Furthermore, they provide information on the long-term effects of a high-fat diet on various factors such as food intake, insulin resistance, energy expenditures, and glucose tolerance (Suleiman et al., 2020) (Lutz & Woods, 2012). In addition to aiding in the understanding of the efficacy of anti-obesity drugs and other therapies in treating obesity and its consequences (Suleiman et al., 2020) (Lutz & Woods, 2012).

DIO animal models are superior to genetically modified models of obesity for studying polygenic diseases because they more closely resemble human obesity, which is a polygenic disease (Lutz & Woods, 2012). Unlike monogenic obesity models, polygenic animal models like DIO mice are representative of human obesity pathogenesis (Nilsson et al., 2012). Multiple dietary factors play an important role in the pathogenesis of human obesity, whereas DIO mouse obesity is affected by the type and content of the diet as well as the strain of mice used (Lutz & Woods, 2012; Nilsson et al., 2012). The most recent diet for constructing a DIO model is a diet high in fat and carbohydrates like sucrose and fructose (Nilsson et al., 2012). There are also some predefined diets of obesity for some strains that could differ in the source of fat and carbohydrates as well as their percentage

of calories leading to distinct phenotypes (Nilsson et al., 2012). DIO mice fed high fat and carbohydrate diets resemble the human diet.

Treatment of DIO mice with anti-obesity drugs, like sibutramine and liraglutide, has shown similar results to those in humans (Nilsson et al., 2012). Sibutramine has been shown to be effective in reducing the food intake (Sharma & Henderson, 2008); it has been shown that sibutramine in DIO rats reduces body weight compared to the placebo used in the study by reducing the food intake (Nilsson et al., 2012). Also, liraglutide drug has been shown to decrease food intake and body weight in DIO rats with a high-fat diet (60%) (Hayes et al., 2011). Moreover, liraglutide decreased energy and body fat intake in DIO mice with 45% of calories from the fat diet (Porter et al., 2010). Therefore, DIO rodents can be used as a valid animal model for indicating the effects noticed in humans while testing for pharmacological drugs that cause a reduction in body weight by affecting the appetite (Nilsson et al., 2012).

The main mechanism by which drugs like sibutramine and liraglutide work on reducing obesity either in humans or animal models is by changing the normal epigenetics in the body.

2.8 Epigenetics

The central dogma of molecular biology involves the transcription of DNA into mRNA, which is then translated into proteins, and it is quite well-established how this process is happening in the human body. However, what is not known now is how genes are regulated and expressed in different behaviors and environments. Epigenetics is a study of stable, inherited factors that interact with genes, affecting the way they are expressed; Epigenetics changes gene expression significantly, but it cannot change the DNA sequence (Al Aboud et

al., 2021). They are mainly molecular factors inherited in mitosis, which regulate the genome's activity and contribute to disease etiology, such as in cancers, cardiovascular, autoimmune diseases, and many other illnesses (Weinhold, 2006).

The mechanisms of epigenetics are involved in the regulation of various cell activities by either repressing or activating gene expression (Weinhold, 2006). Multiple epigenetic mechanisms, such as methylation, ubiquitylation, acetylation, and many others, can alter gene expression. However, the most important epigenetic mechanisms are DNA methylation, histone modification, and non-coding RNAs (Zhang & Pradhan, 2014).

2.8.1 Non-coding RNAs

Non-coding RNAs (ncRNAs) are untranslated RNA molecules, constituting a large proportion of the DNA sequence (Esteller, 2011). Although it is non-coding and does not result in a protein, it has been identified as having a vital functional importance in normal development or disease mechanisms (Esteller, 2011). ncRNAs are classified according to their size as either small ncRNAs of size 19-200 bp or long ncRNAs of more than 200 bp in size (Esteller, 2011). The small ncRNAs consist of microRNAs (miRNAs), PIWI-interacting RNAs (piRNAs), and small nucleolar RNAs (snoRNAs) (Esteller, 2011). On the other hand, long ncRNAs are transcribed into proteins like ultra-conserved regions (T-UCRs) and large intergenic non-coding RNAs (lincRNAs) (Esteller, 2011). The most widely studied ncRNAs are microRNAs.

2.8.2 miRNAs discovery

The discovery of Lin-4 miRNA in 1993 in *Caenorhabditis elegans* (*C. elegans*) by Ambros and Ruvkun caused a revolution in the field of molecular biology (Lee et al., 1993; Wightman et al., 1993). Lin-4 was first thought to be a gene that regulates the development

of *C. elegans* larvae. However, then further studies identified that it is, in fact, a non-coding small RNA that downregulates the lin-14 gene responsible for *C. elegans* larvae development by binding to its 3′ untranslated region (3′ UTR) (O'Brien et al., 2018). Furthermore, since miRNAs have been highly interested in research where they were identified in all animal models, some of which are highly conserved and up to date, new miRNAs are being discovered (O'Brien et al., 2018).

microRNAs are short non-coding small RNA molecules that are 18-25 nucleotides in length and play a significant role in gene expression regulation at the post-transcriptional level by binding to untranslated areas of the gene and affecting the mRNA sequences stability (Landrier et al., 2019; Shi et al., 2016). miRNAs are first transcribed into primary miRNAs (pri-miRNAs) from DNA sequences; thereafter, they are processed into precursor miRNA (pre-miRNAs) and finally into a mature miRNA (O'Brien et al., 2018). Mostly, miRNAs bind to the 3′ UTR of the mRNA and suppress its expression, but binding to other regions like 5′ UTR, the coding sequence or promoters of genes has also been noticed (O'Brien et al., 2018). Furthermore, studies have shown that miRNAs can activate the expression of other genes and can control the translation and transcription rates of multiple genes (O'Brien et al., 2018).

2.8.3 miRNAs biogenesis

miRNAs are first transcribed in the nucleus by polymerase II (pol II) into pri-miRNAs forming a long hairpin loop structure; thereafter, the pri-miRNA is cleaved by the microprocessor complex containing DROSHA and double-stranded RNA binding protein DGCR8 (DiGeorge syndrome critical region 8) into pre-miRNAs of about 60-70 nucleotide (Lin & Gregory, 2015; O'Brien et al., 2018). DROSHA has 2 RNAse III domains, each of which cuts a strand of the pri-miRNA, forming a shorter pre-miRNA with an overhang of 1-

2 nucleotides at the 3' end for transport of the cytoplasm (Lin & Gregory, 2015). The exportin 5 (XPO5) facilities the transport of pre-miRNA from the nucleus to the cytoplasm, where it is picked up by DICER1 that, which is an RNAse enzyme (RIII) cleaves the hairpin loop structure into a short double-stranded miRNA which is the mature miRNA called miRNA: miRNA*duplex (Lin & Gregory, 2015). Transactivation-responsive RNA-binding protein (TRBP) helps DICER1 in the cleavage of pre-miRNA, as well as connects DICER1 with argonaute proteins to help in forming the miRNA-induced silencing complex (miRISC) (Lin & Gregory, 2015). The guide strand of the miRNA remains bound by the argonaute protein and is loaded into the target mRNA for gene suppression by complementary sequence binding (Lin & Gregory, 2015). Gene suppression occurs through the degradation of mRNA by the argonaute protein and repression of the translation through the blocking of ribosomal binding to the mRNA; thus, the target protein will no longer be produced (Lin & Gregory, 2015; O'Brien et al., 2018). Figure 1 shows the biogenesis of miRNA.

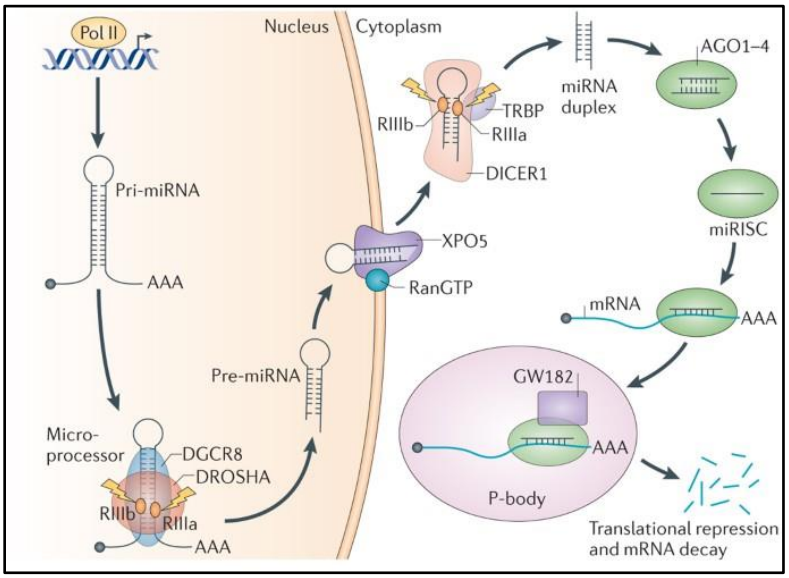

Figure 1:The biogenesis of miRNA (Lin & Gregory, 2015).

2.8.4 Role of miRNA as an epigenetic regulator

miRNAs regulate gene expression and play a role in disease processes (Landrier et al., 2019; Shi et al., 2016). In addition, they can be used as biological biomarkers that help in the early detection of certain diseases, either by being overexpressed or down-expressed. They can be a target of therapy for disease treatment (O'Brien et al., 2018). It has been previously shown that epigenetic regulations control miRNA expression, including RNA modification, DNA methylation, and histone post-translational modifications (Qian Yao et al., 2019). In addition to being regulated by epigenetic mechanisms, miRNAs target histone deacetylases (HDACs), DNA methyltransferases (DNMTs), ten-eleven translocations (TETs), and histone methyltransferases (EZH) enzymes, thereby regulating epigenetic mechanisms (Qian Yao et al., 2019). Furthermore, DNA methylation is regulated by miRNAs, which regulate the expression of DNA methylation enzymes (DNMTs and TETs), affecting the whole methylation profile in the genome (Qian Yao et al., 2019). For example, miR-29b, which belongs to the miR-29 family, works on DNMTs and TETs regulating DNA methylation (Qian Yao et al., 2019). A study has shown that inhibition of miR-29b in the early embryo development of porcine has increased the levels of DNA methylation by DNMT3A/B and TET1 upregulation while downregulating TET2/3 (Zhang et al., 2018).

Moreover, miR-101 has been proven to be complementary to the 3’-UTR of DNMT3A mRNA, and overexpression of miR-101 can inhibit the expression of DNMT3A, thereby suppressing the proliferation of lung cells leading to apoptosis of lung cells (Wang et al., 2017). A study by Xie et al. has suggested that the 3’-UTR regions of DNMT1 mRNA can be targeted by miR-377 as well.

In addition to DNA methyltransferases, histone deacetylases and histone methyltransferases can also be targets of miRNA regulation. Bioinformatics analysis has recognized histone modifications by miRNAs in H3K4me1, H3K27me3, H3K27ac, H3K9ac, H3K4me3, and H2AZ in the process of mammalian spermatogenesis (Taguchi, 2015). For example, miR-34a regulates HDAC1 by binding to the 3'UTR of its mRNA in foam cells, and overexpression of miR-34a decreases expression of HDAC1, leading to increased acetylation of H3K9ac causing abnormal lipid accumulation in foam cells (Zhao et al., 2017). Moreover, miR-138 regulates KDM5B histone demethylase in breast cancer. In patients with breast cancer, overexpression of KDM5B has been noticed. At the same time, there is low expression of miR-138, and restoring the expression of miR-138 reduced KDM5B, inhibiting the proliferation and migration of breast cancer cells (Denis et al., 2016).

All in all, miRNAs regulated by epigenetic regulation can, in reverse, provide epigenetic regulation, thereby providing a closed loop of epigenetic machinery between epigenetic regulators and miRNAs that is not fully understood yet (Qian Yao et al., 2019).

2.8.5 miRNAs and obesity

miRNAs are critical players in pathological conditions, such as obesity, contributing to lipid metabolism (Frost & Olson, 2011; Krützfeldt & Stoffel, 2006) and could act as epigenetic modulators. Additionally, miRNAs are secreted to extracellular fluids, where they act as potential biomarkers for the early detection and diagnosis of diseases or as potential therapeutic targets for other diseases (O'Brien et al., 2018). They also act as a cell-cell communicator by conveying signals from one cell to the other (O'Brien et al., 2018). Many miRNAs are expressed in the white adipose tissue, and it has

been shown in multiple studies that they are related to multiple metabolic factors such as BMI, adipogenesis, glycemia, and leptinemia (Landrier et al., 2019). A study by Heneghan et al. found that expression of miR-17-5p and miR-132 in omental fat and blood differs in obese and non-obese subjects, and they are highly correlated with leptin, BMI, glycated hemoglobin, and fasting blood glucose (Heneghan et al., 2011). Moreover, miR-21 was high in white adipose tissue and positively correlated with BMI for obese subjects than in slim controls (Heneghan et al., 2011). Helge et al. measured the miRNA expression of severely obese individuals before and after a diet for weight loss for 15 weeks. They found a downregulation of miR-20b-5p and an upregulation of miR-29a-3p and miR-29a-5p (Kristensen et al., 2017). Another study identified the upregulation of miR-221 and that it is responsible for fat digestion by tumor necrosis factor-α (TNF-α) and leptin in obese individuals (Meerson et al., 2013). Chartoumpekis et al. study showed that during the development of obesity in mice, upregulation of miR-342-3p, miR-142-3p, miR-142-5p, miR-21, miR-146a, miR-146b, miR-379 and downregulation of miR-122, miR-133b, miR-1, miR-30a, miR-192, and miR-203 occurs (Chartoumpekis et al., 2012).

2.8.6 miRNAs in myogenesis

Some miRNAs are expressed in a tissue-specific manner and named according to their highly expressed tissue (Lagos-Quintana et al., 2002). MyomiRNAs are a class of microRNAs that have been shown to regulate critical genes responsible for muscle development and function, including myogenin, myocyte enhancer factor 2, and myocardin-related transcription factor-A (Ge & Chen, 2011; Harding & Velleman, 2016; Morton et al., 2021). Multiple miRNAs play a role in muscles' myogenesis and regeneration, such as miR-1, miR-133, and miR-206 (Rao Prakash et al., 2006). MiR-1

plays a role in repressing histone deacetylase 4 (HDAC4), promoting differentiation of myoblasts, while miR-133 increases myoblast proliferation by activating serum response factor (SRF) (Chen et al., 2006) (Miano, 2003). On the other hand, miR-206 downregulates Pola 1 subunit of DNA polymerase α, initiating myoblast differentiation (Kim et al., 2006). Additionally, miR-206 indirectly downregulates Id1-3, a DNA-binding protein inhibitor, and myogenic repressor (MyoR), such as MyoD, further regulating myoblast differentiation (Kim et al., 2006). A study by Dey et al. showed that miR-206 and miR-486 promote myoblast differentiation by targeting a paired box transcription factor (Pax7) that usually represses differentiation of myoblasts through negative regulation of MyoD (Dey Bijan et al., 2011). In contrast, miR-23a was shown to target the 3' UTR of myosin-heavy chains 1,2, and 4, inhibiting myoblast differentiation (Li Wang et al., 2012) (Lijun Wang et al., 2012).

Additionally, miR-29 has been suggested in many studies as a regulator of myogenesis. A study by Huating et al. showed repression of miR-29 by Yin Yang 1 (YY1) protein through NF-kB-YY1 pathway activation (Wang et al., 2008). In normal myogenesis, NF-kB and YY1 levels are decreased; however, there is an increased expression of miR-29, this increase of miR-29 could further downregulate YY1 translation through binding to miR-29 binding sites in the 3'UTR of YY1 enhancing myoblast differentiation (Wang et al., 2008). Another study by Wei et al. showed inhibition of myoblast proliferation and enhanced myoblast differentiation by miR-29 through the downregulation of Akt3 (Wei et al., 2013).

De la Garza-Rodea et al. have recently shown that S1P lyase (SPL) can regulate myoblast differentiation by modulating miR-1, miR206, and miR-486 (de la Garza-Rodea

et al., 2014). Both miR-675-3P and miR-675-5P have been found to trigger myogenesis and differentiation of satellite cells (Dey et al., 2014). During skeletal muscle regeneration, miR-675-3P and miR-675-5P target 3'UTR of Cdc6 -initiation factor of DNA replication- and Smads help in the differentiation and regeneration of myoblasts (Dey et al., 2014).

Other miRNAs include miR-27a/b, which both play a role in downregulating myostatin which acts as a myogenesis inhibitor (Huang et al., 2012; McFarlane et al., 2014). McFarlane et al. showed that inhibition of miR-27a/b leads to increased myostatin expression, decreased proliferation of myoblasts, and decreased activation of satellite cells. While overexpression of both miR-27a/b decreased myostatin expression levels, thereby increasing myoblast proliferation and skeletal muscle hypertrophy (McFarlane et al., 2014).

Table 2. 1 miRNA function in myogenesis

Condition	MiRNAs	Function	Reference
Myogenesis	miR-1	Promotes myoblast differentiation and regeneration through HDAC4 downregulation repressing MEF2-activated muscle gene expression.	(Chen et al., 2006) (Miano, 2003) (Rao Prakash et al., 2006)
	miR-23a	Inhibits myoblast differentiation through targeting 3' UTR of myosin heavy chains 1,2 and 4.	(Li Wang et al., 2012)
	miR-27a/b	Downregulates myostatin expression inducing hypertrophy of muscles.	(Huang et al., 2012) (McFarlane et al., 2014)
	miR-29	Represses YY1 protein, enhances myoblast differentiation, and downregulates Akt3 inhibiting muscle proliferation.	(Wang et al., 2008) (Wei et al., 2013)
	miR-133	Negatively regulates SRF enhancing myoblast proliferation.	(Chen et al., 2006) (Miano, 2003)

Condition	MiRNAs	Function	Reference
Myogenesis	miR-206	Targets Pax7 causing myoblast differentiation and regeneration.	(Kim et al., 2006) (Dey Bijan et al., 2011)
	miR675-3p & miR675-5p	Induces satellite cells differentiation and myogenesis in muscle regeneration.	(Dey et al., 2014)

2.8.7 miRNAs and insulin resistance/sensitivity in skeletal muscles

Skeletal muscle accounts for 40-60% of total body weight and 80-90% of glucose uptake by insulin, making it a highly metabolically significant tissue (DeFronzo et al., 1985; Tseng et al., 2010). However, few studies have investigated how insulin resistance impacts skeletal muscle microRNA expression; in fact, various studies have shown the relation between miRNAs and insulin resistance in both in vivo and in vitro insulin resistance models. For example, Zhou et al. discovered that miR-29a is involved in the mechanism of insulin resistance by lowering the levels of GLUT4 transporters in the muscles by targeting PPARδ (Zhou et al., 2016). Furthermore, it was suggested that miR-29a is upregulated in the liver of obese mice, and this was always accompanied by a reduction of phosphoenol pyruvate carboxykinase (PEPCK) inhibition, which is important for gluconeogenesis inhibition by insulin (Zhou et al., 2016). Another study showed that a high-fat diet in mice increased miR-29a expression in muscle cells and disrupted insulin signaling through reduced expression of IRS1 (Pandey et al., 2011). Moreover, miR-135a was upregulated in the skeletal muscle of hyperglycemic db/db mice, and silencing, miR-135a improved glucose tolerance in db/db mice and resolved the hyperglycemic condition (Agarwal et al., 2013). In addition, both miR-24 and miR-126 are significantly upregulated in the skeletal muscles of hyperglycemic Goto-Kakizaki rats compared to normoglycemic Wistar rats (Huang et al., 2009). miR-149, on the other hand, was downregulated in skeletal muscles of DIO C57BL/6J mice, indicating that insulin resistance promotes mitochondrial dysfunction in skeletal muscles

(Mohamed et al., 2014). Finally, the expression of miR-106b was upregulated in a study of C2C12 myotubes with palmitic acid-induced insulin resistance, and silencing miR-106b has retained insulin sensitivity (Y. Zhang et al., 2015).

2.9 Treatment of obesity

Obesity therapies now comprise a balanced nutritional diet of low fat or low carbohydrate consumption or a low fat and carbohydrate intake diet that assures weight loss and exercise (Wirth et al., 2014). Other therapeutical medications that function by either halting the sense of hunger or inhibiting fat absorption by the body, such as orlistat, a weight reduction recommended drug that inhibits the activity of lipase by preventing the digestion of dietary fats in a meal, might also be utilized (Bethesda, 2012; Wirth et al., 2014). Furthermore, bariatric surgery might be performed on severely obese individuals with significant medical issues in whom other weight loss methods have failed (Colquitt et al., 2009). Bariatric surgery refers to a group of surgeries performed in the digestive system to assist people in losing weight, such as gastric bypass, sleeve gastrectomy, and biliopancreatic diversion with a duodenal switch (Colquitt et al., 2009). These procedures either entail decreasing the amount of food consumed by the individual or limiting the amount of nutrients absorbed by the body (Colquitt et al., 2009).

2.10 Sulforaphane

Sulforaphane (SFN), a naturally occurring isothiocyanate compound extracted from cruciferous vegetables such as broccoli and cabbage, acts as an antioxidant, a chemotherapeutic, and an anti-cancerogenic agent (Fan et al., 2012). Several in vitro studies on the obese mouse model have demonstrated that SFN treatment can help resolve and treat obesity (Martins et al., 2018). It has been proven to increase lipolysis, glucose

uptake, oxidative utilization, and up-regulation of the oxidation pathway for fatty acids while repressing triglyceride synthesis and preventing adipocyte differentiation (Martins et al., 2018). Furthermore, SFN has been identified as an inhibitor of adipocyte differentiation by blocking the clonal expansion of 3T3-L1 preadipocytes by the arrest of preadipocytes in the cell cycle (Choi et al., 2014). Furthermore, it also promotes lipolysis by activating lipase and suppresses the NF-κB pathways preventing scar tissue formation (Choi et al., 2014).

Additionally, it inhibits platelet aggregation and blood clots' formation by activating adenylate cyclase and inhibiting PI3-kinase/Akt, p38 MAPK, and PLCγ2-PKC-p47 cascades (Choi et al., 2014). Moreover, SFN interacts with cystine residues of KEAP1, causing the release of Nrf2 to the nucleus and leading to the transcription of antioxidative genes (McWalter et al., 2004). In addition, mice treatment with SFN led to AMPK pathway activation, which plays a role in the energy homeostasis of the cell (Choi et al., 2014). Furthermore, SFN further upregulates the insulin signaling pathway improving glucose intolerance in obese mice (Xu et al., 2018). Hence, SFN supplements for obese patients with type 2 diabetes decreased the fasting blood glucose and HbA1c, marking it as a potential drug for treating diabetes by treating the underlying cause of obesity (Hawley et al., 2002).

According to a recent study conducted in Dr. Nasser's lab, skeletal muscle cells are the primary site of action for SFN in DIO mice (Cakir et al., 2022). This study employed different mice models to prove that SFN can treat obesity (Cakir et al., 2022). They have also shown that SFN, to reverse diet-induced obesity, must have a functioning leptin receptor accompanied by high leptin levels in the blood (Cakir et al., 2022). The

study demonstrated that SFN treatment reduced the body weight of only wild-type DIO mice but not chow-fed wild-type lean, *Lepr db/db*, or leptin-deficient *Lep ob/ob* mice (Cakir et al., 2022). Furthermore, it induced an anorectic response when exogenous leptin was given in wild-type DIO mice as well as chow-fed lean and *Lep ob/ob*, but not in the *Lepr db/db* mice (Cakir et al., 2022). This finding suggests that the SFN can reduce weight upon high levels of leptin circulating in the blood and functional leptin receptor (Cakir et al., 2022). Other observations by this study included a decrease in the body fat mass but not the lean mass. Moreover, the SFN repressed food intake by wild-type DIO mice but not the lean mice (Cakir et al., 2022).

CHAPTER 3: HYPOTHESIS

As the transcription profiling of different tissues following SFN treatment revealed an increase in Nrf2 activity, mainly in the skeletal muscle tissue, this suggests that skeletal muscles are the primary site of action for SFN.

Moreover, SFN increased the antioxidant capacity due to Nrf2 upregulation, which activated additional downstream genes that reduce oxidative stress (Cakir et al., 2022). Furthermore, this increased antioxidant capacity enhanced glucose tolerance and insulin sensitivity (Cakir et al., 2022). Nevertheless, it is unknown how Nrf2 activity in skeletal muscles causes leptin receptor signaling and weight reduction. Hence, we hypothesized that the transcriptional changes occurring are due to the direct SFN action on skeletal muscle tissue affecting the metabolic phenotype and regulation of gene expressions.

CHAPTER 4: OBJECTIVES

The study objectives are as follows

1- To study the miRNA expression profile in the skeletal muscles of SFN-treated DIO mice.

2- To determine the function of miRNAs in the skeletal muscles of DIO mice following SFN treatment. Through their involvement in changing gene expression as upstream regulators, these roles will be detected using bioinformatics methods to pinpoint pathways and gene ontologies involved in the metabolic processes of skeletal muscles.

CHAPTER 5: MATERIALS & METHODS

5.1 Materials

5.1.1 Materials and reagents

miRNeasy Mini Kit for total RNA extraction (catalog number 217084) was supplied by QIAGEN (USA). Agilent (Santa Clara, California) supplied Agilent RNA 6000 Nano Kit (catalog number 5067-1511) and Agilent High sensitivity kit (catalog number 5067-4626). Perkin Elmer (USA) provided kit NEXTFLEX® Small RNA-Seq Kit v3 for Illumina® Platforms (catalog number NOVA-5132-06). KAPA Library Quantification Kit Illumina® Platforms (catalog number KK4824) was provided by kapa Biosystems (UK). Miseq reagent kit v2 (50 cycles) (catalog number MS-102-2001) was provided by illumina (USA)

Table 5. 1 List of kits

Name of kit	**Company**	**Catalogue number**
miRNeasy Mini kit	QIAGEN	217084
Agilent RNA 6000 Nano kit	Agilent	5067-1511
Agilent High sensitivity kit	Agilent	5067-4626

Name of kit	Company	Catalogue number
NEXTFLEX® Small RNA-Seq Kit v3 for Illumina® Platforms	Perkin Elmer	NOVA-5132-06
KAPA Library Quantification Kit Illumina® Platforms	Kapa Biosystems	KK4824
Miseq reagent kit v2 (50 cycles)	Illumina	MS-102-2001

Table 5. 2 List of Instruments

Name of instrument	Company	Catalogue number
2100 Bioanalyzer system	Agilent	G2943CA
Mi-seq Systems	Illumina	SY-411-9001DOC
7500 Fast Real-Time PCR System, laptop	Applied Biosystems	4351106
Veriti™ 96-Well Thermal Cycler	Applied Biosystems	4375786

5.1.2 Ethics statement

All animal procedures were ethically approved by the Institutional Animal Care and Use Committees (IACUC) and Institutional Bio-safety Committee (IBC) at Qatar University, IACUC (1-6/2019-1 and QU-IBC-2021/010.

5.1.3 Animals and treatment

Ten male mice of CD1 strain were used in the study. After two weeks of acclimatization, CD1 mice were randomized at age four weeks and fed a high-fat diet (with 60% fat for 16-20 weeks) to induce diet-induced obesity (DIO). To evaluate SFN's potential as an anti-obesity medication, 5 CD1-DIO were given 5mg/kg body weight

intraperitoneally for 28 days, one hour before the dark cycle. SFN was dissolved in a cocktail of 50% Polyethylene glycol (PEG), 30% Phosphate buffered saline (PBS), and 20% Dimethyl sulfoxide (DMSO). The other five mice were treated with an equal volume of 25 ul of the cocktail solution as the vehicle/control.

5.1.4 Samples collection and blood measurement

After 21 days, a glucose tolerance test was performed as described below and three days following, an insulin tolerance test was performed on all mice as published (cakier 2022).

Finally, after four weeks, all were decapitated, and skeletal muscle tissue was cut, frozen in liquid nitrogen, then stored at -70^{0}C and used for total RNA extraction. Blood samples were collected, and plasma was used for biochemical assays such as glucose and insulin.

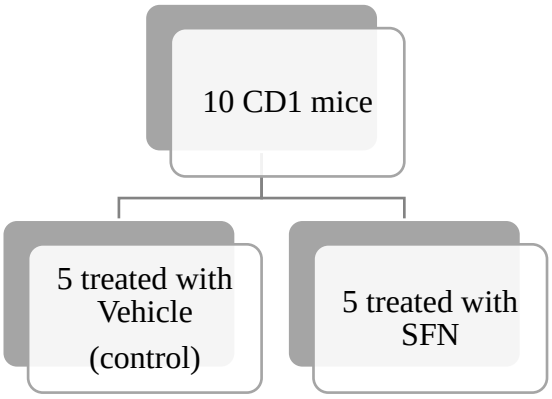

Figure 2: Classification of animals.

5.1.5 Glucose tolerance test (GTT) and Insulin tolerance test (ITT)

On day 21 of injection, GTT was performed, and three days later, ITT was performed to evaluate the effect of SFN on glucose uptake and the whole body's response to insulin action. GTT is used to identify the ability of the body to manage

glucose upload of a standardized quantity of glucose (Eyth et al., 2022). The test shows either normal, impaired, or abnormal glucose tolerance and helps diagnose different types of diabetes (Eyth et al., 2022). On the other hand, ITT is used to evaluate insulin sensitivity in the body by measuring glucose levels in the blood before and after insulin injection (Okita et al., 2014). In each group, animals were further exposed to glucose tolerance testing (GTT) and insulin tolerance testing (ITT). For GTT, mice were given an intraperitoneal injection of glucose (1 g/kg body weight), and blood samples were collected from the tail vein immediately before, and 15, 30, 60, 90, and 120 min after glucose administration, blood glucose levels were measured with glucose reagent strip using Accu-check glucometer. For ITT, the animals were fasted for 4 hours prior to an intraperitoneal injection of insulin (1 U/kg body weight). Blood samples were withdrawn from the tail vein at 0,15,30,60 and 120 min post-injection (Cakir et al., 2022).

5.2 Methodology

5.2.1 Total RNA Extraction

Total RNA was extracted from skeletal muscle cells of DIO mice treated with SFN and DIO control mice using miRNeasy Mini Kit from Qiagen according to the manufacturer's protocol. A piece of skeletal muscle tissue was cut and weighed, ensuring the weight of the tissue was between 30- 50mg as recommended by the protocol. Thereafter tissue was directly placed into 700 µl QIAzol Lysis Reagent in a 1.5ml Eppendorf tube; then, it was immediately homogenized using a homogenizer for 1 minute, and each sample was checked for sufficient homogenization. Samples were then left for 5 minutes at room temperature to enable the separation of nucleoprotein complexes. 140 µl of chloroform was added to the sample, mixed well, and placed for 3 minutes at room

temperature. Afterward, samples were placed in a centrifuge for 15 minutes at 12,000 x g at 4°C. after 15 minutes, and the sample was separated into 3 phases; the first was a colorless phase with the required RNA, an interphase white in color and another pink organic phase. 300-350 µl of the first aqueous, colorless phase was transferred to a separate 1.5ml collection tube without disturbing or transferring any of the lower layers. Then 100% ethanol was added as a 1.5X the volume of the aqueous phase (usually a 525 µl for 350 µl) and mixed well. A 700 µl of the sample is pipetted into a RNeasy Mini spin column in a 2 ml collection tube and then centrifuged at ≥8000 x g (≥10,000 rpm) for 1 minute at room temperature, the resulting flowthrough is then discarded, and the same step is repeated with any remaining volume of the sample. A DNase digestion is conducted where 350 µl of RWT buffer was added and centrifuged for 1 minute at ≥8000 x g (≥10,000 rpm) for washing. Thereafter, 10 µl of DNase I stock and 70 µl RDD buffer are added to each sample, mixed, and then incubated for 15 minutes at room temperature (20-30°C). A 350 µl of RWT buffer is added to the samples and centrifuged ≥8000 x g (≥10,000 rpm) for 1 minute. A 500 µl of RPE buffer was added for washing and centrifuged for 1 minute at ≥8000 x g (≥10,000 rpm); another wash step was done to ensure high-quality RNA extraction. At last, 2-minute centrifugation is done to ensure the complete removal of ethanol. Lastly, the RNA is eluted into a new 1.5 ml collection tube using 50 µl RNase-free water and centrifuge for 1 min at ≥8000 x g (≥10,000 rpm). The quality of the total RNA extracted was measured using the Qubit RNA integrity and quality kit.

5.2.2 Total RNA quality and quantity

The quality and quantity of total RNA were measured using 2100 Agilent bioanalyzer before library preparation with RNA 6000 Nano kit to ensure good quality and quantity of the samples to be sequenced and avoid degraded RNA, which poses complexity to library preparations and sample analysis. The Agilent Bioanalyzer instrument is an automated capillary electrophoresis tool that implements gel electrophoresis to assess samples' quality, quantity, size, integrity, and purity. It generates a report which includes an electropherogram, RNA integrity number (RIN), and RNA concentration. RIN is a scale of the integrity of RNA samples showing a range between 0 to 10, where 0 represents degraded RNA sample and 10 represents highly intact RNA sample. All samples' RIN number was higher than five. Up to date, it is not clear what level of RNA degradation is acceptable for miRNA profiling experiments, but recommendations have suggested that an RNA integrity range from 3.95-8 RIN values should be acceptable depending on the method of analysis (Becker et al., 2010; Ibberson et al., 2009; Imbeaud et al., 2005; Weis et al., 2007).

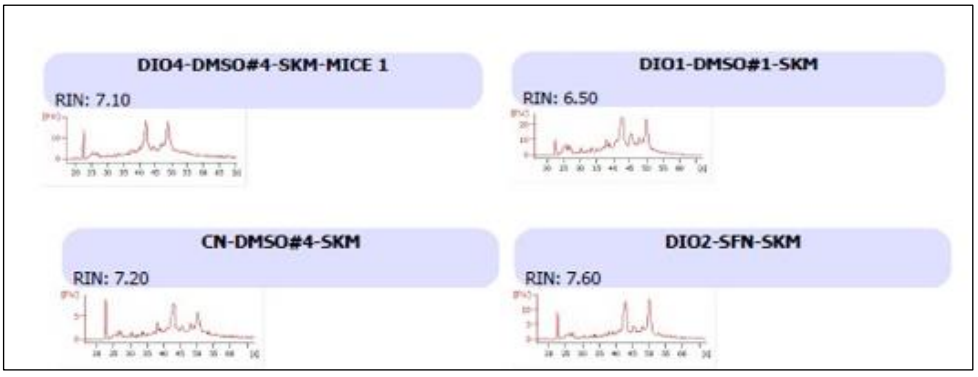

Figure 3: 2100 Agilent Bioanalyzer total RNA quality.

The figure shows total RNA samples quality results prior to library construction depending on the RIN value.

5.2.3 Library preparation and sequencing

The kit used is NEXTFLEX® Small RNA-Seq Kit v3 to prepare libraries of small RNA either from total RNA or pure small RNA. In this project, total RNA samples were utilized. Before sRNA library preparations, samples are normalized for NGS library preparation as 1 µg total RNA in 10.5 µL total volume from each sample. After that, 3' and 5' adapters are ligated to both ends of the sRNA sample -which provide annealing sites for reverse transcription, PCR, and high throughput sequencing primers. The next step is first-strand synthesis by reverse transcription, followed by barcoding, wherein a distinct sequence of 6 nucleotides is assigned to each sample to allow for their differentiation in data analysis. Finally, 15 cycles of amplification and size selection resulted in a library with an approximate size of 150bp. A simplified flowchart of sRNA library preparation is shown in Figure (3).

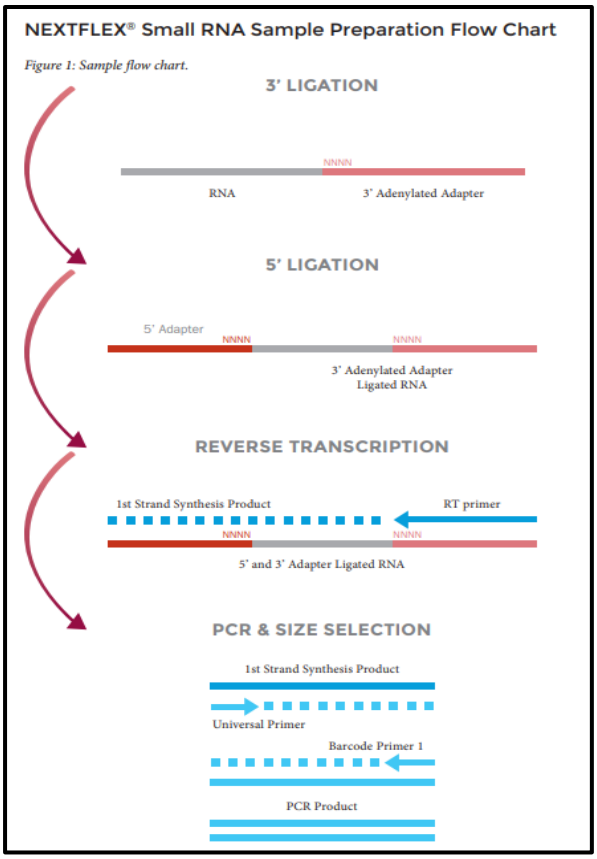

From NEXTFLEX® Small RNA sample preparation protocol

Figure 4: sRNA library preparation flowchart.

5.2.4 Evaluation of sRNA library construction

Evaluation of library construction was successful prior to sequencing. Following library preparation, the quality of the library was checked on 2100 Agilent bioanalyzer with Agilent high sensitivity kit where the presence of a peak at 150 bp indicates a successful library construction. According to the NEXTFLEX® Small RNA-Seq Kit v3 protocol, control from the kit must be run along with the samples as a positive control. We can see in figure 4-D that the miRNA positive control library is successfully constructed.

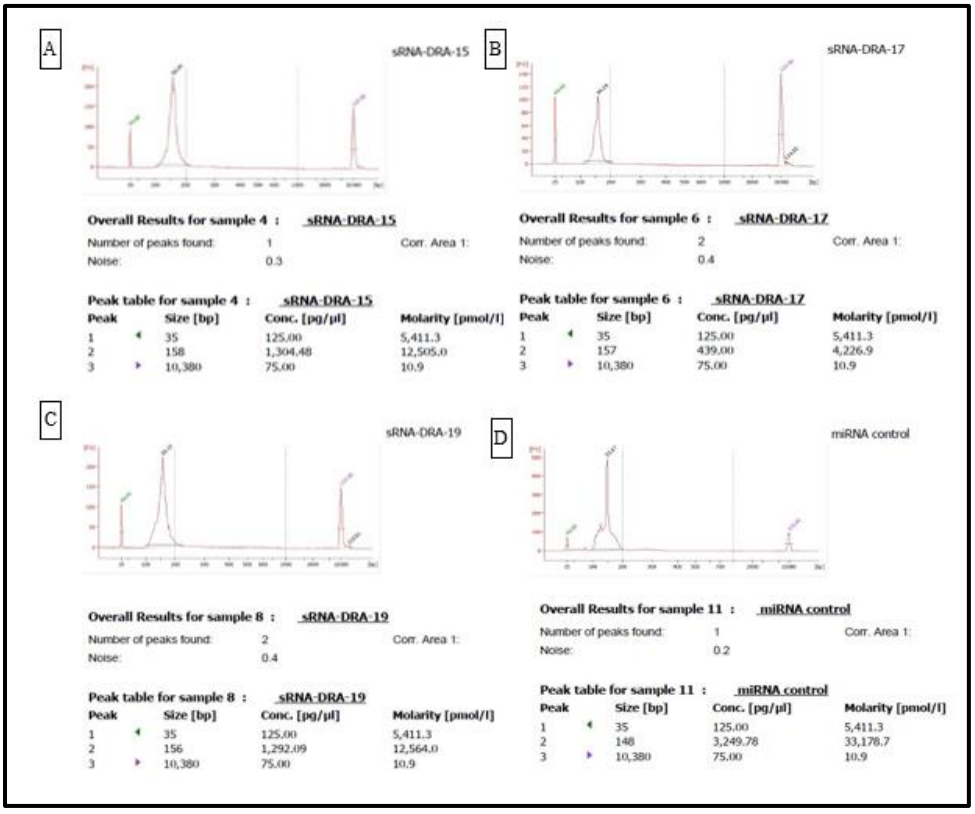

Figure 5: 2100 Agilent Bioanalyzer library validation.

The figure shows the results of library construction by 2100 Agilent bioanalyzer for samples and control prior to sequencing. A, B, and C show three different sample library results, while D shows the kit miRNA control ran along with the samples as a reference.

5.2.5 Library sequencing

Prior to sequencing, the quality of libraries was checked on Agilent Bioanalyzer High sensitivity kit and quantified by qPCR using KAPA Library Quantification Kits for Illumina® platforms on 7500 Fast Real-Time PCR System to avoid over clustering. Moreover, to avoid bias in sequencing, all samples were normalized to 2nM to ensure each of the 29 samples had an equal representation of the reads; then, samples were pooled equally to a final pool with a total volume of 10 µL. Afterward, the pool was denatured and spiked with 1% PhiX, which acts as a control for Illumina sequencing runs.

5.2.6 Data Analysis

5.2.6.1 Bioinformatic analysis

Different bioinformatic analysis software was used to assess miRNA sequence, as shown in the workflow in figure (5). They include FastQC software, which was used to assess the quality of the sequence, Bowtie 2 for reads alignment for analyzing the data, Partek E/M software, v10.0 (Partek Inc. (2020). Partek® Flow® (Version 10.0) [Computer software]. https://www.partek.com/partek-flow/)-, was used for differential gene expression analysis or Gene-specific analysis. Moreover, miRDB (http://mirdb.org/miRDB/), an online miRNA database utilized for target prediction and functional annotation (Chen & Wang, 2020), was used to identify potential target genes. Additionally, gene ontology (GO) and KEGG pathway analysis were employed to find target genes of differentially expressed miRNAs and related pathways (Partek E/M software, v10.0). Using Partek® Flow® software, Fisher's exact p-value ($p<0.05$) was calculated to judge whether the observed difference was significant for differentially expressed miRNA, and the cutoff value for the adjusted p-value was 0.05. The -2-fold change to 2 was selected.

5.2.6.2 Statistical analysis

Figures were constructed using Microsoft Excel 2016 (Microsoft Corp., Redmond, WA) and GraphPad prism 9 (GraphPad Software, Inc.), where the data in figures represents the mean ± standard deviation of the mean (SD) for different mice used in the study unless mentioned otherwise. An appropriate unpaired T-test was used for all analyses to compare the two study groups; SFN-treated and vehicle-treated DIO mice. A two-tailed P-value ≤0.05 is considered significant and rejects the null hypothesis.

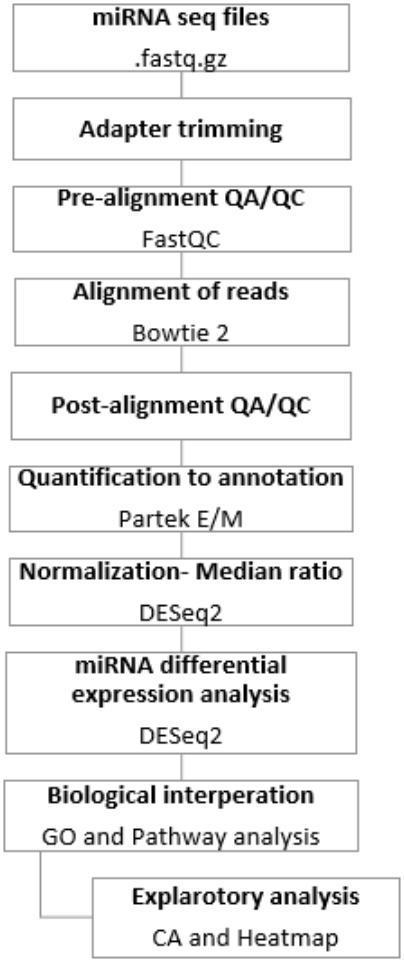

Figure 6: Data analysis workflow.

CHAPTER 6: RESULTS

6.1 Effect of SFN treatment on body weight (BW) and food intake (FI) for CD1-DIO mice

As shown in table 6.1 and figure (7A), treatment with SFN causes a significant decrease in the final body weight (43.57±4.06g) of DIO-SFN compared to DIO-Vehicle with final body weight (52.63±2.31g) and P= 0.001. Unlike the initial body weight in both groups, no significant difference was observed p= 0.64. Moreover, there was a significant difference in the daily food intake during the treatment period between the two groups with DIO-SFN mean (2.55±0.49g), and DIO-Vehicle mean (3.05±0.51g) and p= 0.006 shown in figure (7B).

These results indicate that SFN treatment has contributed to lowering body weight and decreasing food intake in CD1-DIO mice compared to the control. Furthermore, table 6.1 shows that SFN-treated DIO mice significantly reduced plasma glucose and leptin (Fig.8 and Fig.9A) with p= 0.046 and 0.031, respectively. On the other hand, though insulin tends to decrease in response to SFN, it did not reach a significant value, with p= 0.269.

Table 6. 1 Summarizes Body weight, food intake, blood glucose, and plasma insulin levels in the two groups of diet-induced obese [DIO] male CD1 mice.

Phenotype CD1 mice	DIO-SFN	DIO-Vehicle	P-value
Initial body weight (gm)	51.45±3.27	50.77±3.01	0.64
Final body weight (gm)	43.57±4.07	52.67±2.31	0.0016
Food intake (gm)/day	2.55±0.49	3.05±0.51	0.006
Plasma glucose (mg/dl)	244.5±85.9	282.3±71.5	0.046
Plasma glucose (ng/ml)	99.5±36.83	131.97±35.4	0.269
Plasma leptin ng/ml	4.23±2.08	8.11±2.94	0.031

Data are presented as mean ±SD. A two-tailed P value is significant at ≤0.05.

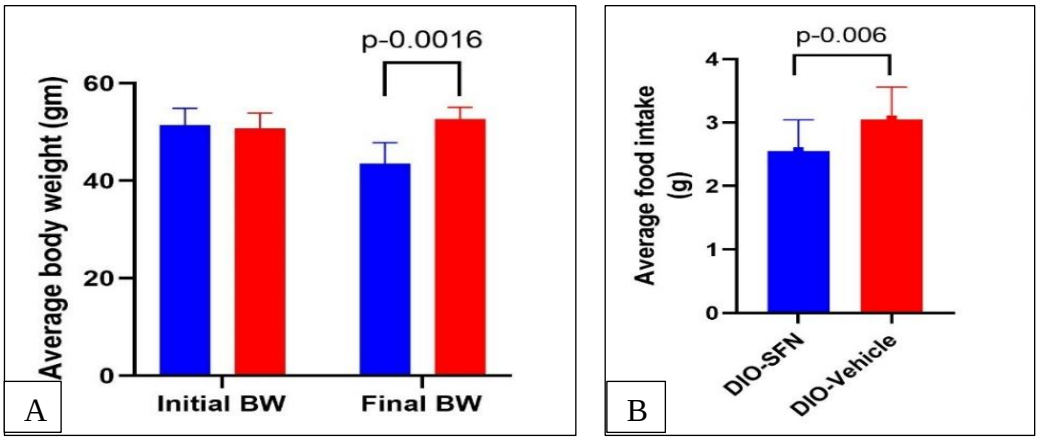

Figure 7: Body weights (BW) and food intake change of DIO mice treated with SFN (n=5) and vehicle (n=5). 7A: Bars represent the mean and SD of the initial and final body weight of DIO mice vehicle (control) groups, and CD1-DIO SFN treated mice. 7B: Daily food intake for DIO mice vehicle (control), and CD1-DIO SFN treated groups. A two-tailed p-value is significant ≤0.05.

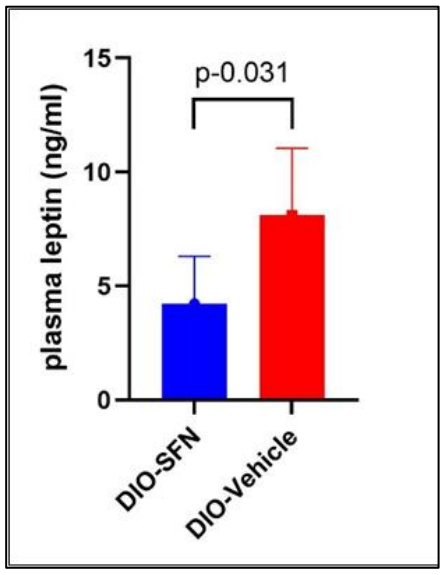

Figure 8: Change in Plasma leptin levels in response to SFN treatment.

Bars represent the mean and SD of plasma leptin measurement for DIO mice treated with SFN (n=5) and vehicle (n=5). A two-tailed p-value is significant ≤0.05.

6.2 Effect of SFN on glucose tolerance test (GTT) and insulin tolerance test (ITT)

After three weeks of treatment by SFN, a glucose tolerance test was performed on both groups of DIO mice. In short, glucose was injected after 6 hours of fasting (1g/kg/BW) via Ip route, and blood was collected via the tail vein at different time points; 0,30,60,90 and 120 minutes, and glucose was measured using an Accu-check glucometer analyzer as shown in figure (9A). The GTT test aimed to determine whether SFN increases glucose uptake by skeletal muscles. Moreover, the ITT test was used to determine whether SFN has an impact on insulin resistance in the body. Following intraperitoneal insulin injection at 0,15,30,60 and 120 minutes, blood glucose levels were measured from tail vein samples. The results are shown in figure (9B). The significant decrease in plasma glucose levels shows that treatment of SFN in obese mice causes increased glucose uptake by peripheral tissue like skeletal muscles, which indicates an improvement of insulin resistance in the muscles.

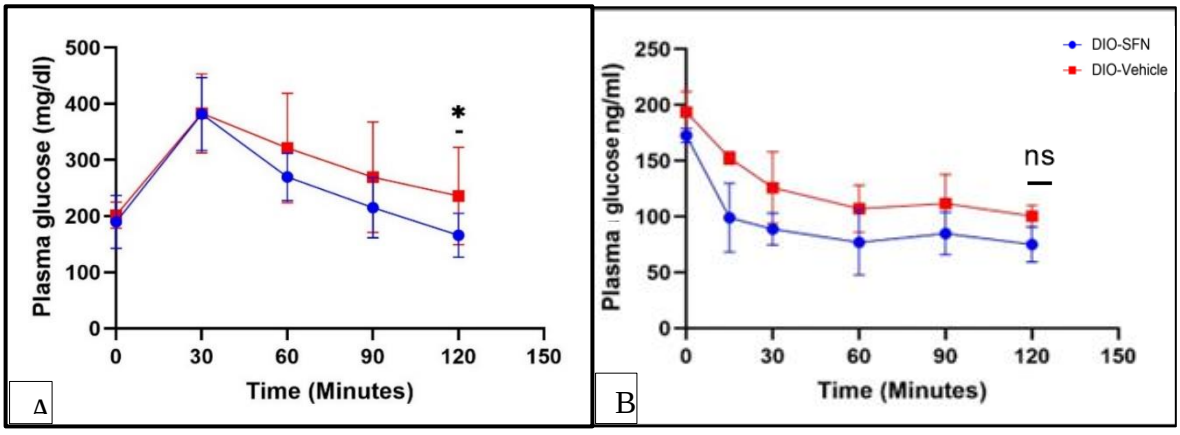

Figure 9: Changes in plasma glucose and insulin levels at different time points throughout the ITT & GTT test between DIO-SFN and DIO-Vehicle groups.

9A: Curve showing GTT in DIO mice treated with SFN versus DIO mice treated with vehicle as control. The X-axis shows the time points in minutes, while the Y-axis shows blood glucose levels (mg/dl). * P value ≤0.05 is significant between both groups.

9B: Curve showing insulin tolerance test (ITT) in DIO mice treated with SFN versus DIO mice treated with vehicle as control. The X-axis shows the time points in minutes, while the Y-axis shows plasma insulin levels (ng/dl). With no significance between groups. A two-tailed p-value is significant ≤0.05.

6.3 Assessment of the quality of microRNA sequencing

Before sequence results analysis, the quality of the run was evaluated by checking the read quality and removing poor-quality reads that could occur due to sequencing errors. Then, using Partek flow software, we evaluated the sequencing quality and GC content, as shown in the appendix (supplementary table 1). The most critical parameter for determining the quality of the run is base calling accuracy, measured by Phred quality score (Q score), which indicates the chance that a base is called incorrectly by the sequencer.

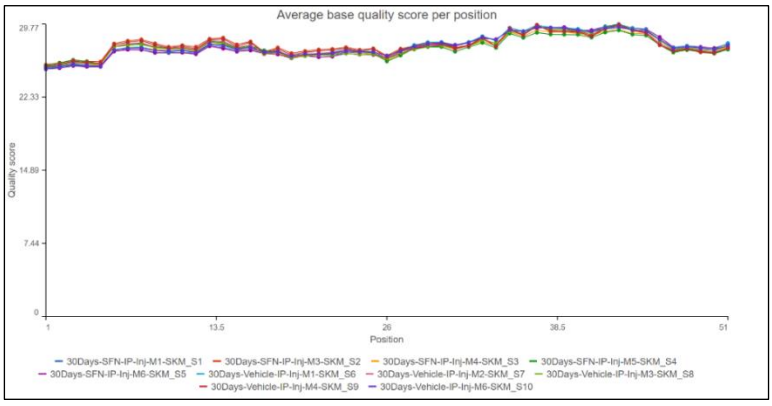

Figure 10: Average Q score post alignment for CD1 samples.

As shown in figure 10, the average Q score of all bases was measured using Phred +33, and it did not go below Q20, which indicates a 99% accuracy of the base calling during sequencing.

6.3.1 Alignment, distribution, and quantification of mature miRNA

After checking the quality of the sequencing run, samples were aligned using Bowtie 2 to a reference genome (mm10 - miRBase mature microRNAs version 22), and quantification was performed to identify mapped reads to each gene. As shown in Table 6.2, we have an average of 29.88% of reads for all CD1 samples found within a miRNA region, while the rest is either partly within a miRNA or not part of a miRNA. Furthermore, figure (S2) in the appendix shows the distribution of raw counts of each sample quantified to mm10. The samples' mean, Q1, and Q3 distribution values after normalization are shown in table S3 in the appendix. PCA was provided in supplementary figure (S1) and was 18% among the treatment group with SFN and 16% among the vehicle-treated group, totaling 48%. A Heatmap cluster was provided to explain the analysis's variation, which reflects biological variability among the DIO mice studied.

Table 6. 2: Distribution of raw count reads for each sample.

Sample name	Total reads	Fully within a microRNA	Partly within a microRNA	Not in a microRNA
30Days-SFN-IP-Inj-M1-SKM_S1	141926	17.76%	0.68%	81.55%
30Days-SFN-IP-Inj-M3-SKM_S2	280527	39.97%	1.55%	58.49%
30Days-SFN-IP-Inj-M4-SKM_S3	131788	25.40%	0.98%	73.63%
30Days-SFN-IP-Inj-M5-SKM_S4	172095	31.41%	1.18%	67.41%
30Days-SFN-IP-Inj-M6-SKM_S5	154856	16.35%	0.61%	83.03%
30Days-Vehicle-IP-Inj-M1-SKM_S6	161187	28.12%	1.05%	70.83%
30Days-Vehicle-IP-Inj-M2-SKM_S7	180546	38.99%	1.60%	59.41%
30Days-Vehicle-IP-Inj-M3-SKM_S8	129008	26.66%	1.07%	72.27%
30Days-Vehicle-IP-Inj-M4-SKM_S9	133863	44.03%	1.66%	54.31%

Sample name	Total reads	Fully within a microRNA	Partly within a microRNA	Not in a microRNA
30Days-Vehicle-IP-Inj-M6-SKM_S10	141070	19.03%	0.68%	80.29%
Average	162686.6	29.88%	1.15%	68.97%

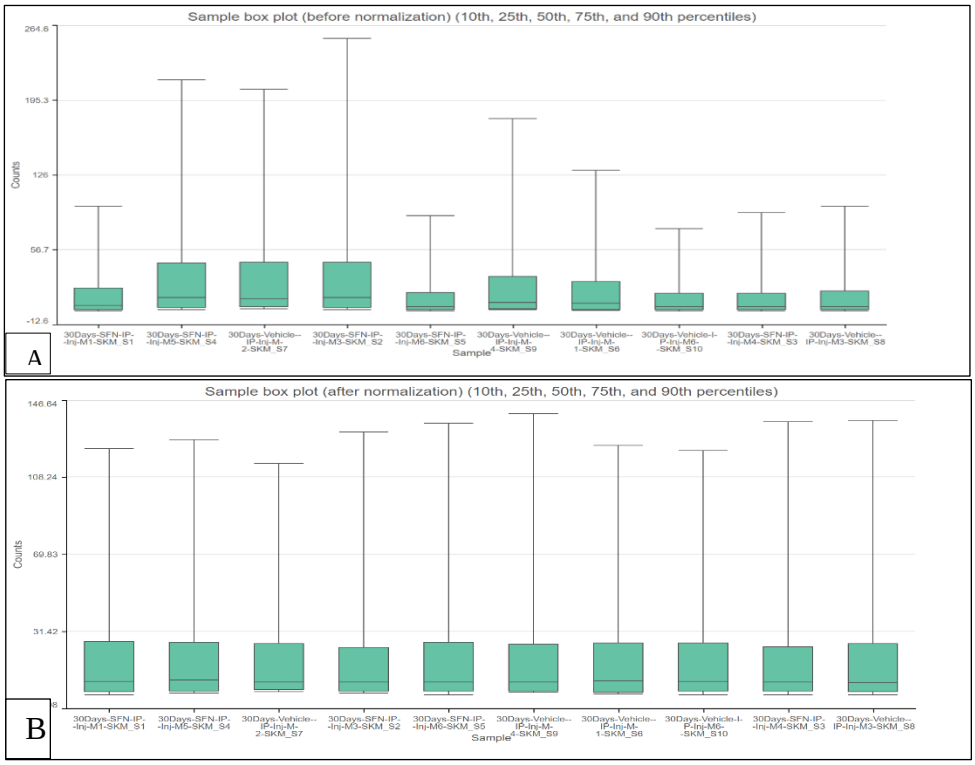

Figure 11: Read count distribution box plot.

As shown in figure 11, the box plot bars show median values and interquartile of the read count distribution of each sample before normalization (A) and after normalization (B). DEseq2 software was used to normalize the reads based on their median value after removing any differences between samples' reads that could have resulted from possible differences in sequencing depth. After normalization, all samples' medians equalized, balancing the reads across all samples.

6.3.2 microRNA expression profiling in skeletal muscle of CD1-DIO mice treated with SFN

To assess whether microRNA expression profiles were affected by SFN as an anti-obesity treatment in the skeletal muscle of DIO mice, we examined the expression profiles of mature microRNAs in the skeletal muscles of the SFN and vehicle-treated control mice. Following mapping, alignments process, and normalization of small RNA seq data, eight mice microRNAs were differentially expressed between the two groups of mice, in which three microRNAs were down-regulated, and five microRNAs were up-regulated in DIO mice treated with SFN (Figure 13, Table 5.3) based on fold regulation of ±2 and FDR of 0.05. Moreover, an appendix provides a supplementary table of all expressed mature miRNAs for both groups.

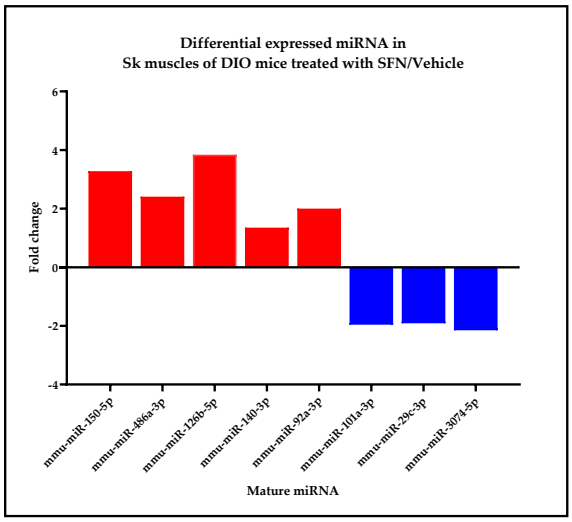

Figure 12: Distribution of differentially expressed miRNAs in DIO mice treated with SFN compared to DIO vehicle/control mice.

Bars show the most significant differentially expressed mature miRNAs in Skeletal muscles in response to SFN with fold change ±2. The red color indicates upregulated miRNA, and the blue color indicates downregulated miRNA expressions.

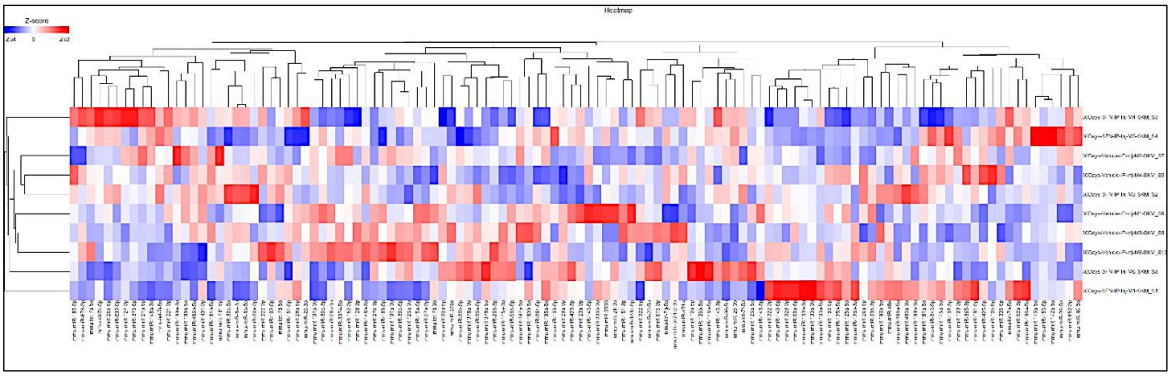

Figure 13: Heatmap of all miRNAs in response to SFN and vehicle treatment in skeletal muscle of DIO mice. The red color indicates upregulated miRNA, and the blue color indicates downregulated miRNA expressions.

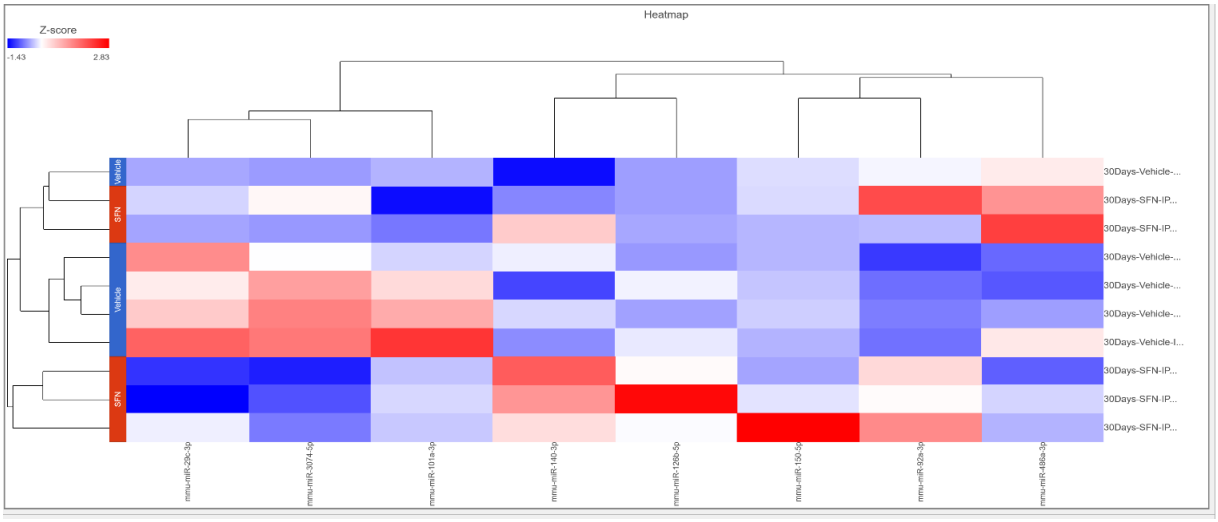

Figure 14: Heatmap of significantly expressed miRNAs in response to SFN in skeletal muscle of DIO mice. Shows the significantly up and downregulated miRNAs in response to SFN treatment in CD1-DIO mice from both DIO-SFN and DIO-Vehicle groups. Blue indicates downregulated

miRNAs, red indicates upregulated miRNAs, and grey or white means no change. Color intensity indicates the z-score of changes in expression.

Table 6. 3: Significant miRNAs in SMs of CD1-DIO mice in response to SFN.

microRNA ID	P-value (SFN vs. Vehicle)	FDR step up (SFN vs. Vehicle)	Ratio (SFN vs. Vehicle)	Fold change (SFN vs. Vehicle)	LSMean (SFN) (SFN vs. Vehicle)	LSMean (Vehicle) (SFN vs. Vehicle)	direction
mmu-miR-150-5p	1.20^{E-13}	1.40^{E-11}	3.28	3.28	2.95	9.01	up
mmu-miR-486a-3p	4.00^{E-09}	2.34^{E-07}	2.41	2.41	2.77	1.15	up
mmu-miR-101a-3p	1.09^{E-08}	4.24^{E-07}	5.10^{E-01}	-1.96	2.30	4.52	down
mmu-miR-126b-5p	1.72^{E-03}	5.03^{E-02}	3.84	3.84	4.78	1.25	up
mmu-miR-140-3p	2.63^{E-03}	5.25^{E-02}	1.35	1.35	4.33	3.22	up
mmu-miR-29c-3p	2.96^{E-03}	5.25^{E-02}	5.25^{E-01}	-1.91	6.09	1.16	down
mmu-miR-92a-3p	3.52^{E-03}	5.25^{E-02}	2.00	2.00	2.79	1.40	up
mmu-miR-3074-5p	3.59^{E-03}	5.25^{E-02}	4.65^{E-01}	-2.15	2.25	4.85	down

LS mean= least squares method is a statistical procedure to find the best fit for a set of data points by minimizing the sum of the offsets or residuals of points from the plotted curve

6.3.3 Target gene prediction, GO, and pathway mapping analysis

We used a pathway enrichment analysis with different web-based applications to identify each miRNA's predicted target genes and the biological pathways overrepresented by the identified differentially expressed miRNAs. Then, by using the GO approach and KEGG pathways, we identified important biological processes and pathways primarily associated with the dysregulated miRNAs; we used the pathway mapping tools to identify the biological pathways of the target genes. The findings revealed a wide range of biological functions linked to the target

genes. For example, GO:0015631 for tubulin binding and GO:0015629 for actin cytoskeleton had 66, and 40 annotated genes from 8 differentially expressed miRNAs found in the study. The top 15 primary gene ontologies are related to cellular metabolism, transcription control, and intracellular signaling are shown in table 6.4. As for the pathway analysis, we can see that the metabolic and inflammatory pathways related to skeletal muscle metabolism associated with obesity, like MAPK signaling pathway (mmu 04010) and PI3K-Akt signaling pathway (mmu 04151), are significantly overrepresented in the SFN-treated CD1-DIO mice. Moreover, the insulin resistance and signaling pathways revealed the list of genes in response to SFN caused by dysregulated miRNA, which reflected changes in phenotypes as evident by improvement of glucose tolerance and insulin resistance as phenotypic changes.

Table 6. 4: Gene ontology (GO) of all dysregulated miRNAs.

Gene set	Description	Enrichment score	P-value
GO:0061470	T follicular helper cell differentiation	8.63191	0.000178
GO:0043559	insulin binding	7.74262	0.000434
GO:0017046	peptide hormone binding	7.63861	0.000481
GO:0016864	intramolecular oxidoreductase activity, transposing S-S bonds	7.01293	0.0009
GO:0003756	protein disulfide isomerase activity	7.01293	0.0009
GO:0098978	glutamatergic synapse	6.88898	0.001019
GO:0051389	inactivation of MAPKK activity	6.65789	0.001284
GO:0008286	insulin receptor signaling pathway	6.63523	0.001313
GO:0016860	intramolecular oxidoreductase activity	6.57325	0.001397
GO:0071863	regulation of cell proliferation in bone marrow	6.5437	0.001439
GO:0071864	positive regulation of cell proliferation in bone marrow	6.5437	0.001439
GO:1905244	regulation of modification of synaptic structure	6.42322	0.001623
GO:0070840	dynein complex binding	6.16395	0.002104
GO:0045934	negative regulation of nucleobase-containing compound metabolic process	6.15699	0.002119

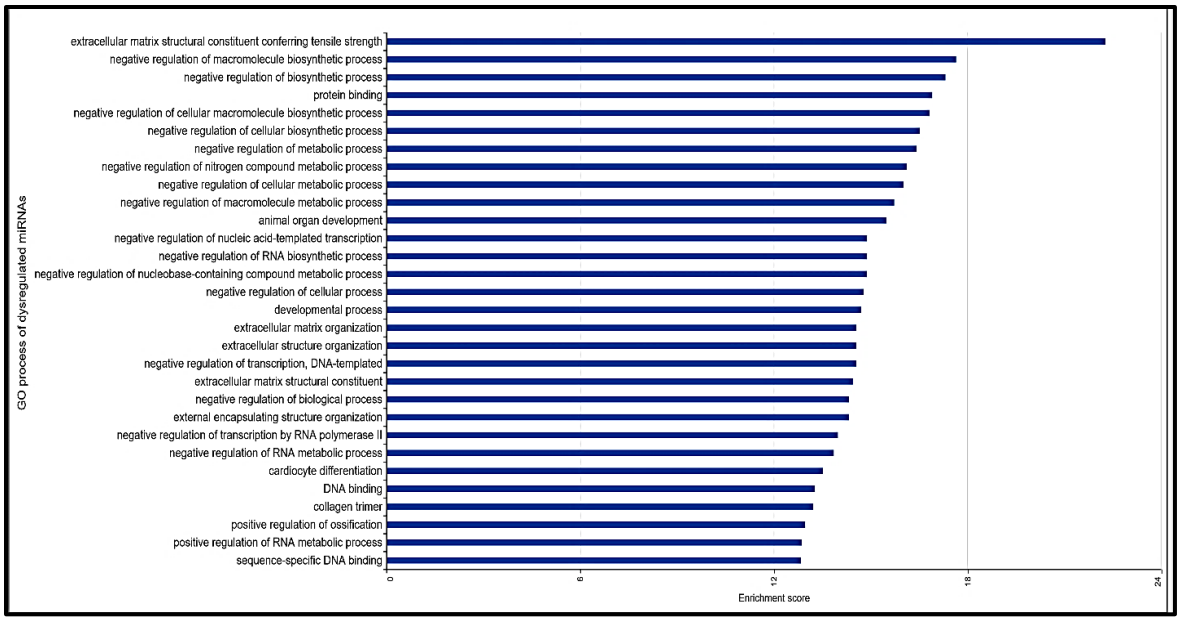

Figure 15: Gene ontology (GO) enrichment analysis of all dysregulated miRNAs.

Functional enrichment analysis of all dysregulated miRNAs in response to SFN: GO enrichment analysis shows GO of the target genes based on cellular component, biological process, and molecular function. The X-axis displays the enrichment score; Y-axis indicates GO terms.

Table 6. 5: Significant KEGG pathways related to muscle metabolism.

Gene set	Description	Enrichment score	P-value
path: mmu 04010	MAPK signaling pathway	5.60755	0.00367
path: mmu 04910	Insulin signaling pathway	5.37476	0.004632
path: mmu 04151	PI3K-Akt signaling pathway	5.28327	0.005076
path: mmu 04931	Insulin resistance	4.48917	0.01123
path: mmu 04668	TNF signaling pathway	3.69996	0.024725
path: mmu 04933	AGE-RAGE signaling pathway in diabetic complications	3.48577	0.03063

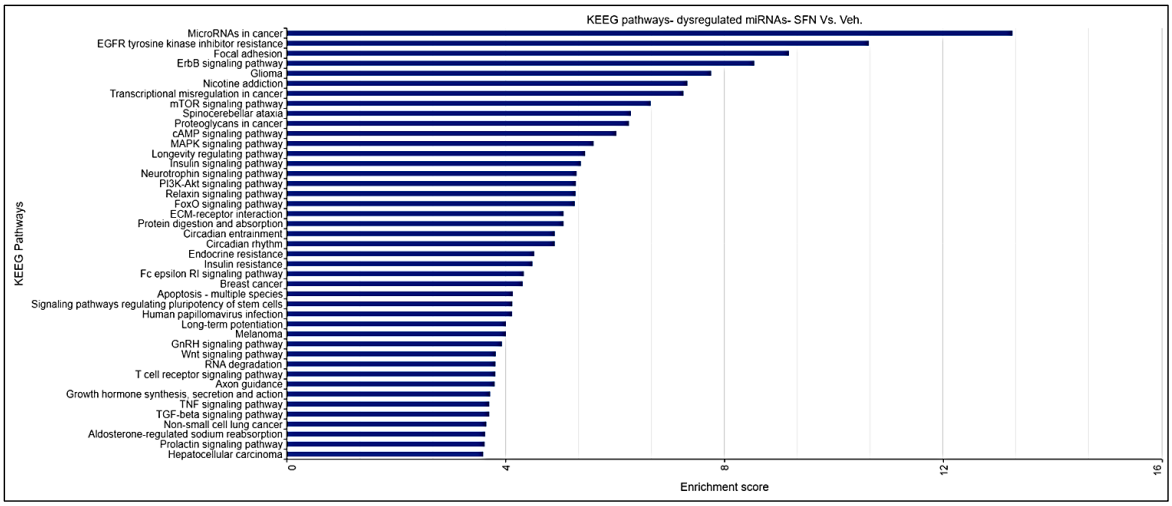

Figure 16: KEGG pathways enrichment analysis of all dysregulated miRNAs.

Enrichment scores of KEGG pathway enrichment analysis. The X-axis displays the enrichment score; Y-axis indicates KEGG pathway. The higher the enrichment score, the more represented the KEGG pathway as a bar length.

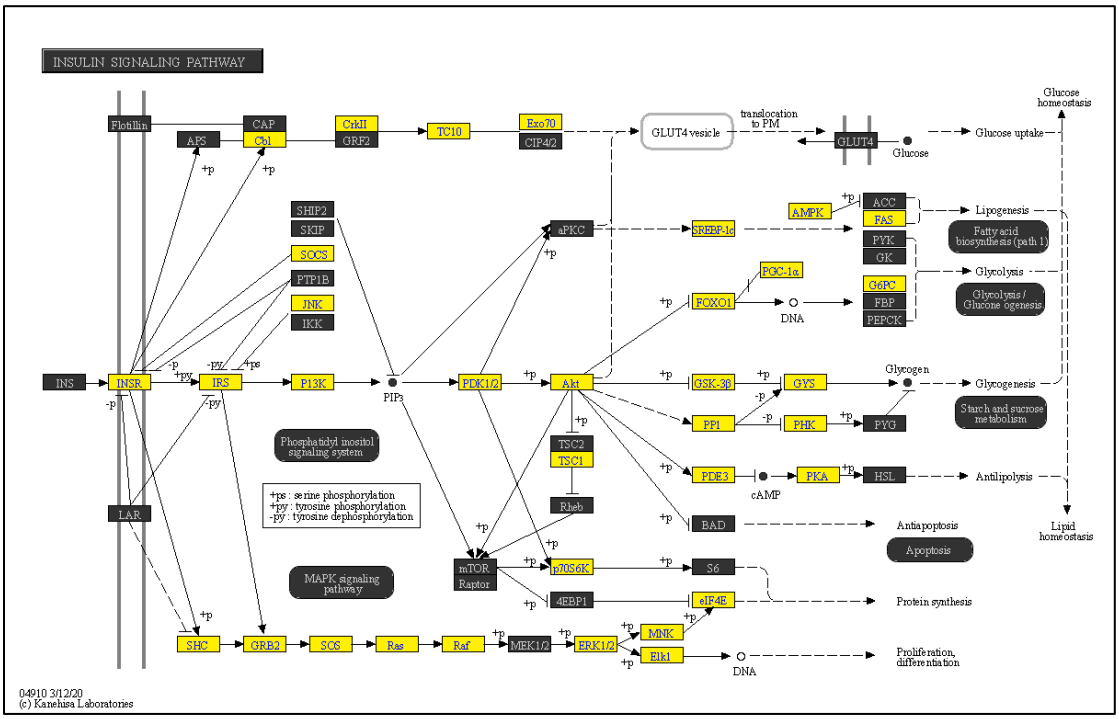

Figure 17: Insulin signaling pathway.

The diagram generated by partek flow software shows genes controlled by all dysregulated miRNAs identified in this study. The figure will be explained in more detail in the discussion.

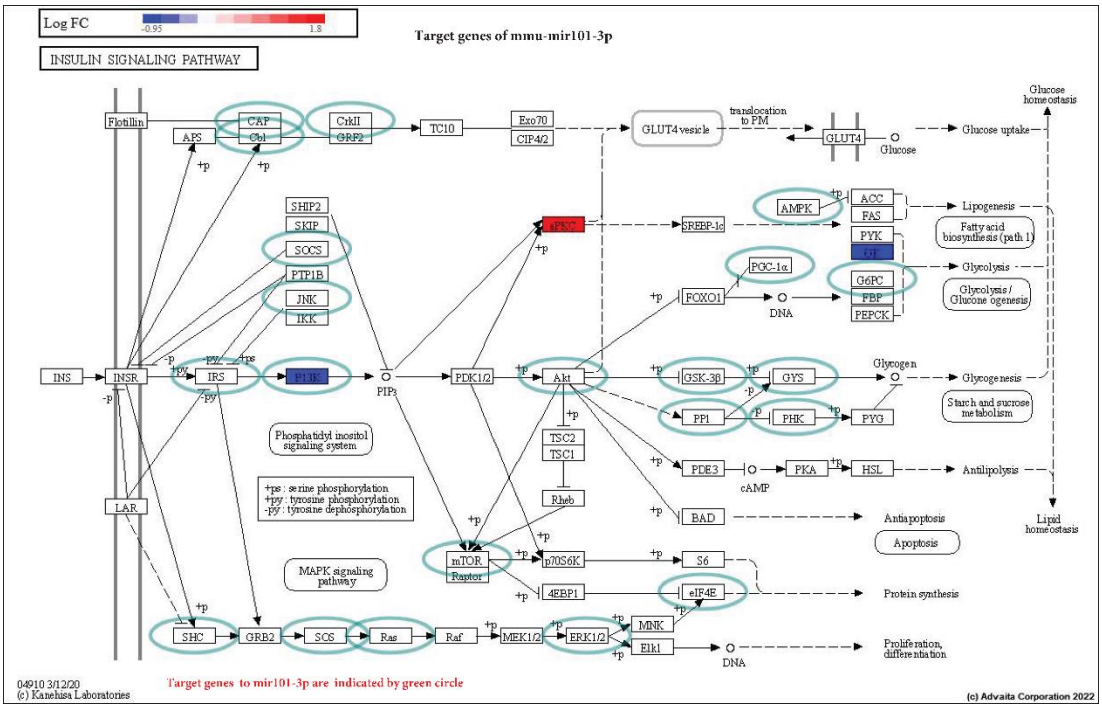

Figure 18: Target genes of mmu-mir101-3p in insulin signaling pathway.

The green circles indicate target genes for mmu-mir101-3p. The red color indicates upregulated genes, and the blue indicates downregulated genes.

CHAPTER 7: DISCUSSION

Obesity is a multifactorial complex metabolic disease that poses a high risk to individuals who are classified as obese or overweight, as it increases the risk of developing other medical conditions like hypertension and diabetes (Martins et al., 2018; Mayoral et al., 2020; Wirth et al., 2014). Bariatric surgery is the most effective obesity treatment, but it is also associated with other health complications (Cakir et al., 2022). Therefore, a new treatment must be found to resolve the problem without inducing other complications in patients. Understanding the molecular mechanism in obesity through identifying expressed genes and their regulatory molecules, such as miRNAs, as well as involved biological pathways, would help to identify the best treatment for it. Sulforaphane (SFN), an isothiocyanate compound extracted from cruciferous vegetables like broccoli and cabbage, is capable of inhibiting histone deacetylases (HDAC) type I and II in different types of cancers like colon and urinary bladder cancer (Abbaoui et al., 2017; Myzak et al., 2006; Rajendran et al., 2011). In addition to being thought to be the cause of epigenetic modulation of the MSTN gene, a regulator of muscle growth and development (H. H. Liu et al., 2019), and a significant contributor to muscle weakness in obese patients (Allen et al., 2011). MicroRNAs play a vital role in diabetes and skeletal muscle dysfunction (Esteves et al., 2017); However, their involvement in regulating metabolism and insulin resistance of skeletal muscles with obesity remains unclear. Only a few studies have investigated the effects of SFN as a treatment for obesity associated with insulin resistance on microRNA expression in skeletal muscle and their impact on skeletal muscle metabolism.

In the current study, diet-induced obese mice were treated with SFN to assess weight loss and identify the expression profile of miRNA affected by the treatment and their target

genes. The significantly expressed miRNAs in the present study for CD1-DIO mice in skeletal muscle tissue in response to SFN are mmu-miR-150-5p, mmu-miR-486a-3p, mmu-miR-101a-3p, mmu-miR-126b-5p, mmu-miR-140-3p, mmu-miR-29c-3p, mmu-miR-92a-3p, mmu-miR-3074-5p.

Intraperitoneal injection of CD1-DIO mice with SFN (5mg/kg/day) for 4 weeks has shown a significant decrease in body weight, food intake, plasma glucose, and leptin levels compared to the vehicle-treated DIO mice. This was in agreement with previous studies; for example, the study by Cakir et al. has shown that treatment of SFN decreases body weight and food intake for C57BL/6J and CD1 obese mice but does not decrease it for the lean wild-type mice. Based on these results, SFN can be considered a potential anti-obesity molecule for decreasing fat mass in the body. Furthermore, the Cakir et al. study also tested the glucose tolerance of obese mice. It showed that SFN-treated DIO mice significantly decreased total plasma glucose levels compared to the controls, indicating improvement in glucose uptake and insulin action (Cakir et al., 2022).

MicroRNAs are short non-coding single-stranded RNA molecules that play a significant role in gene expression regulation, especially at the post-transcriptional level. They are about 22 nucleotides long and capable of regulating gene expression of target mRNA, so they can change mRNA expression and act as upstream regulators. To our knowledge, no previous reports are available on the characterization of microRNAs involved in the response of skeletal muscle insulin resistance of DIO mice to anti-obesity treatment by SFN. Therefore, using a small RNA seq analysis, we compared the microRNA expressions in DIO-treated mice with SFN- and DIO mice treated with vehicle as a control group. We identified eight differentially expressed microRNAs with five upregulated miRNAs (mmu-miR-150-5p, mmu-miR-486a-3p,

mmu-miR-126b-5p, mmu-miR-140-3p, mmu-miR-92a-3p) and three downregulated miRNAs (mmu-miR-101a-3p, mmu-miR-29c-3p, mmu-miR-3074-5p). Multiple miRNAs have been identified to be involved in skeletal muscle development, differentiation, and metabolism, and alteration of these miRNAs' expression profiles could lead to various skeletal muscle diseases. For example, mmu-miR-29c-3p, mmu-miR-92a-3p, mmu-miR-101-3P, mmu-miR-126b-5p, mmu-miR-140-3p, mmu-miR-150-5p, and mmu-486a-3p which has been identified in our study as differentially expressed miRNAs were previously described to be involved in regulating skeletal muscle metabolism and development (Erener et al., 2017; Esguerra et al., 2011; Esteves et al., 2018; Li et al., 2021; Santos et al., 2019; T. Zhang et al., 2015). On the other hand, one miRNA identified in our study (mmu-miR-3074-5p) has not been previously linked to myogenesis.

In order to obtain more information on the molecular mechanisms behind microRNAs' role in the regulation of skeletal muscle metabolism, we predicted the targets of differentially expressed microRNAs using bioinformatic tools. Further, we examined the signaling pathway enrichment and gene annotation. The results showed that the dysregulated microRNA in response to SFN targets genes involved in multiple biological and cellular processes that regulate skeletal muscle metabolism.

miRNA-29 family has been previously described to be involved in cancer pathogenesis (Falcone, 2019) either as a tumor promoter or suppressor. Moreover, it has been linked to skeletal muscle differentiation, function, and disease. Also, miR-29 has been identified as a regulator of myogenesis, downregulating YY1 translation and enhancing myoblast differentiation (Wang et al., 2008). A study by Silva et al. suggested that miR-29c is involved in increasing muscle mass and has shown that mouse muscles with overexpressed miR-29c have

increased size and length and a higher number of serial sarcomeres, and no inflammation. Furthermore, they detected increased levels of activated satellite cells upon overexpression of miR-29c (Silva et al., 2019). Furthermore, this study has proved that overexpression of miR-29c causes skeletal muscle hypertrophy by downregulating MuRF1 and Atrogin 1, regulators of muscle mass (Silva et al., 2019). Skeletal muscle hypertrophy is characterized by the enlargement of pre-existing myofibers and increased synthesis of new myofibrils (Silva et al., 2019); in fact, skeletal muscle hypertrophy occurs due to new proteins and organelles being synthesized, contributing to the larger size of the muscle through different pathways such as insulin/IGF1-Akt-mTOR pathway (Sartori et al., 2021).

Furthermore, miR-29c-3p has been proposed as a repressor of GLUT4 and HK2 protein expression (Esteves et al., 2018). GLUT4 is an essential factor for blood glucose uptake by skeletal muscles (Harriet Wallberg-Henriksson, 2001; Zierath et al., 2000), reported being repressed in diabetic patients. In diabetes, miR-29c-3p expression is upregulated by approximately 51% in skeletal muscles and negatively correlates with expression levels of GLUT4 and HK2 proteins (Esteves et al., 2018). This suggests that miR-29c-3p is a repressor of GLUT4, which has been previously validated (Massart et al., 2017). In our study, we found mmu-miR-29c to be significantly decreased in skeletal muscle tissue of DIO mice upon treatment with SFN, as well as improved insulin sensitivity of skeletal muscles marked by the decreased glucose levels in the blood and enhancement of GTT. This suggests that the reduction of mmu-miR-29c has allowed for the expression of GLUT4 protein on the surface of skeletal muscles, enhancing the glucose uptake of muscles from the blood.

On the other hand, mmu-miR-92a-3p was associated with skeletal muscle proliferation, myofiber specification, and apoptosis (Li et al., 2021). Furthermore, a study by li et al. has

shown that the upregulation of miR-92a-3p had a role in the regulation of skeletal muscle metabolism by regulating MYBL2, STAT1, and IKZF1 transcription factors in skeletal muscles of obese rabbits (Li et al., 2021). Furthermore, a previous study has shown that miR-92a-3p is upregulated in sarcopenia and obesity, and it targets SMAD 7, which is an inhibitor of TGF-β pathway (Zhang et al., 2019) that is an important regulator of muscle atrophy which weakness skeletal muscle regeneration by inhibiting myofiber fusion and satellite cell proliferation (Burks & Cohn, 2011) thereby preventing muscle atrophy. In our study, mmu-miR-92a-3a was upregulated significantly upon treatment of DIO mice with SFN, which could regulate the TGF-β pathway, thereby regulating the skeletal muscle metabolism and helping it to retain its function of glucose uptake.

mmu-miR-101a is a non-muscle-specific miRNA involved in myogenesis regulation (Liu et al., 2021). It has been found to act as a repressor of myogenesis by targeting multiple muscle cell differentiation signaling pathways. Additionally, miR-101 has been previously described as a regulator of epigenesis; hence, it acts as an inhibitor of DNMT3A and suppresses lung cell proliferation leading to their death. Liu et al. have shown that miR-101a was transiently upregulated during C2C12 muscle differentiation accompanied by downregulation of myosin heavy chain (MHC) and concluded that miR-101a works on repressing myoblast differentiation (Liu et al., 2021). Furthermore, it was shown that miR-101a represses myoblast differentiation by downregulating the p38/MAPK pathway through inhibition of up and downstream effectors of the pathway such as MKK3/6, p38, ATF2, and Mef2c (Liu et al., 2021). In the current study, mmu-miR-101a was downregulated in response to SFN treatment, indicating that there is no repression of myoblast differentiation in DIO mice treated with SFN and that skeletal muscles are carrying their normal metabolic function.

mmu-miR-126 is essential in regulating the vascular formation, survival, and maintenance, as well as controlling angiogenesis (Eisenstein, 1991; Fernandes et al., 2012; Fish et al., 2008). The main target of miR-126 is PI3KR2, an important factor in angiogenesis regulation; it acts as a negative regulator of vascular endothelial growth factor (VEGF), thereby inhibiting PI3K signaling pathway and angiogenesis (Pandya et al., 2006; Prior et al., 2004). Obesity decreases the miR-126 expression in skeletal muscles, thereby decreasing the expression of angiogenic protein leading to microvascular refraction (Gomes et al., 2017). In vitro analysis of miR-126 has shown that it is a regulator of multiple developments and growth pathways such as Akt/ Foxo1 and myogenic differentiation 1 (MyoD)/myogenic factor 5 (Myf5) as well as insulin growth factor-1 (IGF-1) signaling (Rivas et al., 2014). Inhibition of miR-126 in proliferating myoblasts has shown a significant increase in protein expression of IRS1 levels and a decrease in FOXO1 levels, whereas upregulated miR-126 decreased myogenic determinants MyoD and Myf5 protein levels (Kamei et al., 2004; Kitamura et al., 2007; Long et al., 2011), these results show that dysregulation of miR-126 affects important regulators of skeletal muscle growth. The current study has shown that mmu-miR-126 is upregulated in response to SFN, showing a decrease in obesity conditions since, commonly, miR-126 is downregulated in obesity. On the contrary, overexpression of miR-126 leads to inhibition of skeletal muscle differentiation.

mmu-miR-140, transcribed from the WWP2 gene, plays a vital role in disease progression (Tardif et al., 2013; Yuan et al., 2013). miR-140-3p, which has been previously linked to myoblast differentiation inhibition (Luo et al., 2015), is usually involved in chondrogenic differentiation (Karlsen et al., 2014), testis differentiation (Rakoczy et al., 2013), and spinal chordoma prognosis (Zou et al., 2014). However, a study by Luo et al. has shown

that in chicken myoblasts overexpressed miR-140-3p binds to the 3'UTR region of Myomaker -a membrane activator of myocyte fusion for muscle development- inhibiting its expression (Millay et al., 2013). Furthermore, although the results showed that myoblast differentiation is inhibited, myoblast proliferation was initiated (Luo et al., 2015). Moreover, it has been previously shown that miR-140 binds explicitly to the WNT11 factor of the WNT signaling pathway involved in cell movement regulation (Gros et al., 2009; Ulrich et al., 2005). Although the WNT/β-catenin signaling pathway is essential for regulating genes associated with cell survival, growth, and differentiation (Moradi et al., 2017), Liu et al. have shown that upregulation of miR-140 downregulates WNT11 inhibiting WNT signaling pathway, thereby suppressing glycolysis and cell atrophy in skeletal muscles in septic mice (L. Liu et al., 2019). Additionally, miR-140-3p has been identified as an indirect activator of p38 MAPK and NF-κB signaling in human airway smooth muscle (Jude et al., 2012). Both p38 MAPK and NF-κB signaling have a role in skeletal muscle differentiation (Bakkar & Guttridge, 2010; Keren et al., 2006; Zetser et al., 1999). However, whereas p38 MAPK is a positive regulator of muscle development (Keren et al., 2006; Zetser et al., 1999), NF-κB signaling pathway acts as an inhibitor of muscle development (Bakkar et al., 2008).

mmu-miR-150 has been described to be an important positive regulator of mitochondrial metabolism in skeletal muscles (Dahlmans et al., 2017). It directly regulates mitochondrial function by targeting PPARGC1a -mitochondrial biogenesis regulator- and mitochondrial transcription factor A (mtTFA) (Dahlmans et al., 2017). A study has shown that miR-150 is upregulated in skeletal muscles of T2D patients, and its potential target is GLUT4 (Karolina et al., 2011), while another study showed that diabetes causes miR-150-5p expression to be downregulated by 32% in skeletal muscle (Esteves et al., 2018). Mmu-miR-150-5p is

upregulated in response to SFN treatment, and plasma glucose levels were decreased in DIO mice indicating alleviation of diabetic condition in the DIO mice in response to SFN application. This is confirmed by the upregulation of mmu-miR-150-5p, which is usually downregulated in diabetic conditions.

mmu-miR-486 has rarely been reported to be involved in regulating skeletal muscle metabolism. However, it has been shown that the main targets of miR-486 are FoxO1, PTEN, and Pax7 and that S1P lyase (SPL) can regulate myoblast differentiation through regulating miR-1, miR206, and miR-486. Moreover, it has been demonstrated that increased plasma circulating miR-486 in prepubertal obese children activates NF-κB signaling pathway (Song et al., 2013), as well as inhibiting FOXO1, which is a crucial factor for glucose and lipid metabolism (Altomonte et al., 2004), causing insulin resistance (Prats-Puig et al., 2013). Moreover, it was the most significantly upregulated miRNA in adipose tissue of periparturient dairy cows, and pathway analysis showed that lysosome-related pathways were overrepresented (Sadri et al., 2022). Lysosomes are important factors that function in adipocyte inflammation (Xu et al., 2013), obesity-associated lipid metabolism in adipose tissue macrophages (Ju et al., 2019; Luo et al., 2020; Rawnsley & Diwan, 2020), and lipid-related disorders (Cabrera-Reyes et al., 2021).

mmu-miR-3074-5p under iron overload conditions was significantly increased in MC3T3-E1 cells and promoted apoptosis by targeting SMAD4 (Feng et al., 2021). Moreover, it is thought to be a biomarker for diagnosing diabetic complications as it was significantly upregulated in the blood of diabetic rabbits (Kotwal et al., 2022). However, no studies have been done on the miRNA effect on skeletal muscle metabolism.

Enrichment analysis revealed that the significant GO processes are related to functions of miRNA as upstream regulators of gene expression of target genes such as GO:1903507, GO:1903508 as negative and positive regulation of nucleic acid-templated transcription, respectively, and GO:1902680, and GO:1902679 assigned for positive and negative regulation of RNA biosynthetic process, respectively. As for the signaling pathway mapping, we found more than 40 KEGG signaling pathways related to the significant differentially expressed miRNAs in the study (Table S5 in Appendix); among these signaling pathways, cell proliferation signal transduction pathways (MAPK, WNT, and TNF), metabolism (Pantothenate and CoA biosynthesis, Protein digestion and absorption), and oncogenic (Breast cancer, Melanoma) signaling pathways. In addition, we found six significant signaling pathways related to insulin resistance and skeletal muscle metabolism.

For example, in multiple animal models, insulin and the MAPK signaling pathway have been previously linked to insulin resistance in skeletal muscle and other tissue (Gehart et al., 2010; Woods et al., 2009). Skeletal muscle insulin resistance is characterized by impaired insulin signaling and multiple post-receptor intracellular defects, such as impaired glucose transport, impaired glucose phosphorylation, and reduced glucose oxidation and glycogen synthesis, leading to decreased insulin-stimulated glucose uptake (Bajaj & DeFronzo, 2003; Bouzakri et al., 2005; Cusi et al., 2000; Karlsson & Zierath, 2007). Insulin resistance is a central problem in type 2 diabetes aand is linked to obesity and metabolic syndrome (DeFronzo & Tripathy, 2009). The development of insulin resistance in skeletal muscle is heavily influenced by the dysregulation of fatty acid metabolism (Bays et al., 2004; Krssak & Roden, 2004; Lettner & Roden, 2008; McGarry, 2002). Moreover, mitochondrial deficiency in oxidative phosphorylation in skeletal muscle has been identified in a number of insulin resistance states in recent years (Abdul-Ghani

& DeFronzo, 2008; Morino et al., 2006; Roden, 2005). The insulin receptor substrate (IRS) activates the PI3K/Akt pathway, resulting in the translocation and expression of GLUT4 (Chang et al., 2004). A decrease in insulin signaling, especially in the insulin receptor substrate (IRS-1/2)/PI3K/protein kinase B (PKB) axis, activates insulin resistance affecting the insulin metabolic function (Wondmkun, 2020). Overrepresentation of insulin signaling/ resistance pathways. The GO and pathway mapping results suggest that they are involved in insulin resistance induced by HFD and enhanced by SFN treatment. For example, in the insulin signaling pathway in our data, several genes are affected by the dysregulated miRNA under SFN treatment, and their expressions were altered, such as INSR, IRS1, PI3K, AKT, GSK-3 involved in insulin signaling mediated glycogen synthesis in skeletal muscle. Furthermore, the dysregulated miRNA under SFN treatment alters the expression of AKT2, Tbc1d4 (As160, Kiaa0603), which is known to promote SLC2A4/GLUT4 translocation at the plasma membrane, thus increasing glucose uptake, as evident in our data by improvement of GTT in DIO mice treated with SFN Vs. Vehicle. For example, mmu-mir101-3P affect the following genes in insulin signaling pathway: cAMP-responsive element binding protein 1 [Creb1], glycogen synthase 2 [Gys2], glycogen synthase kinase 3 beta [Gsk3b], insulin receptor substrate 1 [Irs1], mechanistic target of rapamycin kinase [Mtor], mitogen-activated protein kinase 8 [Mapk8], O-linked N-acetylglucosamine (GlcNAc) transferase (UDP-N-acetylglucosamine: polypeptide-N-acetylglucosaminyl transferase) [Ogt], peroxisome proliferative activated receptor, gamma, coactivator 1 alpha [Ppargc1a], peroxisome proliferative activated receptor, gamma, coactivator 1 beta [Ppargc1b], protein kinase, AMP-activated, alpha 1 catalytic subunit [Prkaa1], protein kinase C, epsilon [Prkce], protein phosphatase 1 catalytic subunit beta [Ppp1cb], ribosomal protein S6 kinase polypeptide 6 [Rps6ka6], and thymoma viral proto-oncogene 3 [Akt3], as shown in Figure 17. All these genes

are parts of important metabolic processes such as glucose and lipid metabolism. For example, one of the target genes is IRS1, downregulating PI3K, disrupting lipogenesis and glycogenesis processes.

The MAPK pathway is a vital signal transduction pathway involved in regulating cell proliferation, differentiation, and apoptosis (Keshet & Seger, 2010; Qi & Elion, 2005; Raman et al., 2007). The upregulation of miR-140-3p, an indirect activator of the MAPK signaling pathway, could be the reason for the overrepresentation of the pathway in the study. In skeletal muscle p38, MAPK pathway helps to phosphorylate and activate glucose and lipid metabolism and facilitates GLUT4 expression on the surface of skeletal muscle cells, thereby enhancing glucose uptake (Bengal et al., 2020). Several studies have shown that there is a role of p38 MAPK in preventing the development of insulin resistance by controlling the expression of MAPK phosphatase-1 (MKP-1), a suppressor of JNK and P38 MAPK activities (Bengal et al., 2020). MKP-1 knockout in the skeletal muscle of mice on HFD has prevented insulin resistance development (Lawan et al., 2018).

Moreover, PI3K/Akt signaling pathway mediates growth factor signals that are important for various cellular processes like lipid metabolism, glucose homeostasis, and protein synthesis (Abeyrathna & Su, 2015). For example, insulin regulates the metabolism of skeletal muscles by initiating glucose uptake into the muscles, glycogen synthesis, and protein synthesis using the PI3K/Akt signaling pathway. Previous studies have shown that knockdown or knockout of either Akt or IRS-1 (insulin receptor substrate-1) decreases the insulin-mediated glucose uptake into the cells, while increased expression of Akt increases glucose uptake (Ng et al., 2008). In addition, Akt is a direct inducer of GLUT4 translocation to the plasma membrane by phosphorylating

AS160, which allows for increased glucose uptake by the cells (Osorio-Fuentealba et al., 2013) (Thorens & Mueckler, 2010).

Functional analysis using target prediction and pathway mapping has proved that microRNA regulated skeletal muscle metabolism by various signaling pathways, although further studies are needed to validate the differentially expressed microRNAs. This study had some limitations that could be referred to and considered for future studies. One of these limitations is the small sample size used in the study. Moreover, due to time limitations, the identified differentially expressed miRNAs were not validated using qPCR, which would have strengthened the study's findings. Another limitation is the use of only SFN as an anti-obesity drug; comparing our results with expression profiles of other anti-obesity drugs like Orlistat could give us more insight into which drug could be better at regulating the metabolism of skeletal muscles. For future studies, more anti-obesity drugs can be compared to the results of SFN to evaluate which drug would be better at resolving obesity. Additionally, the identified miRNAs should be validated using tissue culture and animal models.

CHAPTER 8: CONCLUSION

All in all, the results of this study support the hypothesis that SFN treatment induces a change in microRNA expression profiles in the skeletal muscle of DIO, which regulates the expression of multiple target genes involved in multiple biological processes and signaling pathways which could explain phenotypic changes in DIO mice in response to SFN.

REFERENCES

Abbaoui, B., Telu, K. H., Lucas, C. R., Thomas-Ahner, J. M., Schwartz, S. J., Clinton, S. K., . . . Mortazavi, A. (2017). The impact of cruciferous vegetable isothiocyanates on histone acetylation and histone phosphorylation in bladder cancer. *J Proteomics*, *156*, 94-103. https://doi.org/10.1016/j.jprot.2017.01.013

Abdul-Ghani, M. A., & DeFronzo, R. A. (2008). Mitochondrial dysfunction, insulin resistance, and type 2 diabetes mellitus. *Current diabetes reports*, *8*(3), 173-178.

Abdul-Ghani, M. A., & DeFronzo, R. A. (2010). Pathogenesis of Insulin Resistance in Skeletal Muscle. *Journal of Biomedicine and Biotechnology*, *2010*, 476279. https://doi.org/10.1155/2010/476279

Abeyrathna, P., & Su, Y. (2015). The critical role of Akt in cardiovascular function. *Vascul Pharmacol*, *74*, 38-48. https://doi.org/10.1016/j.vph.2015.05.008

Agarwal, P., Srivastava, R., Srivastava, A. K., Ali, S., & Datta, M. (2013). miR-135a targets IRS2 and regulates insulin signaling and glucose uptake in the diabetic gastrocnemius skeletal muscle. *Biochimica et Biophysica Acta (BBA)-Molecular Basis of Disease*, *1832*(8), 1294-1303.

Ahmadian, M., Abbott, M. J., Tang, T., Hudak, C. S., Kim, Y., Bruss, M., . . . Sul, H. S. (2011). Desnutrin/ATGL is regulated by AMPK and is required for a brown adipose phenotype. *Cell Metab*, *13*(6), 739-748. https://doi.org/10.1016/j.cmet.2011.05.002

Ahmadian, M., Wang, Y., & Sul, H. S. (2010). Lipolysis in adipocytes. *Int J Biochem Cell Biol*, *42*(5), 555-559. https://doi.org/10.1016/j.biocel.2009.12.009

Al Aboud, N. M., Tupper, C., & Ishwarlal, J. (2021). Genetics, Epigenetic Mechanism. In. StatPearls [Internet].

Allen, D. L., Hittel, D. S., & McPherron, A. C. (2011). Expression and function of myostatin in obesity, diabetes, and exercise adaptation. *Med Sci Sports Exerc*, *43*(10), 1828-1835. https://doi.org/10.1249/MSS.0b013e3182178bb4

Altomonte, J., Cong, L., Harbaran, S., Richter, A., Xu, J., Meseck, M., & Dong, H. H. (2004). Foxo1 mediates insulin action on apoC-III and triglyceride metabolism. *J Clin Invest*, *114*(10), 1493-1503. https://doi.org/10.1172/jci19992

Andermann, M. L., & Lowell, B. B. (2017). Toward a Wiring Diagram Understanding of Appetite Control. *Neuron*, *95*(4), 757-778. https://doi.org/10.1016/j.neuron.2017.06.014

Anderson, E. J., Lustig, M. E., Boyle, K. E., Woodlief, T. L., Kane, D. A., Lin, C. T., . . . Neufer, P. D. (2009). Mitochondrial H2O2 emission and cellular redox state link excess fat intake to insulin resistance in both rodents and humans. *J Clin Invest*, *119*(3), 573-581. https://doi.org/10.1172/jci37048

Apovian, C. M. (2016). Obesity: definition, comorbidities, causes, and burden. *Am J Manag Care*, *22*(7 Suppl), s176-185.

Bajaj, M., & DeFronzo, R. A. (2003). Metabolic and molecular basis of insulin resistance. *Journal of Nuclear Cardiology*, *10*(3), 311-323.

Bakkar, N., & Guttridge, D. C. (2010). NF-κB signaling: a tale of two pathways in skeletal myogenesis. *Physiological reviews*, *90*(2), 495-511.

Bakkar, N., Wang, J., Ladner, K. J., Wang, H., Dahlman, J. M., Carathers, M., . . . Guttridge, D. C. (2008). IKK/NF-κB regulates skeletal myogenesis via a signaling switch to inhibit

differentiation and promote mitochondrial biogenesis. *The Journal of cell biology*, *180*(4), 787-802.

Bandyopadhyay, G. K., Yu, J. G., Ofrecio, J., & Olefsky, J. M. (2006). Increased malonyl-CoA levels in muscle from obese and type 2 diabetic subjects lead to decreased fatty acid oxidation and increased lipogenesis; thiazolidinedione treatment reverses these defects. *Diabetes*, *55*(8), 2277-2285. https://doi.org/10.2337/db06-0062

Bartel, D. P. (2004). MicroRNAs: genomics, biogenesis, mechanism, and function. *Cell*, *116*(2), 281-297. https://doi.org/10.1016/s0092-8674(04)00045-5

Batra, S. K., Castelino-Prabhu, S., Wikstrand, C. J., Zhu, X., Humphrey, P. A., Friedman, H. S., & Bigner, D. D. (1995). Epidermal growth factor ligand-independent, unregulated, cell-transforming potential of a naturally occurring human mutant EGFRvIII gene. *Cell Growth Differ*, *6*(10), 1251-1259.

Bays, H., Mandarino, L., & DeFronzo, R. A. (2004). Role of the adipocyte, free fatty acids, and ectopic fat in pathogenesis of type 2 diabetes mellitus: peroxisomal proliferator-activated receptor agonists provide a rational therapeutic approach. *The Journal of Clinical Endocrinology & Metabolism*, *89*(2), 463-478.

Becker, C., Hammerle-Fickinger, A., Riedmaier, I., & Pfaffl, M. W. (2010). mRNA and microRNA quality control for RT-qPCR analysis. *Methods*, *50*(4), 237-243. https://doi.org/10.1016/j.ymeth.2010.01.010

Bengal, E., Aviram, S., & Hayek, T. (2020). p38 MAPK in Glucose Metabolism of Skeletal Muscle: Beneficial or Harmful? *Int J Mol Sci*, *21*(18). https://doi.org/10.3390/ijms21186480

Bethesda. (2012). Orlistat. In *LiverTox: Clinical and Research Information on Drug-Induced Liver Injury*.

Biga, L. M., Dawson, S., Harwell, A., Hopkins, R., Kaufmann, J., LeMaster, M., . . . Runyeon, J. (2020). Anatomy & physiology.

Bjørge, T., Tretli, S., & Engeland, A. (2004). Relation of height and body mass index to renal cell carcinoma in two million Norwegian men and women. *Am J Epidemiol*, *160*(12), 1168-1176. https://doi.org/10.1093/aje/

Bogardus, C., Lillioja, S., Mott, D., Reaven, G. R., Kashiwagi, A., & Foley, J. E. (1984). Relationship between obesity and maximal insulin-stimulated glucose uptake in vivo and in vitro in Pima Indians. *J Clin Invest*, *73*(3), 800-805. https://doi.org/10.1172/jci111274

Bouzakri, K., Koistinen, H. A., & Zierath, J. R. (2005). Molecular mechanisms of skeletal muscle insulin resistance in type 2 diabetes. *Current diabetes reviews*, *1*(2), 167-174.

Burks, T. N., & Cohn, R. D. (2011). Role of TGF-β signaling in inherited and acquired myopathies. *Skeletal Muscle*, *1*(1), 19. https://doi.org/10.1186/2044-5040-1-19

Cabrera-Reyes, F., Parra-Ruiz, C., Yuseff, M. I., & Zanlungo, S. (2021). Alterations in Lysosome Homeostasis in Lipid-Related Disorders: Impact on Metabolic Tissues and Immune Cells. *Front Cell Dev Biol*, *9*, 790568. https://doi.org/10.3389/fcell.2021.790568

Cakir, I., Lining Pan, P., Hadley, C. K., El-Gamal, A., Fadel, A., Elsayegh, D., . . . Ghamari-Langroudi, M. (2022). Sulforaphane reduces obesity by reversing leptin resistance *elife*. https://doi.org/10.7554/eLife.67368

Castro, J.A.C., H.E.G. Nunes, and D.A.S. Silva, *Prevalence of abdominal obesity in adolescents: association between sociodemographic factors and lifestyle.* Revista Paulista de Pediatria, 2016. **34**: p. 343-351.

Chang, L., Chiang, S.-H., & Saltiel, A. R. (2004). Insulin Signaling and the Regulation of Glucose Transport. *Molecular Medicine*, *10*(7), 65-71. https://doi.org/10.2119/2005-00029.Saltiel

Chartoumpekis, D. V., Zaravinos, A., Ziros, P. G., Iskrenova, R. P., Psyrogiannis, A. I., Kyriazopoulou, V. E., & Habeos, I. G. (2012). Differential expression of microRNAs in adipose tissue after long-term high-fat diet-induced obesity in mice. *PLoS One*, *7*(4), e34872. https://doi.org/10.1371/journal.pone.0034872

Cheah, Y. K., Azahadi, M., Mohamad Nor, N. S., Phang, S. N., & Abd Manaf, N. H. (2020). Sociodemographic factors associated with consumption of confectionery among obese and non-obese adults: A secondary analysis. *Obesity Research & Clinical Practice*, *14*(5), 428-436. https://doi.org/https://doi.org/10.1016/j.orcp.2020.07.008

Chen, C. Z., Li, L., Lodish, H. F., & Bartel, D. P. (2004). MicroRNAs modulate hematopoietic lineage differentiation. *Science*, *303*(5654), 83-86. https://doi.org/10.1126/science.1091903

Chen, J.-F., Mandel, E. M., Thomson, J. M., Wu, Q., Callis, T. E., Hammond, S. M., . . . Wang, D.-Z. (2006). The role of microRNA-1 and microRNA-133 in skeletal muscle proliferation and differentiation. *Nature Genetics*, *38*(2), 228-233. https://doi.org/10.1038/ng1725

Chen, Y., & Wang, X. (2020). miRDB: an online database for prediction of functional microRNA targets. *Nucleic Acids Research*, *48*(D1), D127-D131. https://doi.org/10.1093/nar/gkz757

Choi, K.-M., Lee, Y.-S., Kim, W., Kim, S. J., Shin, K.-O., Yu, J.-Y., . . . Yoo, H.-S. (2014). Sulforaphane attenuates obesity by inhibiting adipogenesis and activating the AMPK pathway in obese mice. *The Journal of Nutritional Biochemistry*, *25*(2), 201-207. https://doi.org/https://doi.org/10.1016/j.jnutbio.2013.10.007

Colquitt, J. L., Picot, J., Loveman, E., & Clegg, A. J. (2009). Surgery for obesity. *Cochrane Database Syst Rev*(2), Cd003641. https://doi.org/10.1002/14651858.CD003641.pub3

Cusi, K., Maezono, K., Osman, A., Pendergrass, M., Patti, M. E., Pratipanawatr, T., . . . Mandarino, L. J. (2000). Insulin resistance differentially affects the PI 3-kinase–and MAP kinase–mediated signaling in human muscle. *The Journal of Clinical Investigation*, *105*(3), 311-320.

Dahlmans, D., Houzelle, A., Andreux, P., Jorgensen, J. A., Wang, X., de Windt, L. J., . . . Hoeks, J. (2017). An unbiased silencing screen in muscle cells identifies miR-320a, miR-150, miR-196b, and miR-34c as regulators of skeletal muscle mitochondrial metabolism. *Mol Metab*, *6*(11), 1429-1442. https://doi.org/10.1016/j.molmet.2017.08.007

de la Garza-Rodea, A. S., Baldwin, D. M., Oskouian, B., Place, R. F., Bandhuvula, P., Kumar, A., & Saba, J. D. (2014). Sphingosine phosphate lyase regulates myogenic differentiation via S1P receptor-mediated effects on myogenic microRNA expression [https://doi.org/10.1096/fj.13-233155]. *The FASEB Journal*, *28*(1), 506-519. https://doi.org/https://doi.org/10.1096/fj.13-233155

de Wilde, J., Mohren, R., van den Berg, S., Boekschoten, M., Dijk, K. W.-V., de Groot, P., . . . Smit, E. (2008). Short-term high fat-feeding results in morphological and metabolic adaptations in the skeletal muscle of C57BL/6J mice. *Physiological Genomics*, *32*(3), 360-369. https://doi.org/10.1152/physiolgenomics.00219.2007

DeFronzo, R. A. (1988). Lilly lecture 1987. The triumvirate: beta-cell, muscle, liver. A collusion responsible for NIDDM. *Diabetes*, *37*(6), 667-687. https://doi.org/10.2337/diab.37.6.667

DeFronzo, R. A., Gunnarsson, R., Björkman, O., Olsson, M., & Wahren, J. (1985). Effects of insulin on peripheral and splanchnic glucose metabolism in noninsulin-dependent (type II) diabetes mellitus. *The Journal of Clinical Investigation*, *76*(1), 149-155.

DeFronzo, R. A., & Tripathy, D. (2009). Skeletal muscle insulin resistance is the primary defect in type 2 diabetes. *Diabetes care*, *32*(suppl_2), S157-S163.

Denis, H., Van Grembergen, O., Delatte, B., Dedeurwaerder, S., Putmans, P., Calonne, E., . . . Deplus, R. (2016). MicroRNAs regulate KDM5 histone demethylases in breast cancer cells. *Mol Biosyst*, *12*(2), 404-413. https://doi.org/10.1039/c5mb00513b

Deslypere, J. P., Verdonck, L., & Vermeulen, A. (1985). Fat tissue: a steroid reservoir and site of steroid metabolism. *J Clin Endocrinol Metab*, *61*(3), 564-570. https://doi.org/10.1210/jcem-61-3-564

Dey Bijan, K., Gagan, J., & Dutta, A. (2011). miR-206 and -486 Induce Myoblast Differentiation by Downregulating Pax7. *Molecular and Cellular Biology*, *31*(1), 203-214. https://doi.org/10.1128/MCB.01009-10

Dey, B. K., Pfeifer, K., & Dutta, A. (2014). The H19 long noncoding RNA gives rise to microRNAs miR-675-3p and miR-675-5p to promote skeletal muscle differentiation and regeneration. *Genes & development*, *28*(5), 491-501.

Dohm, G. L., Tapscott, E. B., Pories, W. J., Dabbs, D. J., Flickinger, E. G., Meelheim, D., . . . Caro, J. F. (1988). An in vitro human muscle preparation suitable for metabolic studies. Decreased insulin stimulation of glucose transport in muscle from morbidly obese and diabetic subjects. *J Clin Invest*, *82*(2), 486-494. https://doi.org/10.1172/jci113622

Dostie, J., Mourelatos, Z., Yang, M., Sharma, A., & Dreyfuss, G. (2003). Numerous microRNPs in neuronal cells containing novel microRNAs. *Rna*, *9*(2), 180-186. https://doi.org/10.1261/rna.2141503

Egan, J. J., Greenberg, A. S., Chang, M. K., Wek, S. A., Moos, M. C., Jr., & Londos, C. (1992). Mechanism of hormone-stimulated lipolysis in adipocytes: translocation of hormone-sensitive lipase to the lipid storage droplet. *Proc Natl Acad Sci U S A*, *89*(18), 8537-8541. https://doi.org/10.1073/pnas.89.18.8537

Eisenstein, R. (1991). Angiogenesis in arteries. *Pharmacology & therapeutics*, *49*(1-2), 1-19.

Ellulu, M. S., Patimah, I., Khaza'ai, H., Rahmat, A., & Abed, Y. (2017). Obesity and inflammation: the linking mechanism and the complications. *Arch Med Sci*, *13*(4), 851-863. https://doi.org/10.5114/aoms.2016.58928

Elton, C. W., Tapscott, E. B., Pories, W. J., & Dohm, G. L. (1994). Effect of moderate obesity on glucose transport in human muscle. *Horm Metab Res*, *26*(4), 181-183. https://doi.org/10.1055/s-2007-1000807

Endalifer, M. L., & Diress, G. (2020). Epidemiology, Predisposing Factors, Biomarkers, and Prevention Mechanism of Obesity: A Systematic Review. *J Obes, 2020*, 6134362. https://doi.org/10.1155/2020/6134362

Engeland, A., Tretli, S., & Bjørge, T. (2003). Height, body mass index, and ovarian cancer: a follow-up of 1.1 million Norwegian women. *J Natl Cancer Inst*, *95*(16), 1244-1248. https://doi.org/10.1093/jnci/djg010

Engin, A. (2017). The Definition and Prevalence of Obesity and Metabolic Syndrome. *Adv Exp Med Biol*, *960*, 1-17. https://doi.org/10.1007/978-3-319-48382-5_1

Erener, S., Marwaha, A., Tan, R., Panagiotopoulos, C., & Kieffer, T. J. (2017). Profiling of circulating microRNAs in children with recent onset of type 1 diabetes. *JCI insight*, *2*(4).

Esguerra, J. L. S., Bolmeson, C., Cilio, C. M., & Eliasson, L. (2011). Differential glucose-regulation of microRNAs in pancreatic islets of non-obese type 2 diabetes model Goto-Kakizaki rat. *PLoS One*, *6*(4), e18613.

Esteller, M. (2011). Non-coding RNAs in human disease. *Nature Reviews Genetics*, *12*(12), 861-874. https://doi.org/10.1038/nrg3074

Esteves, J. V., Enguita, F. J., & Machado, U. F. (2017). MicroRNAs-mediated regulation of skeletal muscle GLUT4 expression and translocation in insulin resistance. *Journal of diabetes research*, *2017*.

Esteves, J. V., Yonamine, C. Y., Pinto-Junior, D. C., Gerlinger-Romero, F., Enguita, F. J., & Machado, U. F. (2018). Diabetes Modulates MicroRNAs 29b-3p, 29c-3p, 199a-5p and 532-3p Expression in Muscle: Possible Role in GLUT4 and HK2 Repression. *Front Endocrinol (Lausanne)*, *9*, 536. https://doi.org/10.3389/fendo.2018.00536

Eyth, E., Basit, H., & Smith, C. J. (2022). Glucose tolerance test. In *StatPearls [Internet]*. StatPearls Publishing.

Falcone, G. (2019). A new role of miR-29c as a potent inducer of skeletal muscle hypertrophy [https://doi.org/10.1111/apha.13320]. *Acta Physiologica*, *226*(4), e13320. https://doi.org/https://doi.org/10.1111/apha.13320

Fan, H., Zhang, R., Tesfaye, D., Tholen, E., Looft, C., Hölker, M., . . . Cinar, M. U. (2012). Sulforaphane causes a major epigenetic repression of myostatin in porcine satellite cells. *Epigenetics*, *7*(12), 1379-1390. https://doi.org/10.4161/epi.22609

Felig, P., & Wahren, J. (1975). Fuel homeostasis in exercise. *N Engl J Med*, *293*(21), 1078-1084. https://doi.org/10.1056/nejm197511202932107

Feng, Y., He, P. Y., Kong, W. D., Cen, W. J., Wang, P. L., Liu, C., . . . Jiang, J. W. (2021). Apoptosis-promoting properties of miR-3074-5p in MC3T3-E1 cells under iron overload conditions. In *Cell Mol Biol Lett* (Vol. 26, pp. 37). © 2021. The Author(s). https://doi.org/10.1186/s11658-021-00281-w

Fernandes, T., Magalhães, F. C., Roque, F. R., Phillips, M. I., & Oliveira, E. M. (2012). Exercise training prevents the microvascular rarefaction in hypertension balancing angiogenic and apoptotic factors: role of microRNAs-16,-21, and-126. *Hypertension*, *59*(2), 513-520.

Fish, J. E., Santoro, M. M., Morton, S. U., Yu, S., Yeh, R.-F., Wythe, J. D., . . . Srivastava, D. (2008). miR-126 regulates angiogenic signaling and vascular integrity. *Developmental cell*, *15*(2), 272-284.

Flier, J. S. (1998). Clinical review 94: What's in a name? In search of leptin's physiologic role. *J Clin Endocrinol Metab*, *83*(5), 1407-1413. https://doi.org/10.1210/jcem.83.5.4779

Frederich, R. C., Hamann, A., Anderson, S., Löllmann, B., Lowell, B. B., & Flier, J. S. (1995). Leptin levels reflect body lipid content in mice: Evidence for diet-induced resistance to leptin action. *Nature Medicine*, *1*(12), 1311-1314. https://doi.org/10.1038/nm1295-1311

Friedman, J. E., Caro, J. F., Pories, W. J., Azevedo, J. L., Jr., & Dohm, G. L. (1994). Glucose metabolism in incubated human muscle: effect of obesity and non-insulin-dependent diabetes mellitus. *Metabolism*, *43*(8), 1047-1054. https://doi.org/10.1016/0026-0495(94)90188-0

Friedman, J. M. (2002). The function of leptin in nutrition, weight, and physiology. *Nutr Rev*, *60*(10 Pt 2), S1-14; discussion S68-84, 85-17. https://doi.org/10.1301/002966402320634878

Friedman, J. M. (2009). Leptin at 14 y of age: an ongoing story. *Am J Clin Nutr*, *89*(3), 973s-979s. https://doi.org/10.3945/ajcn.2008.26788B

Fritzen, A. M., Lundsgaard, A. M., & Kiens, B. (2020). Tuning fatty acid oxidation in skeletal muscle with dietary fat and exercise. *Nature reviews. Endocrinology*, *16*(12), 683-696. https://doi.org/10.1038/s41574-020-0405-1

Frost, R. J., & Olson, E. N. (2011). Control of glucose homeostasis and insulin sensitivity by the Let-7 family of microRNAs. *Proc Natl Acad Sci U S A*, *108*(52), 21075-21080. https://doi.org/10.1073/pnas.1118922109

Ge, Y., & Chen, J. (2011). MicroRNAs in skeletal myogenesis. *Cell Cycle*, *10*(3), 441-448. https://doi.org/10.4161/cc.10.3.14710

Gehart, H., Kumpf, S., Ittner, A., & Ricci, R. (2010). MAPK signalling in cellular metabolism: stress or wellness? *EMBO Rep*, *11*(11), 834-840. https://doi.org/10.1038/embor.2010.160

Gomes, J. L., Fernandes, T., Soci, U. P., Silveira, A. C., Barretti, D. L., Negrao, C. E., & Oliveira, E. M. (2017). Obesity Downregulates MicroRNA-126 Inducing Capillary Rarefaction in Skeletal Muscle: Effects of Aerobic Exercise Training. *Oxid Med Cell Longev*, *2017*, 2415246. https://doi.org/10.1155/2017/2415246

Goodpaster, B. H., He, J., Watkins, S., & Kelley, D. E. (2001). Skeletal muscle lipid content and insulin resistance: evidence for a paradox in endurance-trained athletes. *J Clin Endocrinol Metab*, *86*(12), 5755-5761. https://doi.org/10.1210/jcem.86.12.8075

Goodpaster, B. H., Theriault, R., Watkins, S. C., & Kelley, D. E. (2000). Intramuscular lipid content is increased in obesity and decreased by weight loss. *Metabolism*, *49*(4), 467-472. https://doi.org/10.1016/s0026-0495(00)80010-4

Goodyear, L. J., Giorgino, F., Sherman, L. A., Carey, J., Smith, R. J., & Dohm, G. L. (1995). Insulin receptor phosphorylation, insulin receptor substrate-1 phosphorylation, and phosphatidylinositol 3-kinase activity are decreased in intact skeletal muscle strips from obese subjects. *J Clin Invest*, *95*(5), 2195-2204. https://doi.org/10.1172/jci117909

Gregoire, F. M., Smas, C. M., & Sul, H. S. (1998). Understanding adipocyte differentiation. *Physiol Rev*, *78*(3), 783-809. https://doi.org/10.1152/physrev.1998.78.3.783

Groop, L. C., Bonadonna, R. C., DelPrato, S., Ratheiser, K., Zyck, K., Ferrannini, E., & DeFronzo, R. A. (1989). Glucose and free fatty acid metabolism in non-insulin-dependent diabetes mellitus. Evidence for multiple sites of insulin resistance. *J Clin Invest*, *84*(1), 205-213. https://doi.org/10.1172/jci114142

Gros, J., Serralbo, O., & Marcelle, C. (2009). WNT11 acts as a directional cue to organize the elongation of early muscle fibres. *Nature*, *457*(7229), 589-593.

Gupte, A. A., Lyon, C. J., & Hsueh, W. A. (2013). Nuclear factor (erythroid-derived 2)-like-2 factor (Nrf2), a key regulator of the antioxidant response to protect against atherosclerosis and nonalcoholic steatohepatitis. *Curr Diab Rep*, *13*(3), 362-371. https://doi.org/10.1007/s11892-013-0372-1

Harding, R. L., & Velleman, S. G. (2016). MicroRNA regulation of myogenic satellite cell proliferation and differentiation. *Mol Cell Biochem*, *412*(1-2), 181-195. https://doi.org/10.1007/s11010-015-2625-6

Harriet Wallberg-Henriksson, J. R. Z. (2001). GLUT4: a key player regulating glucose homeostasis? Insights from transgenic and knockout mice. *Molecular membrane biology*, *18*(3), 205-211.

Haslam, D. (2010). Obesity and diabetes: the links and common approaches. *Prim Care Diabetes*, *4*(2), 105-112. https://doi.org/10.1016/j.pcd.2010.04.002

Hawley, S. A., Gadalla, A. E., Olsen, G. S., & Hardie, D. G. (2002). The Antidiabetic Drug Metformin Activates the AMP-Activated Protein Kinase Cascade via an Adenine Nucleotide-Independent Mechanism. *Diabetes*, *51*(8), 2420-2425. https://doi.org/10.2337/diabetes.51.8.2420

Hayes, M. R., Kanoski, S. E., Alhadeff, A. L., & Grill, H. J. (2011). Comparative effects of the long-acting GLP-1 receptor ligands, liraglutide and exendin-4, on food intake and body weight suppression in rats. *Obesity (Silver Spring)*, *19*(7), 1342-1349. https://doi.org/10.1038/oby.2011.50

Helge, J. W., Fraser, A. M., Kriketos, A. D., Jenkins, A. B., Calvert, G. D., Ayre, K. J., & Storlien, L. H. (1999). Interrelationships between muscle fibre type, substrate oxidation

and body fat. *International Journal of Obesity*, *23*(9), 986-991. https://doi.org/10.1038/sj.ijo.0801030

Heneghan, H. M., Miller, N., McAnena, O. J., O'Brien, T., & Kerin, M. J. (2011). Differential miRNA expression in omental adipose tissue and in the circulation of obese patients identifies novel metabolic biomarkers. *J Clin Endocrinol Metab*, *96*(5), E846-850. https://doi.org/10.1210/jc.2010-2701

Houmard, J. A., Pories, W. J., & Dohm, G. L. (2011). Is there a metabolic program in the skeletal muscle of obese individuals? *J Obes*, *2011*, 250496. https://doi.org/10.1155/2011/250496

Houmard, J. A., Pories, W. J., & Dohm, G. L. (2012). Severe obesity: evidence for a deranged metabolic program in skeletal muscle? *Exerc Sport Sci Rev*, *40*(4), 204-210. https://doi.org/10.1097/JES.0b013e31825d53fc

Huang, B., Qin, W., Zhao, B., Shi, Y., Yao, C., Li, J., . . . Jin, Y. (2009). MicroRNA expression profiling in diabetic GK rat model. *Acta Biochim Biophys Sin*, *41*(6), 472-477.

Huang, Z., Chen, X., Yu, B., He, J., & Chen, D. (2012). MicroRNA-27a promotes myoblast proliferation by targeting myostatin. *Biochemical and Biophysical Research Communications*, *423*(2), 265-269. https://doi.org/https://doi.org/10.1016/j.bbrc.2012.05.106

Hulver, M. W., Berggren, J. R., Cortright, R. N., Dudek, R. W., Thompson, R. P., Pories, W. J., . . . Houmard, J. A. (2003). Skeletal muscle lipid metabolism with obesity. *Am J Physiol Endocrinol Metab*, *284*(4), E741-747. https://doi.org/10.1152/ajpendo.00514.2002

Ibberson, D., Benes, V., Muckenthaler, M. U., & Castoldi, M. (2009). RNA degradation compromises the reliability of microRNA expression profiling. *BMC Biotechnology*, *9*(1), 102. https://doi.org/10.1186/1472-6750-9-102

Imbeaud, S., Graudens, E., Boulanger, V., Barlet, X., Zaborski, P., Eveno, E., . . . Auffray, C. (2005). Towards standardization of RNA quality assessment using user-independent classifiers of microcapillary electrophoresis traces. *Nucleic Acids Res*, *33*(6), e56. https://doi.org/10.1093/nar/gni054

Jonsson, F., Wolk, A., Pedersen, N. L., Lichtenstein, P., Terry, P., Ahlbom, A., & Feychting, M. (2003). Obesity and hormone-dependent tumors: cohort and co-twin control studies based on the Swedish Twin Registry. *Int J Cancer*, *106*(4), 594-599. https://doi.org/10.1002/ijc.11266

Ju, L., Han, J., Zhang, X., Deng, Y., Yan, H., Wang, C., . . . Jia, W. (2019). Obesity-associated inflammation triggers an autophagy-lysosomal response in adipocytes and causes degradation of perilipin 1. *Cell Death Dis*, *10*(2), 121. https://doi.org/10.1038/s41419-019-1393-8

Jude, J. A., Dileepan, M., Subramanian, S., Solway, J., Panettieri Jr, R. A., Walseth, T. F., & Kannan, M. S. (2012). miR-140-3p regulation of TNF-α-induced CD38 expression in human airway smooth muscle cells. *American Journal of Physiology-Lung Cellular and Molecular Physiology*, *303*(5), L460-L468.

Kahn, B. B., & Flier, J. S. (2000). Obesity and insulin resistance. *The Journal of Clinical Investigation*, *106*(4), 473-481. https://doi.org/10.1172/JCI10842

Kamei, Y., Miura, S., Suzuki, M., Kai, Y., Mizukami, J., Taniguchi, T., . . . Aburatani, H. (2004). Skeletal Muscle FOXO1 (FKHR) Transgenic Mice Have Less Skeletal Muscle

Mass, Down-regulated Type I (Slow Twitch/Red Muscle) Fiber Genes, and Impaired Glycemic Control*[boxs]. *Journal of Biological Chemistry*, *279*(39), 41114-41123.

Karlsen, T. A., Jakobsen, R. B., Mikkelsen, T. S., & Brinchmann, J. E. (2014). microRNA-140 targets RALA and regulates chondrogenic differentiation of human mesenchymal stem cells by translational enhancement of SOX9 and ACAN. *Stem cells and development*, *23*(3), 290-304.

Karlsson, H. K. R., & Zierath, J. R. (2007). Insulin signaling and glucose transport in insulin resistant human skeletal muscle. *Cell biochemistry and biophysics*, *48*(2), 103-113.

Karolina, D. S., Armugam, A., Tavintharan, S., Wong, M. T., Lim, S. C., Sum, C. F., & Jeyaseelan, K. (2011). MicroRNA 144 impairs insulin signaling by inhibiting the expression of insulin receptor substrate 1 in type 2 diabetes mellitus. *PLoS One*, *6*(8), e22839. https://doi.org/10.1371/journal.pone.0022839

Kaul, N., & Forman, H. J. (1996). Activation of NFκB by the respiratory burst of macrophages. *Free Radical Biology and Medicine*, *21*(3), 401-405. https://doi.org/https://doi.org/10.1016/0891-5849(96)00178-5

Keaver, L., Webber, L., Dee, A., Shiely, F., Marsh, T., Balanda, K., & Perry, I. J. (2013). Application of the UK foresight obesity model in Ireland: the health and economic consequences of projected obesity trends in Ireland. *PLoS One*, *8*(11), e79827. https://doi.org/10.1371/journal.pone.0079827

Kelley, D. E., Goodpaster, B., Wing, R. R., & Simoneau, J. A. (1999). Skeletal muscle fatty acid metabolism in association with insulin resistance, obesity, and weight loss. *Am J Physiol*, *277*(6), E1130-1141. https://doi.org/10.1152/ajpendo.1999.277.6.E1130

Keren, A., Tamir, Y., & Bengal, E. (2006). The p38 MAPK signaling pathway: a major regulator of skeletal muscle development. *Molecular and cellular endocrinology*, *252*(1-2), 224-230.

Kerkadi, A., et al., *The Relationship between Lifestyle Factors and Obesity Indices among Adolescents in Qatar*. International journal of environmental research and public health, 2019. **16**(22): p. 4428.

Keshet, Y., & Seger, R. (2010). The MAP kinase signaling cascades: a system of hundreds of components regulates a diverse array of physiological functions. *Methods Mol Biol*, *661*, 3-38. https://doi.org/10.1007/978-1-60761-795-2_1

Kim, H. K., Lee, Y. S., Sivaprasad, U., Malhotra, A., & Dutta, A. (2006). Muscle-specific microRNA miR-206 promotes muscle differentiation. *Journal of Cell Biology*, *174*(5), 677-687. https://doi.org/10.1083/jcb.200603008

Kim, J. Y., Hickner, R. C., Cortright, R. L., Dohm, G. L., & Houmard, J. A. (2000). Lipid oxidation is reduced in obese human skeletal muscle. *Am J Physiol Endocrinol Metab*, *279*(5), E1039-1044. https://doi.org/10.1152/ajpendo.2000.279.5.E1039

Kim, S., & Moustaid-Moussa, N. (2000). Secretory, endocrine and autocrine/paracrine function of the adipocyte. *J Nutr*, *130*(12), 3110s-3115s. https://doi.org/10.1093/jn/130.12.3110S

Kitamura, T., Kitamura, Y. I., Funahashi, Y., Shawber, C. J., Castrillon, D. H., Kollipara, R., . . . Accili, D. (2007). A Foxo/Notch pathway controls myogenic differentiation and fiber type specification. *The Journal of Clinical Investigation*, *117*(9), 2477-2485.

Kley, H. K., Deselaers, T., Peerenboom, H., & Krüskemper, H. L. (1980). Enhanced conversion of androstenedione to estrogens in obese males. *J Clin Endocrinol Metab*, *51*(5), 1128-1132. https://doi.org/10.1210/jcem-51-5-1128

Klok, M. D., Jakobsdottir, S., & Drent, M. L. (2007). The role of leptin and ghrelin in the regulation of food intake and body weight in humans: a review. *Obes Rev*, *8*(1), 21-34. https://doi.org/10.1111/j.1467-789X.2006.00270.x

Kotwal, G. J., Waigel, S., Chariker, J., Rouchka, E., & Chien, S. (2022). Distinct MicroRNAs identified in rabbit blood arising from, induced diabetes and a surgically simulated diabetic ischemia complication. *Microrna*. https://doi.org/10.2174/2211536611666221005091351

Kristensen, D. E., Albers, P. H., Prats, C., Baba, O., Birk, J. B., & Wojtaszewski, J. F. P. (2015). Human muscle fibre type-specific regulation of AMPK and downstream targets by exercise [https://doi.org/10.1113/jphysiol.2014.283267]. *The Journal of Physiology*, *593*(8), 2053-2069. https://doi.org/https://doi.org/10.1113/jphysiol.2014.283267

Kristensen, M. M., Davidsen, P. K., Vigelsø, A., Hansen, C. N., Jensen, L. J., Jessen, N., . . . Helge, J. W. (2017). miRNAs in human subcutaneous adipose tissue: Effects of weight loss induced by hypocaloric diet and exercise. *Obesity (Silver Spring)*, *25*(3), 572-580. https://doi.org/10.1002/oby.21765

Krssak, M., & Roden, M. (2004). The role of lipid accumulation in liver and muscle for insulin resistance and type 2 diabetes mellitus in humans. *Reviews in Endocrine and Metabolic Disorders*, *5*(2), 127-134.

Krützfeldt, J., & Stoffel, M. (2006). MicroRNAs: a new class of regulatory genes affecting metabolism. *Cell Metab*, *4*(1), 9-12. https://doi.org/10.1016/j.cmet.2006.05.009

Lagos-Quintana, M., Rauhut, R., Yalcin, A., Meyer, J., Lendeckel, W., & Tuschl, T. (2002). Identification of tissue-specific microRNAs from mouse. *Curr Biol*, *12*(9), 735-739. https://doi.org/10.1016/s0960-9822(02)00809-6

Landrier, J. F., Derghal, A., & Mounien, L. (2019). MicroRNAs in Obesity and Related Metabolic Disorders. *Cells*, *8*(8). https://doi.org/10.3390/cells8080859

Lawan, A., Min, K., Zhang, L., Canfran-Duque, A., Jurczak, M. J., Camporez, J. P. G., . . . Bennett, A. M. (2018). Skeletal Muscle-Specific Deletion of MKP-1 Reveals a p38 MAPK/JNK/Akt Signaling Node That Regulates Obesity-Induced Insulin Resistance. *Diabetes*, *67*(4), 624-635. https://doi.org/10.2337/db17-0826

Leroy, P., Dessolin, S., Villageois, P., Moon, B. C., Friedman, J. M., Ailhaud, G., & Dani, C. (1996). Expression of ob gene in adipose cells. Regulation by insulin. *J Biol Chem*, *271*(5), 2365-2368. https://doi.org/10.1074/jbc.271.5.2365

Lettner, A., & Roden, M. (2008). Ectopic fat and insulin resistance. *Current diabetes reports*, *8*(3), 185-191.

Li, S., Zhao, J. H., Luan, J., Luben, R. N., Rodwell, S. A., Khaw, K. T., . . . Loos, R. J. (2010). Cumulative effects and predictive value of common obesity-susceptibility variants identified by genome-wide association studies. *Am J Clin Nutr*, *91*(1), 184-190. https://doi.org/10.3945/ajcn.2009.28403

Li, Y., Wang, J., Elzo, M. A., Gan, M., Tang, T., Shao, J., . . . Lai, S. (2021). Multi-Omics Analysis of Key microRNA-mRNA Metabolic Regulatory Networks in Skeletal Muscle of Obese Rabbits. *International journal of molecular sciences*, *22*(8), 4204. https://doi.org/10.3390/ijms22084204

Lin, S., & Gregory, R. I. (2015). MicroRNA biogenesis pathways in cancer. *Nature Reviews Cancer*, *15*(6), 321-333. https://doi.org/10.1038/nrc3932

Liu, H. H., Mao, H. G., Dong, X. Y., Cao, H. Y., Liu, K., & Yin, Z. Z. (2019). Expression of MSTN gene and its correlation with pectoralis muscle fiber traits in the domestic

pigeons (Columba livia). *Poultry Science*, *98*(11), 5265-5271. https://doi.org/https://doi.org/10.3382/ps/pez399

Liu, L., Li, T. M., Liu, X. R., Bai, Y. P., Li, J., Tang, N., & Wang, X. B. (2019). MicroRNA-140 inhibits skeletal muscle glycolysis and atrophy in endotoxin-induced sepsis in mice via the WNT signaling pathway. *Am J Physiol Cell Physiol*, *317*(2), C189-C199. https://doi.org/10.1152/ajpcell.00419.2018

Liu, S., Xie, S., Chen, H., Li, B., Chen, Z., Tan, Y., . . . Qu, L. (2021). The functional analysis of transiently upregulated miR-101 suggests a "braking" regulatory mechanism during myogenesis. *Science China Life Sciences*, *64*(10), 1612-1623. https://doi.org/10.1007/s11427-020-1856-5

Londos, C., Brasaemle, D. L., Schultz, C. J., Adler-Wailes, D. C., Levin, D. M., Kimmel, A. R., & Rondinone, C. M. (1999). On the control of lipolysis in adipocytes. *Ann N Y Acad Sci*, *892*, 155-168. https://doi.org/10.1111/j.1749-6632.1999.tb07794.x

Long, Y. C., Cheng, Z., Copps, K. D., & White, M. F. (2011). Insulin receptor substrates Irs1 and Irs2 coordinate skeletal muscle growth and metabolism via the Akt and AMPK pathways. *Molecular and Cellular Biology*, *31*(3), 430-441.

Lugrin, J., Rosenblatt-Velin, N., Parapanov, R., & Liaudet, L. (2014). The role of oxidative stress during inflammatory processes. *Biological Chemistry*, *395*(2), 203-230. https://doi.org/doi:10.1515/hsz-2013-0241

Luo, W., Li, E., Nie, Q., & Zhang, X. (2015). Myomaker, Regulated by MYOD, MYOG and miR-140-3p, Promotes Chicken Myoblast Fusion. *Int J Mol Sci*, *16*(11), 26186-26201. https://doi.org/10.3390/ijms161125946

Luo, X., Li, Y., Yang, P., Chen, Y., Wei, L., Yu, T., . . . Zhao, L. (2020). Obesity induces preadipocyte CD36 expression promoting inflammation via the disruption of lysosomal calcium homeostasis and lysosome function. *EBioMedicine, 56*, 102797. https://doi.org/10.1016/j.ebiom.2020.102797

Lutz, T. A., & Woods, S. C. (2012). Overview of animal models of obesity. *Curr Protoc Pharmacol, Chapter 5*, Unit5.61. https://doi.org/10.1002/0471141755.ph0561s58

Manna, P., & Jain, S. K. (2015). Obesity, Oxidative Stress, Adipose Tissue Dysfunction, and the Associated Health Risks: Causes and Therapeutic Strategies. *Metab Syndr Relat Disord, 13*(10), 423-444. https://doi.org/10.1089/met.2015.0095

Martins, T., Colaço, B., Venâncio, C., Pires, M. J., Oliveira, P. A., Rosa, E., & Antunes, L. M. (2018). Potential effects of sulforaphane to fight obesity. *J Sci Food Agric*, *98*(8), 2837-2844. https://doi.org/10.1002/jsfa.8898

Massart, J., Sjögren, R. J. O., Lundell, L. S., Mudry, J. M., Franck, N., O'Gorman, D. J., . . . Krook, A. (2017). Altered miR-29 expression in type 2 diabetes influences glucose and lipid metabolism in skeletal muscle. *Diabetes*, *66*(7), 1807-1818.

Mayoral, L. P., Andrade, G. M., Mayoral, E. P., Huerta, T. H., Canseco, S. P., Rodal Canales, F. J., . . . Perez-Campos, E. (2020). Obesity subtypes, related biomarkers & heterogeneity. *Indian J Med Res*, *151*(1), 11-21. https://doi.org/10.4103/ijmr.IJMR_1768_17

McFarlane, C., Vajjala, A., Arigela, H., Lokireddy, S., Ge, X., Bonala, S., . . . Sharma, M. (2014). Negative auto-regulation of myostatin expression is mediated by Smad3 and microRNA-27. *PLoS One*, *9*(1), e87687.

McGarry, J. D. (2002). Banting lecture 2001: dysregulation of fatty acid metabolism in the etiology of type 2 diabetes. *Diabetes*, *51*(1), 7-18.

McWalter, G. K., Higgins, L. G., McLellan, L. I., Henderson, C. J., Song, L., Thornalley, P. J., . . . Hayes, J. D. (2004). Transcription Factor Nrf2 Is Essential for Induction of NAD(P)H:Quinone Oxidoreductase 1, Glutathione S-Transferases, and Glutamate Cysteine Ligase by Broccoli Seeds and Isothiocyanates. *The Journal of Nutrition*, *134*(12), 3499S-3506S. https://doi.org/10.1093/jn/134.12.3499S

Meerson, A., Traurig, M., Ossowski, V., Fleming, J. M., Mullins, M., & Baier, L. J. (2013). Human adipose microRNA-221 is upregulated in obesity and affects fat metabolism downstream of leptin and TNF-α. *Diabetologia*, *56*(9), 1971-1979. https://doi.org/10.1007/s00125-013-2950-9

Mengeste, A. M., Rustan, A. C., & Lund, J. (2021). Skeletal muscle energy metabolism in obesity. *Obesity (Silver Spring)*, *29*(10), 1582-1595. https://doi.org/10.1002/oby.23227

Miano, J. M. (2003). Serum response factor: toggling between disparate programs of gene expression. *Journal of molecular and cellular cardiology*, *35*(6), 577-593.

Millay, D. P., O'Rourke, J. R., Sutherland, L. B., Bezprozvannaya, S., Shelton, J. M., Bassel-Duby, R., & Olson, E. N. (2013). Myomaker is a membrane activator of myoblast fusion and muscle formation. *Nature*, *499*(7458), 301-305. https://doi.org/10.1038/nature12343

Mogensen, M., Sahlin, K., Fernström, M., Glintborg, D., Vind, B. F., Beck-Nielsen, H., & Højlund, K. (2007). Mitochondrial respiration is decreased in skeletal muscle of patients with type 2 diabetes. *Diabetes*, *56*(6), 1592-1599. https://doi.org/10.2337/db06-0981

Mohamed, J. S., Hajira, A., Pardo, P. S., & Boriek, A. M. (2014). MicroRNA-149 inhibits PARP-2 and promotes mitochondrial biogenesis via SIRT-1/PGC-1α network in skeletal muscle. *Diabetes*, *63*(5), 1546-1559. https://doi.org/10.2337/db13-1364

Moller, D. E., & Flier, J. S. (1991). Insulin resistance--mechanisms, syndromes, and implications. *N Engl J Med*, *325*(13), 938-948. https://doi.org/10.1056/nejm199109263251307

Moradi, A., Ghasemi, F., Anvari, K., Hassanian, S. M., Simab, S. A., Ebrahimi, S., . . . ShahidSales, S. (2017). The cross-regulation between SOX15 and Wnt signaling pathway. *Journal of Cellular Physiology*, *232*(12), 3221-3225.

Morino, K., Petersen, K. F., & Shulman, G. I. (2006). Molecular mechanisms of insulin resistance in humans and their potential links with mitochondrial dysfunction. *Diabetes*, *55*(Supplement_2), S9-S15.

Moro, C., & Capel, F. (2019). Chapter 22 - Regulation of Skeletal Muscle Metabolism by Saturated and Monounsaturated Fatty Acids. In S. Walrand (Ed.), *Nutrition and Skeletal Muscle* (pp. 367-378). Academic Press. https://doi.org/https://doi.org/10.1016/B978-0-12-810422-4.00021-X

Morton, S. U., Sefton, C. R., Zhang, H., Dai, M., Turner, D. L., Uhler, M. D., & Agrawal, P. B. (2021). microRNA-mRNA Profile of Skeletal Muscle Differentiation and Relevance to Congenital Myotonic Dystrophy. *Int J Mol Sci*, *22*(5). https://doi.org/10.3390/ijms22052692

Myers, M. G., Jr., Leibel, R. L., Seeley, R. J., & Schwartz, M. W. (2010). Obesity and leptin resistance: distinguishing cause from effect. *Trends in Endocrinology & Metabolism*, *21*(11), 643-651. https://doi.org/10.1016/j.tem.2010.08.002

Myzak, M. C., Dashwood, W. M., Orner, G. A., Ho, E., & Dashwood, R. H. (2006). Sulforaphane inhibits histone deacetylase in vivo and suppresses tumorigenesis in Apc-minus mice. *FASEB J*, *20*(3), 506-508. https://doi.org/10.1096/fj.05-4785fje

Narkar, V. A., Downes, M., Yu, R. T., Embler, E., Wang, Y. X., Banayo, E., . . . Evans, R. M. (2008). AMPK and PPARdelta agonists are exercise mimetics. *Cell, 134*(3), 405-415. https://doi.org/10.1016/j.cell.2008.06.051

Ng, Y., Ramm, G., Lopez, J. A., & James, D. E. (2008). Rapid activation of Akt2 is sufficient to stimulate GLUT4 translocation in 3T3-L1 adipocytes. *Cell Metab, 7*(4), 348-356. https://doi.org/10.1016/j.cmet.2008.02.008

Niemelä, S., Miettinen, S., Sarkanen, J. R., & Ashammakhi, N. (2008). Adipose tissue and adipocyte differentiation: molecular and cellular aspects and tissue engineering applications. *Topics in Tissue Engineering, 4*(1), 26.

Nilsson, C., Raun, K., Yan, F. F., Larsen, M. O., & Tang-Christensen, M. (2012). Laboratory animals as surrogate models of human obesity. *Acta Pharmacol Sin, 33*(2), 173-181. https://doi.org/10.1038/aps.2011.203

Nimrod, A., & Ryan, K. J. (1975). Aromatization of androgens by human abdominal and breast fat tissue. *J Clin Endocrinol Metab, 40*(3), 367-372. https://doi.org/10.1210/jcem-40-3-367

O'Brien, J., Hayder, H., Zayed, Y., & Peng, C. (2018). Overview of MicroRNA Biogenesis, Mechanisms of Actions, and Circulation [10.3389/fendo.2018.00402]. *Frontiers in Endocrinology, 9*, 402.

Obesity and overweight. (2021). Retrieved 8/10 from

Okita, K., Iwahashi, H., Kozawa, J., Okauchi, Y., Funahashi, T., Imagawa, A., & Shimomura, I. (2014). Usefulness of the insulin tolerance test in patients with type 2 diabetes receiving insulin therapy. *Journal of diabetes investigation, 5*(3), 305-312.

Ortega, F. J., Mercader, J. M., Catalan, V., Moreno-Navarrete, J. M., Pueyo, N., Sabater, M., . . . Fernandez-Real, J. M. (2013). Targeting the circulating microRNA signature of obesity. *Clin Chem*, *59*(5), 781-792. https://doi.org/10.1373/clinchem.2012.195776

Osorio-Fuentealba, C., Contreras-Ferrat, A. E., Altamirano, F., Espinosa, A., Li, Q., Niu, W., . . . Jaimovich, E. (2013). Electrical stimuli release ATP to increase GLUT4 translocation and glucose uptake via PI3Kγ-Akt-AS160 in skeletal muscle cells. *Diabetes*, *62*(5), 1519-1526. https://doi.org/10.2337/db12-1066

Oswal, A., & Yeo, G. S. (2007). The leptin melanocortin pathway and the control of body weight: lessons from human and murine genetics. *Obes Rev*, *8*(4), 293-306. https://doi.org/10.1111/j.1467-789X.2007.00378.x

Pandey, A. K., Verma, G., Vig, S., Srivastava, S., Srivastava, A. K., & Datta, M. (2011). miR-29a levels are elevated in the db/db mice liver and its overexpression leads to attenuation of insulin action on PEPCK gene expression in HepG2 cells. *Mol Cell Endocrinol*, *332*(1-2), 125-133. https://doi.org/10.1016/j.mce.2010.10.004

Pandya, N. M., Dhalla, N. S., & Santani, D. D. (2006). Angiogenesis—a new target for future therapy. *Vascular pharmacology*, *44*(5), 265-274.

Poitras, V.J., et al., *Systematic review of the relationships between objectively measured physical activity and health indicators in school-aged children and youth.* Applied physiology, nutrition, and metabolism, 2016. **41**(6): p. S197-S239.

Porter, D. W., Kerr, B. D., Flatt, P. R., Holscher, C., & Gault, V. A. (2010). Four weeks administration of Liraglutide improves memory and learning as well as glycaemic control in mice with high fat dietary-induced obesity and insulin resistance. *Diabetes Obes Metab*, *12*(10), 891-899. https://doi.org/10.1111/j.1463-1326.2010.01259.x

Prats-Puig, A., Ortega, F. J., Mercader, J. M., Moreno-Navarrete, J. M., Moreno, M., Bonet, N., . . . Fernández-Real, J. M. (2013). Changes in Circulating MicroRNAs Are Associated With Childhood Obesity. *The Journal of Clinical Endocrinology & Metabolism*, *98*(10), E1655-E1660. https://doi.org/10.1210/jc.2013-1496

Price, R. A., & Gottesman, II. (1991). Body fat in identical twins reared apart: roles for genes and environment. *Behav Genet*, *21*(1), 1-7. https://doi.org/10.1007/bf01067662

Prior, B. M., Yang, H. T., & Terjung, R. L. (2004). What makes vessels grow with exercise training? *Journal of applied physiology*, *97*(3), 1119-1128.

Qi, M., & Elion, E. A. (2005). MAP kinase pathways. *J Cell Sci*, *118*(Pt 16), 3569-3572. https://doi.org/10.1242/jcs.02470

Rajendran, P., Delage, B., Dashwood, W. M., Yu, T.-W., Wuth, B., Williams, D. E., . . . Dashwood, R. H. (2011). Histone deacetylase turnover and recovery in sulforaphane-treated colon cancer cells: competing actions of 14-3-3 and Pin1 in HDAC3/SMRT corepressor complex dissociation/reassembly. *Molecular Cancer*, *10*(1), 68. https://doi.org/10.1186/1476-4598-10-68

Rakoczy, J., Fernandez-Valverde, S. L., Glazov, E. A., Wainwright, E. N., Sato, T., Takada, S., . . . Grimmond, S. M. (2013). MicroRNAs-140-5p/140-3p modulate Leydig cell numbers in the developing mouse testis. *Biology of reproduction*, *88*(6), 143-141.

Raman, M., Chen, W., & Cobb, M. H. (2007). Differential regulation and properties of MAPKs. *Oncogene*, *26*(22), 3100-3112. https://doi.org/10.1038/sj.onc.1210392

Rao Prakash, K., Kumar Roshan, M., Farkhondeh, M., Baskerville, S., & Lodish Harvey, F. (2006). Myogenic factors that regulate expression of muscle-specific microRNAs.

Proceedings of the National Academy of Sciences, *103*(23), 8721-8726. https://doi.org/10.1073/pnas.0602831103

Rawnsley, D. R., & Diwan, A. (2020). Lysosome impairment as a trigger for inflammation in obesity: The proof is in the fat. *EBioMedicine*, *56*, 102824. https://doi.org/10.1016/j.ebiom.2020.102824

Rivas, D. A., Lessard, S. J., Rice, N. P., Lustgarten, M. S., So, K., Goodyear, L. J., . . . Fielding, R. A. (2014). Diminished skeletal muscle microRNA expression with aging is associated with attenuated muscle plasticity and inhibition of IGF-1 signaling. *Faseb j*, *28*(9), 4133-4147. https://doi.org/10.1096/fj.14-254490

Roden, M. (2005). Muscle triglycerides and mitochondrial function: possible mechanisms for the development of type 2 diabetes. *International Journal of Obesity*, *29*(2), S111-S115.

Rossi, M. A., & Stuber, G. D. (2018). Overlapping Brain Circuits for Homeostatic and Hedonic Feeding. *Cell metabolism*, *27*(1), 42-56. https://doi.org/10.1016/j.cmet.2017.09.021

Sadri, H., Ghaffari, M. H., Trakooljul, N., Ceciliani, F., & Sauerwein, H. (2022). MicroRNA profiling of subcutaneous adipose tissue in periparturient dairy cows at high or moderate body condition. *Scientific reports*, *12*(1), 14748. https://doi.org/10.1038/s41598-022-18956-5

Santos, A. S., Cunha Neto, E., Fukui, R. T., Ferreira, L. R. P., & Silva, M. E. R. (2019). Increased Expression of Circulating microRNA 101-3p in Type 1 Diabetes Patients: New Insights Into miRNA-Regulated Pathophysiological Pathways for Type 1 Diabetes. *Front Immunol*, *10*, 1637. https://doi.org/10.3389/fimmu.2019.01637

Sartori, R., Romanello, V., & Sandri, M. (2021). Mechanisms of muscle atrophy and hypertrophy: implications in health and disease. *Nat Commun*, *12*(1), 330. https://doi.org/10.1038/s41467-020-20123-1

Seebacher, F., Tallis, J., McShea, K., & James, R. S. (2017). Obesity-induced decreases in muscle performance are not reversed by weight loss. *International Journal of Obesity*, *41*(8), 1271-1278. https://doi.org/10.1038/ijo.2017.81

Sharma, B., & Henderson, D. C. (2008). Sibutramine: current status as an anti-obesity drug and its future perspectives. *Expert Opin Pharmacother*, *9*(12), 2161-2173. https://doi.org/10.1517/14656566.9.12.2161

Shi, C., Huang, F., Gu, X., Zhang, M., Wen, J., Wang, X., . . . Guo, X. (2016). Adipogenic miRNA and meta-signature miRNAs involved in human adipocyte differentiation and obesity. *Oncotarget*, *7*(26), 40830-40845. https://doi.org/10.18632/oncotarget.8518

Silva, W. J., Graca, F. A., Cruz, A., Silvestre, J. G., Labeit, S., Miyabara, E. H., . . . Moriscot, A. S. (2019). miR-29c improves skeletal muscle mass and function throughout myocyte proliferation and differentiation and by repressing atrophy-related genes. *Acta Physiol (Oxf)*, *226*(4), e13278. https://doi.org/10.1111/apha.13278

Simoneau, J. A., Veerkamp, J. H., Turcotte, L. P., & Kelley, D. E. (1999). Markers of capacity to utilize fatty acids in human skeletal muscle: relation to insulin resistance and obesity and effects of weight loss. *FASEB J*, *13*(14), 2051-2060. https://doi.org/10.1096/fasebj.13.14.2051

Song, L., Lin, C., Gong, H., Wang, C., Liu, L., Wu, J., . . . Li, J. (2013). miR-486 sustains NF-κB activity by disrupting multiple NF-κB-negative feedback loops. *Cell Res*, *23*(2), 274-289. https://doi.org/10.1038/cr.2012.174

Spiegelman, B. M., Choy, L., Hotamisligil, G. S., Graves, R. A., & Tontonoz, P. (1993). Regulation of adipocyte gene expression in differentiation and syndromes of obesity/diabetes. *J Biol Chem*, *268*(10), 6823-6826.

Steinberg, G. R. (2018). Cellular Energy Sensing and Metabolism—Implications for Treating Diabetes: The 2017 Outstanding Scientific Achievement Award Lecture. *Diabetes*, *67*(2), 169-179. https://doi.org/10.2337/dbi17-0039

Steinberg, G. R., Michell, B. J., van Denderen, B. J., Watt, M. J., Carey, A. L., Fam, B. C., . . . Kemp, B. E. (2006). Tumor necrosis factor alpha-induced skeletal muscle insulin resistance involves suppression of AMP-kinase signaling. *Cell Metab*, *4*(6), 465-474. https://doi.org/10.1016/j.cmet.2006.11.005

Sternson, S. M., Shepherd, G. M., & Friedman, J. M. (2005). Topographic mapping of VMH --> arcuate nucleus microcircuits and their reorganization by fasting. *Nat Neurosci*, *8*(10), 1356-1363. https://doi.org/10.1038/nn1550

Stuart, C. A., McCurry, M. P., Marino, A., South, M. A., Howell, M. E. A., Layne, A. S., . . . Stone, M. H. (2013). Slow-Twitch Fiber Proportion in Skeletal Muscle Correlates With Insulin Responsiveness. *The Journal of Clinical Endocrinology & Metabolism*, *98*(5), 2027-2036. https://doi.org/10.1210/jc.2012-3876

Suleiman, J. B., Mohamed, M., & Bakar, A. B. A. (2020). A systematic review on different models of inducing obesity in animals: Advantages and limitations. *J Adv Vet Anim Res*, *7*(1), 103-114. https://doi.org/10.5455/javar.2020.g399

Taguchi, Y. H. (2015). Apparent microRNA-Target-specific histone modification in mammalian spermatogenesis. *Evolutionary Bioinformatics*, *11*, EBO-S21832.

Tallis, J., James, R. S., & Seebacher, F. (2018). The effects of obesity on skeletal muscle contractile function. *J Exp Biol*, *221*(Pt 13). https://doi.org/10.1242/jeb.163840

Tamakoshi, K., Wakai, K., Kojima, M., Watanabe, Y., Hayakawa, N., Toyoshima, H., . . . Tamakoshi, A. (2004). A prospective study of body size and colon cancer mortality in Japan: The JACC Study. *Int J Obes Relat Metab Disord*, *28*(4), 551-558. https://doi.org/10.1038/sj.ijo.0802603

Tang, Q. Q., & Lane, M. D. (2012). Adipogenesis: from stem cell to adipocyte. *Annu Rev Biochem*, *81*, 715-736. https://doi.org/10.1146/annurev-biochem-052110-115718

Tanner, C. J., Barakat, H. A., Dohm, G. L., Pories, W. J., MacDonald, K. G., Cunningham, P. R. G., . . . Houmard, J. A. (2002). Muscle fiber type is associated with obesity and weight loss. *American Journal of Physiology-Endocrinology and Metabolism*, *282*(6), E1191-E1196. https://doi.org/10.1152/ajpendo.00416.2001

Tanaka, C., J.J. Reilly, and W.Y. Huang, *Longitudinal changes in objectively measured sedentary behaviour and their relationship with adiposity in children and adolescents: systematic review and evidence appraisal.* Obesity Reviews, 2014. **15**(10): p. 791-803.

Tardif, G., Pelletier, J.-P., Fahmi, H., Hum, D., Zhang, Y., Kapoor, M., & Martel-Pelletier, J. (2013). NFAT3 and TGF-β/SMAD3 regulate the expression of miR-140 in osteoarthritis. *Arthritis research & therapy*, *15*(6), 1-14.

Thorens, B., & Mueckler, M. (2010). Glucose transporters in the 21st Century. *Am J Physiol Endocrinol Metab*, *298*(2), E141-145. https://doi.org/10.1152/ajpendo.00712.2009

Tseng, Y.-H., Cypess, A. M., & Kahn, C. R. (2010). Cellular bioenergetics as a target for obesity therapy. *Nature reviews Drug discovery*, *9*(6), 465-482.

Ulrich, F., Krieg, M., Schötz, E.-M., Link, V., Castanon, I., Schnabel, V., . . . Heisenberg, C.-P. (2005). Wnt11 functions in gastrulation by controlling cell cohesion through Rab5c and E-cadherin. *Developmental cell*, *9*(4), 555-564.

Vomund, S., Schäfer, A., Parnham, M. J., Brüne, B., & von Knethen, A. (2017). Nrf2, the Master Regulator of Anti-Oxidative Responses. *Int J Mol Sci*, *18*(12). https://doi.org/10.3390/ijms18122772

Wahren, J. (1977). Glucose turnover during exercise in man. *Ann N Y Acad Sci*, *301*, 45-55. https://doi.org/10.1111/j.1749-6632.1977.tb38184.x

Wang, H., Garzon, R., Sun, H., Ladner, K. J., Singh, R., Dahlman, J., . . . Chandler, D. S. (2008). NF-κB–YY1–miR-29 regulatory circuitry in skeletal myogenesis and rhabdomyosarcoma. *Cancer cell*, *14*(5), 369-381.

Wang, L., Chen, X., Zheng, Y., Li, F., Lu, Z., Chen, C., . . . Chen, H. (2012). MiR-23a inhibits myogenic differentiation through down regulation of fast myosin heavy chain isoforms. *Experimental Cell Research*, *318*(18), 2324-2334. https://doi.org/https://doi.org/10.1016/j.yexcr.2012.06.018

Wang, L., Yao, J., Sun, H., He, K., Tong, D., Song, T., & Huang, C. (2017). MicroRNA-101 suppresses progression of lung cancer through the PTEN/AKT signaling pathway by targeting DNA methyltransferase 3A. *Oncol Lett*, *13*(1), 329-338. https://doi.org/10.3892/ol.2016.5423

Wang, L., Zhou, L., Jiang, P., Lu, L., Chen, X., Lan, H., . . . Wang, H. (2012). Loss of miR-29 in myoblasts contributes to dystrophic muscle pathogenesis. *Molecular Therapy*, *20*(6), 1222-1233.

Wang, Y., Keys, D. N., Au-Young, J. K., & Chen, C. (2009). MicroRNAs in embryonic stem cells. *J Cell Physiol*, *218*(2), 251-255. https://doi.org/10.1002/jcp.21607

Wei, W., He, H. B., Zhang, W. Y., Zhang, H. X., Bai, J. B., Liu, H. Z., . . . Zhao, S. H. (2013). miR-29 targets Akt3 to reduce proliferation and facilitate differentiation of myoblasts in skeletal muscle development. *Cell Death & Disease*, *4*(6), e668-e668. https://doi.org/10.1038/cddis.2013.184

Weinhold, B. (2006). Epigenetics: the science of change. In *Environ Health Perspect* (Vol. 114, pp. A160-167). https://doi.org/10.1289/ehp.114-a160

Weis, S., Llenos, I. C., Dulay, J. R., Elashoff, M., Martínez-Murillo, F., & Miller, C. L. (2007). Quality control for microarray analysis of human brain samples: The impact of postmortem factors, RNA characteristics, and histopathology. *J Neurosci Methods*, *165*(2), 198-209. https://doi.org/10.1016/j.jneumeth.2007.06.001

Weisberg, S. P., McCann, D., Desai, M., Rosenbaum, M., Leibel, R. L., & Ferrante, A. W., Jr. (2003). Obesity is associated with macrophage accumulation in adipose tissue. *The Journal of Clinical Investigation*, *112*(12), 1796-1808. https://doi.org/10.1172/JCI19246

Wellen, K. E., & Hotamisligil, G. S. (2003). Obesity-induced inflammatory changes in adipose tissue. *The Journal of Clinical Investigation*, *112*(12), 1785-1788. https://doi.org/10.1172/JCI20514

Wirth, A., Wabitsch, M., & Hauner, H. (2014). The prevention and treatment of obesity. *Dtsch Arztebl Int*, *111*(42), 705-713. https://doi.org/10.3238/arztebl.2014.0705

Wondmkun, Y. T. (2020). Obesity, Insulin Resistance, and Type 2 Diabetes: Associations and Therapeutic Implications. *Diabetes Metab Syndr Obes*, *13*, 3611-3616. https://doi.org/10.2147/dmso.s275898

Woods, Y. L., Petrie, J. R., & Sutherland, C. (2009). Dissecting insulin signaling pathways: individualised therapeutic targets for diagnosis and treatment of insulin resistant states. *Endocr Metab Immune Disord Drug Targets*, *9*(2), 187-198. https://doi.org/10.2174/187153009788452408

Wright, S. M., & Aronne, L. J. (2012). Causes of obesity. *Abdom Imaging*, *37*(5), 730-732. https://doi.org/10.1007/s00261-012-9862-x

Xu, L., Nagata, N., & Ota, T. (2018). Glucoraphanin: a broccoli sprout extract that ameliorates obesity-induced inflammation and insulin resistance. *Adipocyte*, *7*(3), 218-225. https://doi.org/10.1080/21623945.2018.1474669

Xu, P., Vernooy, S. Y., Guo, M., & Hay, B. A. (2003). The Drosophila microRNA Mir-14 suppresses cell death and is required for normal fat metabolism. *Curr Biol*, *13*(9), 790-795. https://doi.org/10.1016/s0960-9822(03)00250-1

Xu, X., Grijalva, A., Skowronski, A., van Eijk, M., Serlie, M. J., & Ferrante, A. W., Jr. (2013). Obesity activates a program of lysosomal-dependent lipid metabolism in adipose tissue macrophages independently of classic activation. *Cell Metab*, *18*(6), 816-830. https://doi.org/10.1016/j.cmet.2013.11.001

Yao, Q., Chen, Y., & Zhou, X. (2019). The roles of microRNAs in epigenetic regulation. *Curr Opin Chem Biol*, *51*, 11-17. https://doi.org/10.1016/j.cbpa.2019.01.024

Yuan, Y., Shen, Y., Xue, L., & Fan, H. (2013). miR-140 suppresses tumor growth and metastasis of non-small cell lung cancer by targeting insulin-like growth factor 1 receptor. *PLoS One*, *8*(9), e73604. https://doi.org/10.1371/journal.pone.0073604

Zetser, A., Gredinger, E., & Bengal, E. (1999). p38 mitogen-activated protein kinase pathway promotes skeletal muscle differentiation: participation of the Mef2c transcription factor. *Journal of Biological Chemistry*, *274*(8), 5193-5200.

Zhang, G., & Pradhan, S. (2014). Mammalian epigenetic mechanisms. *IUBMB Life*, *66*(4), 240-256. https://doi.org/10.1002/iub.1264

Zhang, T., Li, L., Shang, Q., Lv, C., Wang, C., & Su, B. (2015). Circulating miR-126 is a potential biomarker to predict the onset of type 2 diabetes mellitus in susceptible individuals. *Biochemical and Biophysical Research Communications*, *463*(1-2), 60-63.

Zhang, Y., Proenca, R., Maffei, M., Barone, M., Leopold, L., & Friedman, J. M. (1994). Positional cloning of the mouse obese gene and its human homologue. *Nature*, *372*(6505), 425-432. https://doi.org/10.1038/372425a0

Zhang, Y., Zhao, Y. P., Gao, Y. F., Fan, Z. M., Liu, M. Y., Cai, X. Y., . . . Gao, C. L. (2015). Silencing miR-106b improves palmitic acid-induced mitochondrial dysfunction and insulin resistance in skeletal myocytes. *Molecular Medicine Reports*, *11*(5), 3834-3841.

Zhang, Z., Cao, Y., Zhai, Y., Ma, X., An, X., Zhang, S., & Li, Z. (2018). MicroRNA-29b regulates DNA methylation by targeting Dnmt3a/3b and Tet1/2/3 in porcine early embryo development [https://doi.org/10.1111/dgd.12537]. *Development, Growth & Differentiation*, *60*(4), 197-204. https://doi.org/https://doi.org/10.1111/dgd.12537

Zhang, Z., Jiang, H., Li, X., Chen, X., & Huang, Y. (2019). MiR-92a regulates brown adipocytes differentiation, mitochondrial oxidative respiration, and heat generation by targeting SMAD7. *J Cell Biochem*. https://doi.org/10.1002/jcb.29539

Zhao, Q., Li, S., Li, N., Yang, X., Ma, S., Yang, A., . . . Jiang, Y. (2017). miR-34a Targets HDAC1-Regulated H3K9 Acetylation on Lipid Accumulation Induced by

Homocysteine in Foam Cells [https://doi.org/10.1002/jcb.26126]. *Journal of Cellular Biochemistry*, *118*(12), 4617-4627. https://doi.org/https://doi.org/10.1002/jcb.26126

Zheng, H., Whitman, S. A., Wu, W., Wondrak, G. T., Wong, P. K., Fang, D., & Zhang, D. D. (2011). Therapeutic potential of Nrf2 activators in streptozotocin-induced diabetic nephropathy. *Diabetes*, *60*(11), 3055-3066. https://doi.org/10.2337/db11-0807

Zhou, Y., Gu, P., Shi, W., Li, J., Hao, Q., Cao, X., . . . Zeng, Y. (2016). MicroRNA-29a induces insulin resistance by targeting PPARδ in skeletal muscle cells. *International journal of molecular medicine*, *37*(4), 931-938. https://doi.org/10.3892/ijmm.2016.2499

Zierath, J. R., Krook, A., & Wallberg-Henriksson, H. (2000). Insulin action and insulin resistance in human skeletal muscle. *Diabetologia*, *43*(7), 821-835.

Zou, M.-X., Huang, W., Wang, X.-B., Lv, G.-H., Li, J., & Deng, Y.-W. (2014). Identification of miR-140-3p as a marker associated with poor prognosis in spinal chordoma. *International journal of clinical and experimental pathology*, *7*(8), 4877.

Appendix

Table S1- showing post-alignment QC.

Sample name	Groups	Total reads	Total alignment	Aligned Mature miRNA base22	Coverage	Avg. coverage depth	Avg. length	Avg. quality Phred-33	%GC
30Days-SFN-IP-Inj-M1-SKM_S1	SFN	272380	141926	52.105	0.0562	2.65677	49.508	27.532	50.0779
30Days-SFN-IP-Inj-M3-SKM_S2	SFN	486085	280527	57.711	0.0610	4.52007	49.569	27.747	47.9603
30Days-SFN-IP-Inj-M4-SKM_S3	SFN	257391	131788	51.201	0.0435	3.0553	49.467	27.458	48.4231
30Days-SFN-IP-Inj-M5-SKM_S4	SFN	334458	172095	51.454	0.0422	4.0387	49.542	27.468	48.4858
30Days-SFN-IP-Inj-M6-SKM_S5	SFN	326559	154856	47.420	0.0642	2.45799	49.410	27.527	49.1936
30Days-Vehicle-IP-Inj-M1-SKM_S6	Vehicle	301203	161187	53.514	0.0499	3.24654	49.501	27.655	48.514
30Days-Vehicle-IP-Inj-M2-SKM_S7	Vehicle	356216	180546	50.684	0.04530	3.78184	49.322	27.629	48.4632
30Days-Vehicle-IP-Inj-M3-SKM_S8	Vehicle	299438	129008	43.083	0.0457	2.67171	48.976	27.628	49.0246
30Days-Vehicle-IP-Inj-M4-SKM_S9	Vehicle	241452	133863	55.440	0.0277	4.64721	49.471	27.691	47.8092
30Days-Vehicle-IP-Inj-M6-SKM_S10	Vehicle	291448	141070	48.403	0.0533	2.70705	49.363	27.636	49.3294

Table S2- Normalization data for all study samples- count

Gene Symbol	30Days-SFN-IP-Inj-M1-SKM_S1	30Days-SFN-IP-Inj-M5-SKM_S4	30Days-Vehicle-IP-Inj-M2-SKM_S7	30Days-SFN-IP-Inj-M3-SKM_S2	30Days-SFN-IP-Inj-M6-SKM_S5	30Days-Vehicle-IP-Inj-M4-SKM_S9	30Days-Vehicle-IP-Inj-M1-SKM_S6	30Days-Vehicle-IP-Inj-M6-SKM_S10	30Days-SFN-IP-Inj-M4-SKM_S3	30Days-Vehicle-IP-Inj-M3-SKM_S8
mmu-let-7a-1-3p	5.05387	1.18593	3.37078	2.59159	0	0.784612	0.95268	3.19447	0	1.40768
mmu-let-7a-5p	34.1136	46.8443	37.6403	46.6486	27.6111	44.7229	36.2019	59.0977	62.6689	35.192
mmu-let-7b-5p	16.4251	12.4523	14.6067	10.3664	10.7377	7.06151	7.62144	9.58341	17.9054	7.0384
mmu-let-7c-2-3p	2.52693	0	1.68539	1.03664	1.53395	2.35384	0	3.19447	4.47635	4.22304
mmu-let-7c-5p	22.7424	29.6483	20.2247	23.8426	12.2716	24.323	21.9117	15.9723	46.2556	16.8922
mmu-let-7d-3p	10.1077	7.70856	6.17976	8.29309	7.66975	3.92306	12.3848	14.3751	8.95269	8.44608
mmu-let-7d-5p	35.3771	27.8694	25.2808	41.4654	26.0772	36.8768	19.0536	46.3198	31.3344	29.5613
mmu-let-7e-5p	5.05387	4.74373	1.68539	4.14654	0	0.784612	2.85804	1.59723	5.96846	5.63072
mmu-let-7f-5p	128.874	149.427	114.045	163.789	173.336	139.661	125.754	122.987	153.688	136.545
mmu-let-7g-5p	130.137	164.252	131.46	165.862	161.065	165.553	103.842	121.39	129.814	178.775
mmu-let-7i-3p	2.52693	0.592966	2.80898	1.55495	4.60185	0.784612	1.90536	3.19447	0	4.22304
mmu-let-7i-5p	68.2272	126.895	93.2581	124.915	75.1636	102	81.9305	71.8756	110.417	83.0531
mmu-miR-100-5p	66.9638	40.9146	39.8875	44.057	61.358	57.2767	57.1608	39.9309	32.8265	43.6381
mmu-miR-101a-3p	7.5808	29.0553	54.4942	19.6961	30.679	26.6768	30.4858	81.459	28.3502	43.6381
mmu-miR-101b-3p	8.84427	16.603	17.9775	13.4763	9.2037	18.0461	20.959	20.7641	11.9369	19.7075
mmu-miR-103-3p	22.7424	21.9397	22.4718	17.1045	10.7377	15.6922	15.2429	14.3751	13.429	12.6691
mmu-miR-106b-3p	2.52693	1.7789	2.24718	1.55495	0	1.56922	0.95268	1.59723	0	2.81536

mmu-miR-107-3p	3.7904	5.92966	3.37078	2.59159	3.0679	3.92306	2.85804	3.19447	1.49212	1.40768
mmu-miR-10a-5p	58.1195	64.0403	73.5953	49.7585	102.775	66.692	42.8706	57.5005	77.59	59.1226
mmu-miR-10b-5p	96.0235	195.086	115.168	76.1928	134.988	265.199	115.274	138.959	104.448	142.176
mmu-miR-122-5p	0	0.296483	0	3.36907	0	1.56922	0	7.98617	0.746058	3.5192
mmu-miR-122b-3p	0	0.296483	0	3.36907	0	1.56922	0	7.98617	0.746058	3.5192
mmu-miR-1249-3p	6.31734	0	1.12359	0	6.1358	0	0	1.59723	1.49212	4.22304
mmu-miR-125a-5p	44.2213	26.0905	23.5954	32.654	42.9506	43.1537	42.8706	36.7364	16.4133	32.3766
mmu-miR-125b-2-3p	0	0	1.12359	1.55495	4.60185	1.56922	0.95268	1.59723	0	0
mmu-miR-125b-5p	50.5387	16.603	15.7303	21.251	35.2809	37.6614	26.6751	28.7502	7.46058	22.5229
mmu-miR-126a-3p	375.982	417.535	525.863	355.259	573.068	434.933	484.619	624.313	484.768	559.272
mmu-miR-126a-5p	10.6598	36.4738	58.4249	21.0076	118.277	63.7643	70.6324	71.4423	39.8255	31.1067
mmu-miR-126b-3p	27.2442	7.40561	7.3052	0.243478	1.37084	9.98931	0.818633	19.6001	0.461577	16.7544
mmu-miR-126b-5p	0.532386	4.06126	0.542994	0.825943	23.6382	0.526649	0.29293	3.40269	4.64614	3.80045
mmu-miR-127-3p	8.84427	6.52262	16.8539	9.32973	7.66975	10.9846	9.5268	4.7917	32.8265	1.40768
mmu-miR-128-3p	17.6885	18.9749	13.4831	16.5862	13.8056	16.4769	20.0063	23.9585	5.96846	25.3382
mmu-miR-130a-3p	1.26347	0.592966	1.12359	0.518318	1.53395	1.56922	0.95268	1.59723	1.49212	0
mmu-miR-133a-3p	3329.24	580.514	934.267	1163.11	1165.8	943.104	1162.27	1006.26	1007.18	1230.31
mmu-miR-133a-5p	24.0059	7.11559	5.05616	10.3664	15.3395	11.7692	10.4795	17.5696	16.4133	9.85376
mmu-miR-133b-3p	415.681	79.4574	151.685	174.155	164.133	143.584	172.435	145.348	164.133	140.768
mmu-miR-136-3p	0.631734	0.296483	1.96629	0.518318	0	0.784612	0.47634	3.19447	2.23817	1.40768
mmu-miR-139-5p	8.84427	11.8593	4.49437	4.66486	9.2037	3.92306	7.62144	7.98617	7.46058	4.22304
mmu-miR-140-3p	31.5867	41.5076	35.9549	43.5387	49.0864	25.1076	37.1545	31.9447	55.2083	28.1536
mmu-miR-140-5p	1.26347	2.37186	3.37078	1.03664	1.53395	3.92306	6.66876	1.59723	1.49212	1.40768
mmu-miR-142a-5p	6.31734	93.0956	7.86514	5.7015	1.53395	2.35384	7.62144	1.59723	8.95269	9.85376
mmu-miR-142b	1.26213	3.75931	1.1224	0	0	0	1.90334	0	0	1.40619
mmu-miR-143-3p	1351.91	2753.73	2899.99	2594.7	3497.41	2845.79	3760.23	2667.38	2679.84	2747.79
mmu-miR-143-5p	0	1.7789	1.12359	0.518318	0	2.35384	0	1.59723	2.98423	1.40768
mmu-miR-144-5p	3.7904	0	1.12359	0.518318	0	0.784612	0	3.19447	1.49212	4.22304
mmu-miR-145a-3p	12.6347	13.6382	11.7977	9.84804	18.4074	8.63074	12.3848	17.5696	10.4448	18.2998
mmu-miR-145a-5p	58.1195	56.9247	53.3706	48.7219	47.5525	56.4921	42.8706	41.5281	29.8423	38.0074
mmu-miR-146a-5p	10.1077	55.7388	15.7303	12.958	9.2037	14.9076	9.5268	6.38894	17.9054	9.85376
mmu-miR-146b-5p	2.52693	7.11559	5.05616	5.18318	12.2716	7.06151	3.81072	3.19447	4.47635	2.81536
mmu-miR-148a-3p	13.8981	49.2162	47.1909	37.8372	26.0772	34.5229	31.4385	19.1668	62.6689	29.5613
mmu-miR-148b-3p	6.31734	9.48745	11.2359	12.958	4.60185	7.06151	7.62144	15.9723	8.95269	12.6691

mmu-miR-149-5p	35.3771	8.89449	10.6741	12.4396	16.8735	14.9076	15.2429	20.7641	7.46058	11.2614
mmu-miR-150-5p	11.3712	80.6434	9.55053	6.73814	12.2716	11.7692	6.66876	6.38894	4.47635	8.44608
mmu-miR-151-3p	6.31734	8.30152	4.49437	5.18318	6.1358	8.63074	11.4322	3.19447	4.47635	12.6691
mmu-miR-151-5p	24.0059	10.0804	17.9775	23.3243	10.7377	26.6768	21.9117	27.153	23.8738	23.9306
mmu-miR-152-3p	13.8981	20.1608	26.4044	19.6961	18.4074	18.8307	20.0063	27.153	10.4448	19.7075
mmu-miR-155-5p	5.05387	8.89449	0.561796	2.59159	1.53395	1.56922	1.90536	1.59723	1.49212	0
mmu-miR-15a-5p	1.26347	5.92966	6.17976	3.62823	4.60185	1.56922	9.5268	7.98617	4.47635	8.44608
mmu-miR-15b-5p	6.31734	13.0452	4.49437	4.14654	12.2716	7.06151	0	3.19447	7.46058	1.40768
mmu-miR-16-5p	88.4427	93.6886	80.3368	72.5645	75.1636	69.0459	74.3091	68.6811	82.0664	80.2377
mmu-miR-181a-2-3p	1.26347	1.7789	1.68539	4.14654	0	5.49229	0	1.59723	0	4.22304
mmu-miR-181a-5p	15.1616	16.0101	12.9213	19.1778	10.7377	18.0461	14.2902	7.98617	4.47635	7.0384
mmu-miR-181b-5p	2.52693	2.96483	6.74155	6.21982	4.60185	7.06151	3.81072	4.7917	4.47635	7.0384
mmu-miR-181c-5p	1.26347	1.7789	0.561796	1.03664	1.53395	1.56922	3.81072	1.59723	1.49212	2.81536
mmu-miR-182-5p	2.52693	0	13.4831	0.518318	0	1.56922	0	0	1.49212	0
mmu-miR-1839-5p	7.5808	5.92966	5.05616	3.62823	1.53395	3.92306	6.66876	4.7917	5.96846	9.85376
mmu-miR-1843a-5p	0	2.96483	6.74155	1.55495	3.0679	2.35384	0.95268	1.59723	4.47635	2.81536
mmu-miR-1843b-5p	2.52693	2.37186	3.37078	3.62823	7.66975	1.56922	0.95268	0	2.98423	0
mmu-miR-185-5p	3.7904	3.5578	2.24718	5.7015	4.60185	7.84612	4.7634	4.7917	7.46058	4.22304
mmu-miR-186-5p	15.1616	10.0804	20.7864	16.5862	18.4074	18.0461	22.8643	25.5558	16.4133	18.2998
mmu-miR-190a-5p	0	0	2.24718	1.03664	0	0	0.95268	3.19447	1.49212	0
mmu-miR-191-5p	42.9579	29.6483	26.9662	31.6174	18.4074	33.7383	20.959	22.3613	20.8896	25.3382
mmu-miR-192-5p	2.52693	1.7789	2.24718	4.66486	4.60185	3.92306	0.95268	7.98617	1.49212	2.81536
mmu-miR-193b-3p	1.26347	1.7789	5.05616	0.518318	0	0	0	0	2.98423	0
mmu-miR-194-5p	0	2.96483	1.12359	0.518318	0	0	1.90536	3.19447	1.49212	1.40768
mmu-miR-195a-5p	34.1136	27.8694	30.337	23.8426	30.679	17.2615	28.5804	19.1668	16.4133	26.7459
mmu-miR-196a-5p	15.1616	10.0804	6.17976	9.32973	4.60185	7.84612	5.71608	6.38894	10.4448	8.44608
mmu-miR-196b-5p	5.05387	2.37186	3.37078	5.18318	3.0679	3.13845	1.90536	3.19447	2.98423	5.63072
mmu-miR-199a-3p	13.8981	14.2312	33.7078	20.7327	12.2716	11.7692	19.0536	14.3751	23.8738	19.7075
mmu-miR-199a-5p	8.84427	10.6734	19.6629	16.0679	1.53395	7.06151	16.1956	3.19447	14.9212	9.85376
mmu-miR-199b-3p	24.0059	13.6382	24.719	27.4709	10.7377	11.7692	16.1956	12.7779	14.9212	16.8922
mmu-miR-199b-5p	0	0.592966	2.24718	2.07327	0	0.784612	2.85804	1.59723	2.98423	1.40768
mmu-miR-1a-3p	10146.9	11373.7	14557.3	24402.4	13544.8	18272.1	15998.4	16175.2	20236.1	19364
mmu-miR-1b-5p	10038.2	10666.9	13612.3	22370.1	12504.8	17264.6	14971.4	14983.7	18269.5	17448.2
mmu-miR-203-3p	0.0117293	0.033029	5.50734	0.024059	0.056961	0.007284	3.81063	0.074139	0.0554078	0.0130681

mmu-miR-203b-5p	1.25174	3.52477	1.23421	2.56753	6.07884	0.777328	9.48E-05	7.91204	5.91305	1.39461
mmu-miR-204-5p	5.05387	0	0	2.59159	3.0679	0	0.95268	0	1.49212	0
mmu-miR-206-3p	25.2693	17.789	29.7752	18.6595	53.6883	24.323	29.5331	62.2922	7.46058	33.7843
mmu-miR-20a-5p	0	1.18593	1.12359	0.518318	3.0679	1.56922	1.90536	0	2.98423	0
mmu-miR-214-3p	0	2.37186	5.61796	2.59159	3.0679	2.35384	1.90536	1.59723	4.47635	0
mmu-miR-21a-5p	200.891	540.785	761.795	397.032	326.731	318.553	333.438	362.572	795.298	354.735
mmu-miR-22-3p	492.752	262.684	503.369	407.398	473.991	466.06	599.236	578.199	735.613	506.765
mmu-miR-22-5p	15.1616	14.2312	10.1123	14.5129	21.4753	14.123	14.2902	7.98617	17.9054	19.7075
mmu-miR-221-3p	2.52693	8.89449	5.61796	5.18318	4.60185	8.63074	7.62144	3.19447	10.4448	2.81536
mmu-miR-222-3p	3.7904	2.96483	4.49437	2.59159	1.53395	6.2769	0.95268	7.98617	5.96846	2.81536
mmu-miR-223-3p	0	8.89449	5.05616	1.55495	0	3.92306	5.71608	3.19447	4.47635	0
mmu-miR-23a-3p	130.137	136.975	123.595	111.957	136.522	116.907	150.524	121.39	135.783	129.507
mmu-miR-23b-3p	89.7062	58.7036	51.1234	80.8576	65.9599	78.4612	97.1734	95.8341	50.7319	53.4918
mmu-miR-24-2-5p	0.0938344	0.077067	6.14878	0.0818	0.113923	0.101974	7.36359	0.103795	0.0554078	0.182953
mmu-miR-24-3p	87.4373	64.1715	62.6402	79.6224	104.371	80.3529	132.182	64.688	90.0605	56.3072
mmu-miR-25-3p	11.3712	24.9046	21.3482	18.1411	26.0772	18.0461	7.62144	7.98617	22.3817	5.63072
mmu-miR-26a-5p	519.285	463.699	419.1	629.238	507.738	631.613	543.981	578.199	429.729	380.074
mmu-miR-26b-5p	84.6523	125.116	103.932	130.616	75.1636	100.43	116.227	113.404	162.641	105.576
mmu-miR-27a-3p	55.5926	70.5629	75.8425	59.6066	73.6296	56.4921	109.558	113.404	77.59	87.2761
mmu-miR-27b-3p	151.616	143.498	150.561	178.301	213.219	174.969	218.164	236.391	143.243	229.452
mmu-miR-28a-3p	2.52693	1.7789	0	2.59159	1.53395	2.35384	0	0	1.49212	0
mmu-miR-28a-5p	7.5808	2.37186	3.93257	4.66486	6.1358	5.49229	6.66876	4.7917	7.46058	7.0384
mmu-miR-29a-3p	320.921	295.89	255.617	221.84	360.478	189.092	336.296	327.433	314.836	339.251
mmu-miR-29b-3p	1.26347	1.18593	3.37078	5.18318	1.53395	2.35384	1.90536	0	4.47635	2.81536
mmu-miR-29c-3p	7.5808	8.30152	11.7977	6.21982	1.53395	6.2769	15.2429	17.5696	2.98423	9.85376
mmu-miR-300-3p	1.26347	0	1.12359	2.07327	1.53395	0	0	1.59723	2.98423	0
mmu-miR-3068-3p	2.52693	1.18593	0.561796	0.518318	1.53395	1.56922	3.81072	1.59723	1.49212	1.40768
mmu-miR-3071-5p	0.631734	0.296483	1.96629	0.518318	0	0.784612	0.47634	3.19447	2.23817	1.40768
mmu-miR-3074-2-3p	10.0139	8.22446	5.08714	8.72961	12.1577	10.8826	0.257854	11.0768	5.91305	19.5246
mmu-miR-3074-5p	37.6459	21.2157	62.6402	24.5595	16.8109	24.7852	35.4896	64.688	11.4034	56.3072
mmu-miR-30a-3p	26.5328	26.6835	40.4493	66.3447	38.3488	32.1691	38.1072	46.3198	34.3187	26.7459
mmu-miR-30a-5p	899.589	765.519	1009.55	1395.31	1394.36	796.381	898.378	1140.43	1063.88	1271.13
mmu-miR-30b-5p	65.7003	42.6935	67.4155	67.3814	76.6975	58.8459	60.0189	68.6811	64.161	61.9379
mmu-miR-30c-2-3p	3.7904	0.592966	1.12359	3.10991	0	3.13845	1.90536	1.59723	0	0

mmu-miR-30c-5p	122.556	90.7238	133.146	187.631	122.716	142.015	123.848	148.543	143.243	149.214
mmu-miR-30d-5p	314.603	315.458	305.617	340.017	391.157	378.183	370.593	332.225	222.325	374.443
mmu-miR-30e-3p	12.6021	25.4009	20.7524	22.7786	15.3395	20.7858	30.3747	27.9253	12.683	19.4652
mmu-miR-30e-5p	118.766	126.895	250.561	157.569	260.772	147.507	196.252	340.211	241.723	285.759
mmu-miR-30f	0.0325581	0.096666	0.034069	0.027392	15.3395	1.96799	0.111037	0.824959	12.683	0.242308
mmu-miR-3102-3p	3.7904	0.592966	1.68539	0.518318	0	0.784612	0	1.59723	0	0
mmu-miR-320-3p	2.52693	1.18593	0.561796	0	1.53395	0.784612	0.95268	1.59723	2.98423	1.40768
mmu-miR-322-3p	8.84427	4.15076	4.49437	6.21982	4.60185	4.70767	5.71608	6.38894	1.49212	4.22304
mmu-miR-322-5p	2.52693	4.74373	3.93257	4.14654	6.1358	5.49229	5.71608	3.19447	7.46058	7.0384
mmu-miR-328-3p	15.1616	2.37186	5.61796	6.73814	4.60185	3.13845	6.66876	7.98617	1.49212	1.40768
mmu-miR-335-3p	0	2.96483	2.24718	1.03664	0	0.784612	1.90536	0	0	0
mmu-miR-335-5p	10.1077	20.7538	6.74155	9.32973	7.66975	20.3999	9.5268	15.9723	16.4133	2.81536
mmu-miR-337-5p	0	0.592966	1.12359	1.55495	3.0679	2.35384	0	0.798617	2.98423	2.81536
mmu-miR-339-5p	3.7904	2.96483	0	2.59159	4.60185	1.56922	0.95268	1.59723	0	0
mmu-miR-340-3p	3.7904	2.96483	3.37078	1.03664	1.53395	2.35384	0.95268	0	0	2.81536
mmu-miR-340-5p	7.5808	9.48745	5.61796	6.73814	4.60185	7.06151	5.71608	4.7917	1.49212	5.63072
mmu-miR-342-3p	3.7904	7.11559	1.68539	0.518318	3.0679	0.784612	1.90536	0	0	0
mmu-miR-34a-5p	0	2.37186	1.12359	0.518318	4.60185	2.35384	0	1.59723	0	0
mmu-miR-350-3p	1.26347	2.37186	1.12359	1.55495	0	0.784612	0.95268	0	0	0
mmu-miR-351-5p	3.7904	1.7789	3.37078	4.66486	4.60185	0	1.90536	7.98617	4.47635	1.40768
mmu-miR-3535	11.3712	11.2664	1.68539	8.29309	7.66975	3.92306	20.0063	3.19447	7.46058	1.40768
mmu-miR-361-3p	0	1.18593	1.12359	1.03664	0	0.784612	0.95268	0	1.49212	2.81536
mmu-miR-361-5p	6.31734	8.30152	6.74155	7.25645	7.66975	3.13845	8.57412	4.7917	2.98423	9.85376
mmu-miR-362-3p	0	1.7789	2.24718	0.518318	0	0.784612	0.95268	1.59723	0	0
mmu-miR-365-3p	8.84427	4.74373	6.74155	5.7015	4.60185	9.41535	5.71608	4.7917	4.47635	4.22304
mmu-miR-369-3p	1.26347	0.592966	2.24718	3.62823	0	3.13845	2.85804	0	1.49212	0
mmu-miR-374b-5p	0	3.45676	2.7946	1.03664	0.001163	0.000595	3.81072	0.002423	8.69846	0
mmu-miR-378a-3p	312.076	186.191	335.954	369.042	470.923	265.984	289.615	392.92	256.644	367.404
mmu-miR-378a-5p	11.3712	5.92966	8.42694	7.25645	16.8735	6.2769	8.57412	11.1806	5.96846	9.85376
mmu-miR-378b	1.26347	1.7789	1.68539	1.03664	3.0679	2.35384	1.90536	0	0	1.40768
mmu-miR-378c	27.7963	16.603	28.6516	34.7273	38.3488	26.6768	25.7224	23.9585	11.9369	42.2304
mmu-miR-379-5p	3.7904	3.5578	20.7864	11.403	9.2037	7.84612	8.57412	11.1806	37.3029	8.44608
mmu-miR-411-5p	2.52693	2.37186	11.2359	6.21982	6.1358	5.49229	1.90536	3.19447	5.96846	4.22304
mmu-miR-423-3p	5.05387	5.92966	2.80898	2.07327	9.2037	2.35384	8.57412	3.19447	4.47635	4.22304
mmu-miR-425-5p	5.05387	5.33669	5.61796	4.14654	1.53395	8.63074	0.95268	4.7917	2.98423	1.40768

mmu-miR-434-3p	7.5808	5.33669	5.05616	8.81141	3.0679	7.06151	8.57412	1.59723	7.46058	7.0384
mmu-miR-434-5p	1.26347	0	2.24718	1.55495	1.53395	0	0.95268	0	2.98423	0
mmu-miR-451a	16.4251	17.789	19.6629	14.5129	24.5432	28.246	16.1956	25.5558	26.8581	33.7843
mmu-miR-484	3.7904	1.7789	2.24718	3.62823	3.0679	1.56922	1.90536	3.19447	1.49212	2.81536
mmu-miR-486a-3p	36.6775	10.972	8.96595	51.7884	13.9154	21.1376	4.15245	21.7343	3.32552	2.51952
mmu-miR-486a-5p	57.6178	13.0452	37.5284	56.5077	38.3469	41.2013	31.3861	17.6458	29.6903	18.1553
mmu-miR-486b-3p	0.501733	11.8593	2.35904	13.9836	0.001825	0.38317	0.052354	17.4933	7.61258	0.144519
mmu-miR-486b-5p	3.75347	12.7466	20.8092	16.6295	1.42407	18.0931	15.8538	2.22423	22.0404	20.0034
mmu-miR-497a-5p	3.7904	5.33669	6.74155	1.03664	1.53395	0.784612	4.7634	1.59723	2.98423	8.44608
mmu-miR-499-5p	1.26347	0.592966	0	0	9.2037	0.784612	0.95268	20.7641	0	8.44608
mmu-miR-501-3p	0	1.7789	2.80898	1.55495	0	2.35384	0.95268	0	0	1.40768
mmu-miR-532-5p	2.52693	5.33669	2.80898	6.21982	1.53395	3.92306	1.90536	3.19447	8.95269	2.81536
mmu-miR-574-3p	0	0.592966	0.561796	3.62823	1.53395	0	0.95268	0	0	0
mmu-miR-615-3p	2.52693	1.18593	0.561796	1.55495	4.60185	1.56922	1.90536	1.59723	2.98423	4.22304
mmu-miR-652-3p	3.7904	6.52262	5.05616	3.10991	1.53395	3.13845	0.95268	1.59723	5.96846	4.22304
mmu-miR-664-3p	2.52693	1.18593	1.12359	2.07327	3.0679	0.784612	0.95268	1.59723	0	1.40768
mmu-miR-674-3p	0	0.592966	1.68539	2.59159	0	0.784612	0	0	0	0
mmu-miR-676-3p	1.26347	2.37186	0.561796	2.07327	1.53395	3.13845	1.90536	3.19447	4.47635	2.81536
mmu-miR-744-5p	0	2.37186	0.561796	0.518318	1.53395	1.56922	0.95268	0	1.49212	1.40768
mmu-miR-7a-1-3p	0	1.7789	1.12359	1.03664	0	0	0	0	1.49212	2.81536
mmu-miR-7a-5p	1.26347	4.15076	1.68539	1.55495	0	0.784612	2.85804	0	5.96846	0
mmu-miR-872-5p	0	2.37186	2.24718	2.07327	1.53395	0.784612	3.81072	4.7917	2.98423	1.40768
mmu-miR-92a-3p	41.6944	34.392	13.4831	17.1045	21.4753	20.3999	9.5268	12.7779	25.366	12.6691
mmu-miR-93-5p	7.5808	15.4171	10.6741	10.3664	4.60185	5.49229	3.81072	9.58341	7.46058	8.44608
mmu-miR-98-5p	5.05387	10.6734	11.2359	11.403	15.3395	8.63074	9.5268	4.7917	11.9369	7.0384
mmu-miR-99a-5p	161.724	71.7489	100.561	97.9621	98.1728	82.3843	102.889	83.0562	73.1137	118.245
mmu-miR-99b-5p	25.2693	24.9046	23.5954	21.251	32.213	18.0461	29.5331	28.7502	17.9054	26.7459

Table S3- Distribution of samples after normalization

Sample name	Mean	Median	Q1	Q3
30Days-SFN-IP-Inj-M1-SKM_S1	175.748	6.31734	1.26347	26.5328
30Days-SFN-IP-Inj-M3-SKM_S2	320.802	6.21982	1.55495	23.3243
30Days-SFN-IP-Inj-M4-SKM_S3	275.446	5.96846	1.49212	23.8738
30Days-SFN-IP-Inj-M5-SKM_S4	176.688	7.11559	1.7789	26.0905
30Days-SFN-IP-Inj-M6-SKM_S5	214.245	6.1358	1.53395	26.0772
30Days-Vehicle-IP-Inj-M1-SKM_S6	238.27	6.66876	0.95268	25.7224
30Days-Vehicle-IP-Inj-M2-SKM_S7	218.182	6.14878	2.24718	25.2808
30Days-Vehicle-IP-Inj-M3-SKM_S8	267.21	5.63072	1.40768	25.3382
30Days-Vehicle-IP-Inj-M4-SKM_S9	255.155	6.2769	1.56922	24.7852
30Days-Vehicle-IP-Inj-M6-SKM_S10	236.581	6.38894	1.59723	25.5558
All samples	237.833	6.21982	1.59723	25.3382

Table S4- differentially expressed miRNAs in skeletal muscle of CD1 mice (SFN vs. Vehicle)

microRNA ID	Chromosome	P-value (SFN vs. Vehicle)	FDR step up (SFN vs. Vehicle)	Fold change (SFN vs. Vehicle)
mmu-miR-150-5p	7	1.20E-13	1.40E-11	3.28E+00
mmu-miR-486a-3p	8	4.00E-09	2.34E-07	2.41E+00
mmu-miR-101a-3p	4	1.09E-08	4.24E-07	-1.96E+00
mmu-miR-126b-5p	2	1.72E-03	5.03E-02	3.84E+00
mmu-miR-140-3p	8	2.63E-03	5.25E-02	1.35E+00
mmu-miR-29c-3p	1	2.96E-03	5.25E-02	-1.91E+00
mmu-miR-92a-3p	14	3.52E-03	5.25E-02	2.00E+00

microRNA ID	Chromosome	P-value (SFN vs. Vehicle)	FDR step up (SFN vs. Vehicle)	Fold change (SFN vs. Vehicle)
mmu-miR-3074-5p	8	3.59E-03	5.25E-02	-2.15E+00
mmu-miR-25-3p	5	1.30E-02	1.70E-01	1.44E+00
mmu-miR-27a-3p	8	1.67E-02	1.95E-01	-1.30E+00
mmu-miR-186-5p	3	3.37E-02	3.23E-01	-1.41E+00
mmu-miR-101b-3p	19	3.48E-02	3.23E-01	-1.51E+00
mmu-miR-3535	1	3.59E-02	3.23E-01	1.60E+00
mmu-miR-196a-5p	11	7.11E-02	5.94E-01	1.46E+00
mmu-miR-146a-5p	11	7.77E-02	6.06E-01	1.88E+00
mmu-miR-126a-3p	2	1.00E-01	6.59E-01	-1.19E+00
mmu-miR-27b-3p	13	1.09E-01	6.59E-01	-1.21E+00
mmu-miR-139-5p	7	1.11E-01	6.59E-01	1.54E+00
mmu-let-7f-5p	13	1.11E-01	6.59E-01	1.21E+00
mmu-miR-140-5p	8	1.13E-01	6.59E-01	-2.29E+00
mmu-let-7i-5p	10	1.25E-01	6.98E-01	1.19E+00
mmu-miR-532-5p	X	1.39E-01	7.37E-01	1.74E+00
mmu-miR-451a	11	1.47E-01	7.50E-01	-1.27E+00
mmu-miR-30e-5p	4	1.70E-01	8.12E-01	-1.35E+00
mmu-miR-152-3p	11	1.74E-01	8.12E-01	-1.30E+00
mmu-let-7c-5p	15	1.94E-01	8.73E-01	1.33E+00
mmu-miR-411-5p	12	2.25E-01	9.37E-01	-1.37E+00
mmu-miR-15a-5p	14	2.36E-01	9.37E-01	-1.59E+00
mmu-let-7b-5p	15	2.41E-01	9.37E-01	1.41E+00
mmu-miR-151-5p	15	2.42E-01	9.37E-01	-1.27E+00
mmu-miR-10b-5p	2	2.48E-01	9.37E-01	-1.28E+00
mmu-miR-30e-3p	4	2.56E-01	9.37E-01	-1.16E+00
mmu-miR-133a-3p	2	2.83E-01	9.64E-01	1.37E+00
mmu-miR-128-3p	1	2.95E-01	9.64E-01	-1.21E+00
mmu-miR-30d-5p	15	2.99E-01	9.64E-01	-1.11E+00
mmu-miR-133b-3p	1	3.05E-01	9.64E-01	1.32E+00
mmu-miR-133a-5p	2	3.20E-01	9.64E-01	1.34E+00
mmu-miR-206-3p	1	3.22E-01	9.64E-01	-1.47E+00
mmu-miR-146b-5p	19	3.43E-01	9.64E-01	1.28E+00
mmu-miR-16-5p	3	3.64E-01	9.64E-01	1.10E+00

microRNA ID	Chromosome	P-value (SFN vs. Vehicle)	FDR step up (SFN vs. Vehicle)	Fold change (SFN vs. Vehicle)
mmu-miR-199a-3p	1	3.78E-01	9.64E-01	-1.20E+00
mmu-miR-222-3p	X	4.01E-01	9.64E-01	-1.38E+00
mmu-miR-22-5p	11	4.09E-01	9.64E-01	1.24E+00
mmu-miR-10a-5p	11	4.15E-01	9.64E-01	1.15E+00
mmu-miR-486a-5p	8	4.21E-01	9.64E-01	1.32E+00
mmu-miR-98-5p	X	4.22E-01	9.64E-01	1.24E+00
mmu-miR-497a-5p	11	4.27E-01	9.64E-01	-1.51E+00
mmu-miR-151-3p	15	4.42E-01	9.64E-01	-1.29E+00
mmu-miR-181b-5p	1	4.62E-01	9.64E-01	-1.41E+00
mmu-miR-127-3p	12	4.64E-01	9.64E-01	1.40E+00
mmu-miR-652-3p	X	4.85E-01	9.64E-01	1.36E+00
mmu-miR-191-5p	9	4.98E-01	9.64E-01	1.12E+00
mmu-miR-126a-5p	2	5.08E-01	9.64E-01	-1.32E+00
mmu-miR-22-3p	11	5.21E-01	9.64E-01	-1.12E+00
mmu-miR-93-5p	5	5.31E-01	9.64E-01	1.26E+00
mmu-miR-143-3p	18	5.41E-01	9.64E-01	-1.16E+00
mmu-miR-126b-3p	2	5.52E-01	9.64E-01	-1.47E+00
mmu-miR-26b-5p	1	5.73E-01	9.64E-01	1.08E+00
mmu-miR-181c-5p	8	5.85E-01	9.64E-01	-1.39E+00
mmu-miR-148a-3p	6	5.89E-01	9.64E-01	1.16E+00
mmu-miR-378c	14	5.95E-01	9.64E-01	-1.13E+00
mmu-miR-1839-5p	7	5.97E-01	9.64E-01	-1.18E+00
mmu-miR-148b-3p	15	6.01E-01	9.64E-01	-1.21E+00
mmu-let-7g-5p	9	6.10E-01	9.64E-01	1.08E+00
mmu-miR-486b-5p	8	6.13E-01	9.64E-01	-1.36E+00
mmu-miR-423-3p	11	6.16E-01	9.64E-01	1.20E+00
mmu-miR-30a-5p	1	6.38E-01	9.64E-01	1.08E+00
mmu-miR-615-3p	15	6.44E-01	9.64E-01	1.29E+00
mmu-miR-3068-3p	12	6.50E-01	9.64E-01	-1.33E+00
mmu-miR-335-5p	6	6.56E-01	9.64E-01	1.17E+00
mmu-miR-23b-3p	13	6.60E-01	9.64E-01	-1.08E+00

microRNA ID	Chromosome	P-value (SFN vs. Vehicle)	FDR step up (SFN vs. Vehicle)	Fold change (SFN vs. Vehicle)
mmu-miR-181a-5p	1	6.61E-01	9.64E-01	1.11E+00
mmu-miR-328-3p	8	6.63E-01	9.64E-01	1.21E+00
mmu-miR-199b-3p	2	6.72E-01	9.64E-01	1.11E+00
mmu-miR-125a-5p	17	6.78E-01	9.64E-01	-1.10E+00
mmu-miR-196b-5p	6	6.89E-01	9.64E-01	1.15E+00
mmu-miR-365-3p	11	6.91E-01	9.64E-01	-1.14E+00
mmu-miR-484	16	6.93E-01	9.64E-01	1.23E+00
mmu-miR-195a-5p	11	6.98E-01	9.64E-01	1.05E+00
mmu-miR-1b-5p	18	7.11E-01	9.64E-01	-1.06E+00
mmu-miR-107-3p	19	7.39E-01	9.64E-01	1.16E+00
mmu-miR-24-3p	8	7.39E-01	9.64E-01	1.06E+00
mmu-miR-145a-5p	18	7.42E-01	9.64E-01	1.03E+00
mmu-miR-30a-3p	1	7.47E-01	9.64E-01	1.07E+00
mmu-let-7a-5p	9	7.48E-01	9.64E-01	1.05E+00
mmu-miR-434-3p	12	7.50E-01	9.64E-01	1.10E+00
mmu-miR-149-5p	1	7.55E-01	9.64E-01	1.11E+00
mmu-miR-1a-3p	2	7.60E-01	9.64E-01	-1.06E+00
mmu-let-7d-5p	13	7.66E-01	9.64E-01	1.06E+00
mmu-miR-30c-5p	1	7.85E-01	9.64E-01	-1.04E+00
mmu-miR-340-5p	11	7.93E-01	9.64E-01	1.10E+00
mmu-miR-221-3p	X	7.93E-01	9.64E-01	1.06E+00
mmu-miR-103-3p	2	8.17E-01	9.64E-01	1.07E+00
mmu-miR-29a-3p	6	8.21E-01	9.64E-01	1.05E+00
mmu-miR-425-5p	9	8.28E-01	9.64E-01	-1.12E+00
mmu-miR-379-5p	12	8.34E-01	9.64E-01	1.10E+00
mmu-miR-21a-5p	11	8.37E-01	9.64E-01	1.06E+00
mmu-miR-199a-5p	1	8.44E-01	9.64E-01	-1.08E+00
mmu-miR-378a-3p	18	8.46E-01	9.64E-01	-1.04E+00
mmu-miR-99b-5p	17	8.53E-01	9.64E-01	-1.04E+00
mmu-miR-192-5p	19	8.61E-01	9.64E-01	-1.09E+00
mmu-miR-99a-5p	16	8.70E-01	9.64E-01	1.03E+00
mmu-miR-676-3p	X	8.78E-01	9.64E-01	1.08E+00
mmu-miR-28a-5p	16	8.84E-01	9.64E-01	-1.05E+00
mmu-miR-145a-3p	18	8.84E-01	9.64E-01	-1.03E+00

microRNA ID	Chromosome	P-value (SFN vs. Vehicle)	FDR step up (SFN vs. Vehicle)	Fold change (SFN vs. Vehicle)
mmu-miR-30b-5p	15	8.94E-01	9.64E-01	-1.02E+00
mmu-miR-185-5p	16	9.00E-01	9.64E-01	1.05E+00
mmu-miR-378a-5p	18	9.03E-01	9.64E-01	1.04E+00
mmu-miR-322-5p	X	9.05E-01	9.64E-01	-1.04E+00
mmu-miR-361-5p	X	9.06E-01	9.64E-01	1.04E+00
mmu-miR-23a-3p	8	9.29E-01	9.71E-01	1.01E+00
mmu-miR-100-5p	9	9.34E-01	9.71E-01	1.01E+00
mmu-miR-322-3p	X	9.38E-01	9.71E-01	1.03E+00
mmu-miR-125b-5p	9	9.67E-01	9.90E-01	-1.01E+00
mmu-let-7d-3p	13	9.79E-01	9.90E-01	-1.01E+00
mmu-miR-3074-2-3p	8	9.82E-01	9.90E-01	-1.01E+00
mmu-miR-26a-5p	9	9.97E-01	9.97E-01	1.00E+00

Table S5. KEGG pathways for all dysregulated miRNAs in skeletal muscles of treated DIO mice with SFN

Gene set	Description	Enrichment score	P-value
path: mmu05206	MicroRNAs in cancer	13.2626	1.74E-06
path: mmu 01521	EGFR tyrosine kinase inhibitor resistance	10.6374	2.40E-05
path: mmu 04510	Focal adhesion	9.17701	0.000103
path: mmu 04012	ErbB signaling pathway	8.54312	0.000195
path: mmu 05214	Glioma	7.75544	0.000428
path: mmu 05033	Nicotine addiction	7.32196	0.000661
path: mmu 05202	Transcriptional misregulation in cancer	7.24997	0.00071
path: mmu 04150	mTOR signaling pathway	6.65138	0.001292
path: mmu 05017	Spinocerebellar ataxia	6.28779	0.001859
path: mmu 05205	Proteoglycans in cancer	6.25344	0.001924
path: mmu 04024	cAMP signaling pathway	6.02279	0.002423
path: mmu 04010	MAPK signaling pathway	5.60755	0.00367
path: mmu 04211	Longevity regulating pathway	5.45265	0.004285
path: mmu 04910	Insulin signaling pathway	5.37476	0.004632
path: mmu 04722	Neurotrophin signaling pathway	5.29621	0.005011
path: mmu 04151	PI3K-Akt signaling pathway	5.28327	0.005076
path: mmu 04926	Relaxin signaling pathway	5.27685	0.005109
path: mmu 04068	FoxO signaling pathway	5.26318	0.005179

Gene set	Description	Enrichment score	P-value
path: mmu 04974	Protein digestion and absorption	5.05791	0.006359
path: mmu 04512	ECM-receptor interaction	5.05791	0.006359
path: mmu 04713	Circadian entrainment	4.89679	0.007471
path: mmu 04710	Circadian rhythm	4.89639	0.007474
path: mmu 01522	Endocrine resistance	4.52217	0.010865
path: mmu 04931	Insulin resistance	4.48917	0.01123
path: mmu 04664	Fc epsilon RI signaling pathway	4.33226	0.013138
path: mmu 05224	Breast cancer	4.31169	0.013411
path: mmu 04215	Apoptosis - multiple species	4.13011	0.016081
path: mmu 04550	Signaling pathways regulating pluripotency of stem cells	4.12167	0.016218
path: mmu 05165	Human papillomavirus infection	4.11662	0.0163
path: mmu 05218	Melanoma	4.00327	0.018256
path: mmu 04720	Long-term potentiation	4.00327	0.018256
path: mmu 04912	GnRH signaling pathway	3.9316	0.019612
path: mmu 04310	Wnt signaling pathway	3.81826	0.021966
path: mmu 03018	RNA degradation	3.81363	0.022068
path: mmu 04660	T cell receptor signaling pathway	3.81179	0.022109
path: mmu 04360	Axon guidance	3.7995	0.022382
path: mmu 04935	Growth hormone synthesis, secretion, and action	3.71712	0.024304
path: mmu 04350	TGF-beta signaling pathway	3.69996	0.024725
path: mmu 04668	TNF signaling pathway	3.69996	0.024725
path: mmu 05223	Non-small cell lung cancer	3.64677	0.026075
path: mmu 04960	Aldosterone-regulated sodium reabsorption	3.6231	0.0267
path: mmu 04917	Prolactin signaling pathway	3.61592	0.026892
path: mmu 05225	Hepatocellular carcinoma	3.58976	0.027605
path: mmu 04933	AGE-RAGE signaling pathway in diabetic complications	3.48577	0.03063
path: mmu 05215	Prostate cancer	3.48577	0.03063
path: mmu 05231	Choline metabolism in cancer	3.28164	0.037567
path: mmu 04929	GnRH secretion	3.13899	0.043327
path: mmu 04810	Regulation of actin cytoskeleton	3.06602	0.046606
path: mmu 04930	Type II diabetes mellitus	3.04076	0.047799
path: mmu 00770	Pantothenate and CoA biosynthesis	2.98153	0.050715

Table S6- Top 50 GO biological processes for dysregulated miRNA in skeletal muscles of treated DIO mice with SFN

Gene set	Description	Enrichment score	P-value
GO:0061470	T follicular helper cell differentiation	8.63191	0.000178
GO:0043559	insulin binding	7.74262	0.000434
GO:0017046	peptide hormone binding	7.63861	0.000481
GO:0016864	intramolecular oxidoreductase activity, transposing S-S bonds	7.01293	0.0009
GO:0003756	protein disulfide isomerase activity	7.01293	0.0009
GO:0098978	glutamatergic synapse	6.88898	0.001019
GO:0051389	inactivation of MAPKK activity	6.65789	0.001284
GO:0008286	insulin receptor signaling pathway	6.63523	0.001313
GO:0016860	intramolecular oxidoreductase activity	6.57325	0.001397
GO:0071863	regulation of cell proliferation in bone marrow	6.5437	0.001439
GO:0071864	positive regulation of cell proliferation in bone marrow	6.5437	0.001439
GO:0051172	negative regulation of nitrogen compound metabolic process	6.53437	0.001453
GO:1905244	regulation of modification of synaptic structure	6.42322	0.001623
GO:0070840	dynein complex binding	6.16395	0.002104
GO:0045934	negative regulation of nucleobase-containing compound metabolic process	6.15699	0.002119
GO:0031670	cellular response to nutrient	6.10054	0.002242
GO:0042562	hormone binding	6.03348	0.002397
GO:0051348	negative regulation of transferase activity	5.9153	0.002698
GO:0033673	negative regulation of kinase activity	5.80786	0.003004
GO:0050807	regulation of synapse organization	5.80692	0.003007
GO:0051253	negative regulation of RNA metabolic process	5.78245	0.003081
GO:0031324	negative regulation of cellular metabolic process	5.73334	0.003236
GO:0000288	nuclear-transcribed mRNA catabolic process, deadenylation-dependent decay	5.72188	0.003274
GO:0030877	beta-catenin destruction complex	5.72188	0.003274
GO:0030334	regulation of cell migration	5.60785	0.003669
GO:0006469	negative regulation of protein kinase activity	5.592	0.003728
GO:0045990	carbon catabolite regulation of transcription	5.58335	0.00376
GO:0045991	carbon catabolite activation of transcription	5.58335	0.00376
GO:0008332	low voltage-gated calcium channel activity	5.58335	0.00376
GO:0035425	autocrine signaling	5.58335	0.00376
GO:0043565	sequence-specific DNA binding	5.54161	0.00392
GO:0043005	neuron projection	5.5408	0.003923
GO:0048736	appendage development	5.53968	0.003928

Gene set	Description	Enrichment score	P-value
GO:0060173	limb development	5.53968	0.003928
GO:0044306	neuron projection terminus	5.43852	0.004346
GO:0048009	insulin-like growth factor receptor signaling pathway	5.39195	0.004553
GO:0010369	chromocenter	5.39195	0.004553
GO:0033688	regulation of osteoblast proliferation	5.29813	0.005001
GO:0048523	negative regulation of cellular process	5.25519	0.00522
GO:1902679	negative regulation of RNA biosynthetic process	5.1649	0.005714
GO:1903507	negative regulation of nucleic acid-templated transcription	5.1649	0.005714
GO:2000145	regulation of cell motility	5.1582	0.005752
GO:0001701	in utero embryonic development	5.12468	0.005948
GO:0030501	positive regulation of bone mineralization	5.11732	0.005992
GO:1902683	regulation of receptor localization to synapse	5.11505	0.006006
GO:0140030	modification-dependent protein binding	5.11258	0.006021
GO:0042288	MHC class I protein binding	5.1002	0.006096
GO:0099159	regulation of modification of postsynaptic structure	5.1002	0.006096
GO:0030889	negative regulation of B cell proliferation	5.1002	0.006096
GO:0033690	positive regulation of osteoblast proliferation	5.1002	0.006096

S1-Figure, PCA

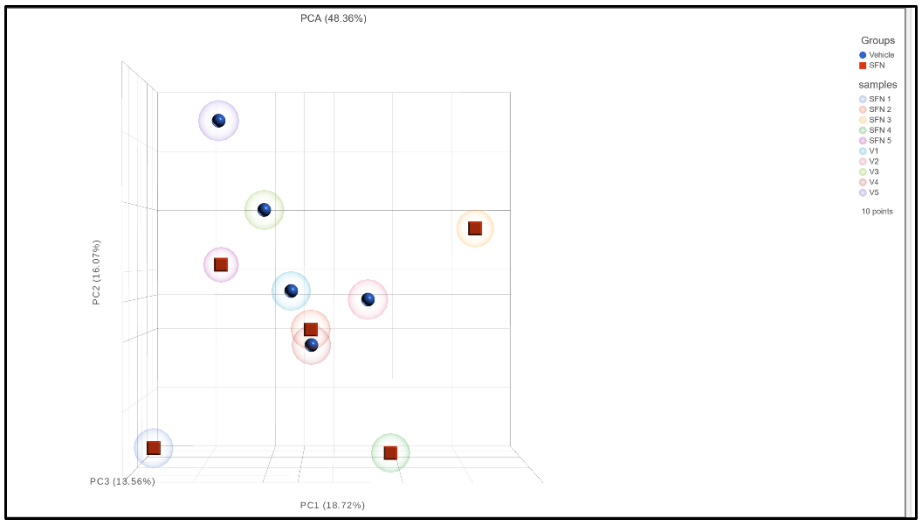

S2- Figure shows the distribution of raw counts of each sample

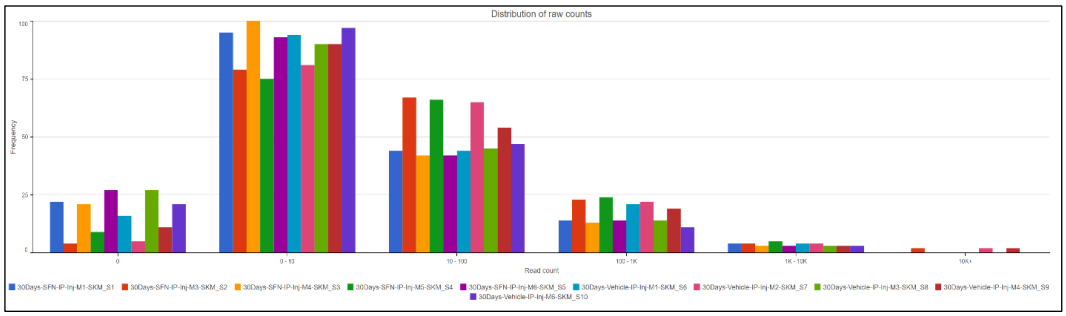

The graph represents the number of genes expressed by each sample, whereas frequency represents the gene counts expressed by a sample. The graph shows that most of the expressed genes had read counts in the 0-10 and 10-100 reads region.

Grants: QUST-1-CHS-2022-353
QNRP grant: This study was supported by the Qatar National Research Fund grant (NPRP9-351-3-075)

IACUC approval
Qatar University (protocol number: QU-IACUC 1-62019-1)
approved the experimental protocols and euthanasia procedures used in this study.

Qatar University
Institutional Bio-safety Committee

To: Nasser Moustafa Rizk
Qatar University

October 19, 2022

Ref: Project Titled Project Titled "Differential Expression of lncRNA /mRNA in the Visceral Adipose Tissue of NrF2 Knockout Mouse Model on HFD
Grant: QUST-2-CHS-2020- 5

Dear Dr. Nasser Moustafa Rizk,
We would like to inform you that your application along with supporting documents provided for the above proposal have been reviewed by QU-IBC, and having met all the requirements, has been granted approval.

Date of Approval: October 19, 2022

Date of Expiration: November 9, 2023

Please note that QU-IBC approval is contingent upon your adherence to the following QU-IBC Guidelines:

- Ensuring compliance with QU Safety Plans and applicable national and international regulations.
- Ensuring experiments that require prior IBC approval are not conducted until IBC approval is obtained and making initial determination of containment levels required for experiments.
- Notifying the IBC of any changes to other hazardous material experiments previously approved by the IBC.
- Reporting any significant problems, violations of QU Safety Plans and applicable regulations/ guidelines, or any significant research-related accidents and illnesses to the QU-IBC. Also, ensuring personnel receive appropriate orientation and specific training for the safe performance of the work.

Your research approval No. is: **QU-IBC-2020/076-REN2**. Please refer to this approval number in all your future correspondence pertaining to this research.

Best wishes,
Chairperson, QU-IBC

Institutional Bio-safety Committee
(IBC)
Office Of Academic Research

Approved Date: October 19, 2022
Qatar University Institutional Biohazard Committee (QU-IBC)

IBC:

جامعة قطر
QATAR UNIVERSITY

Institutional Animal Care & Use Committee (QU-IACUC)

QATAR UNIVERSITY, PO BOX 2713, DOHA, QATAR
TEL: +974 4403-6676 FAX: +974 4403-3901
Email: QU.IACUC@qu.edu.qa
Assurance Registration #: IACUC-QU-2019-002
Assurance #: IACUC-A-QU-2019-0004

August 14, 2020

TO: **Dr. Nasser Moustafa Ragheb Rizk,** Department of Biomedical Sciences, College of Health Sciences, Qatar University
Email: nassrizk@qu.edu.qa

FROM: Qatar University – Institutional Animal Care & Use Committee (QU-IACUC)

SUBJECT: **Letter of Exemption for research project**
Project Title: *"Anti-obesity and anti-diabetic interventions by small molecule compounds".*

NPRP9-351-3-075

Dear Dr. Nasser,

The Qatar University Institutional Animal Care and Use Committee (QU-IACUC) has **APPROVED** your request seeking **IACUC exemption** for the use of archived/stored tissues that were collected under your previously approved IACUC protocol (QU-IACUC 1-6/2019-1) for the above-mentioned project funded by QNRF grant NPRP9-351-3-075.

The animals were cared for and tissue samples were collected under a valid IACUC protocol and hence the further use of these banked tissues is within the spirit of high animal care standards that encourage protocol refinement and reduction of animal numbers. Institutional Biohazard Committee (IBC) approval is sufficient to proceed with the proposed work for use of stored animal tissues. Please note that this exemption letter does not allow, however, any use of live of animals.

Kindly refer to the above Animal Use Protocol number in all of your future correspondence with us pertaining to this project.

Sincerely,

Dr. Abdelali Agouni, MSc, PhD, FHEA
Chair of QU-IACUC
Qatar University
Doha, Qatar

جامعة قطر
QATAR UNIVERSITY
IACUC
Institutional Animal Care and Use Committee

copy: QU-IACUC files